Earth-Science Reviews 201 (2020) 103065

Contents lists available at ScienceDirect

Earth-Science Reviews

journal homepage: www.elsevier.com/locate/earscirev

Carbonates before skeletons: A database approach

Marjorie D. Cantine[a], Andrew H. Knoll[b], Kristin D. Bergmann[a,*]

[a] Department of Earth, Atmospheric and Planetary Sciences, Massachusetts Institute of Technology, Cambridge, MA 02139, USA
[b] Department of Organismic and Evolutionary Biology, Harvard University, Cambridge, MA 02138, USA

ARTICLE INFO

Keywords:
Carbonate precipitation
Dolomite
Carbonate facies
Seafloor precipitate textures
Stromatolites
Molar tooth structures
Intraclasts
Ooids

ABSTRACT

Carbonate minerals have precipitated from seawater for at least the last 3.8 billion years, but changes in the physical and chemical properties of carbonate rocks demonstrate that the nature, loci, and causes of this precipitation have varied markedly through time. Biomineralization is perhaps the most obvious time-bounded driver. However, other changes in the sedimentological character of Archean and Proterozoic carbonates offer an under-considered record of fluctuations in Earth's chemical, biological, and physical systems before and during the rise of animal life. Geobiologists and geochemists have successfully used large geochemical datasets to track changes in Earth's surface chemistry through time, but inconsistencies between proxies make the recognition of clear spatial-temporal patterns challenging. In order to place new constraints on the environmental history of Archean and Proterozoic oceans, especially with regard to redox state, we present for the first time a high-resolution database of global Precambrian and Cambrian carbonate sedimentation.

Our initial datasbase, named *Microstrat*, comprises carbonate-bearing successions dating from c. 3.4 billion to ~500 million years old; these include more than 130 carbonate-bearing formations, digitized at the highest stratigraphic resolution possible and classified by environment of deposition. Lithofacies details are recorded at the finest scale available, including a range of microbial and other depositional fabrics, mineralogy, environment of deposition, age and location. We interrogate the Archean, Proterozoic, and Cambrian carbonate records, testing both long-standing and novel hypotheses about changes in Earth's carbonate system through time. Changes in carbonate sedimentology illuminate global changes in bioturbation and microbial community structure; the depth-dependent timing of marine oxygenation and the transition from anaerobic to aerobic respiration at and within the seafloor; and temporal changes in patterns of dolomitization. Shifts in both the loci of carbonate precipitation and in markers of animal activity are consistent with time- and depth-dependent trends in ocean oxygenation. We also note changes through time in the morphologies of stromatolites and thrombolites, which we suggest reflect secular shifts in carbonate precipitation, clastic sediment transport, and eukaryotic evolution. Observations from the database and petrographic studies confirm that the nature and extent of Proterozoic dolomite contrasts with that of dolomite in the Phanerozoic, consistent with dolomite being an early or even, in some cases, primary precipitate prior to the Cambrian Period. Because this database preserves environmental context and the stratigraphic relationships of carbonate features rather than tracking the occurrence of single features through time, it permits new and detailed analyses of the physical sedimentology of Precambrian carbonates and correlations in time and space among different features.

We also consider how to build upon this initial dataset. Capturing and analyzing sedimentological data is difficult. Analysis becomes more challenging when data have been collected by multiple researchers working across Earth's entire history and surface. Field observations have a great deal of power to describe and explain changes in Earth's surface environments, yet they are often reported in idiosyncratic ways that make it difficult to compare them, obscuring their true explanatory power. *Microstrat* is an effort to pool idiosyncratic sedimentological data in hopes of illuminating Archaean, Proterozoic, and Cambrian carbonate depositional environments, yet it is unavoidably limited. We describe how other researchers can help to build *Microstrat* into a community-curated database by reporting and sharing data.

* Corresponding author.
E-mail address: kdberg@mit.edu (K.D. Bergmann).

https://doi.org/10.1016/j.earscirev.2019.103065
Received 8 March 2019; Received in revised form 10 December 2019; Accepted 11 December 2019
Available online 20 December 2019
0012-8252/

1. Introduction

In the modern ocean, carbonate deposition largely reflects the abundance and distribution of biomineralizing organisms, modulated by the dissolution of carbonate in the deep ocean. The accumulation of marine carbonates in sedimentary basins, however, long predates the evolution of skeletal eukaryotes, extending backward at least as far as the oldest known sedimentary rocks, deposited some 3.8 billion years ago. What does this older carbonate record tell us about life and environments in early oceans?

Many studies have examined the geochemistry of Precambrian sedimentary rocks, assessing the fidelity of environmental and metabolic signatures through burial, deformation, and exhumation. Here, we focus instead on the physical sedimentology and textural characteristics of Archean, Proterozoic and Cambrian carbonates. There is no shortage of papers arguing for secular variation in particular carbonate textures, generally anecdotal accounts based on the (often extensive) experiences of individual geologists. Such arguments provide key hypotheses about Earth's early history, but they require quantification and testing against the record as a whole. As a step in this direction, we present the first iteration of a novel tool: *Microstrat*, a global compilation of Precambrian to Cambrian carbonate strata. It gathers data from theses and published literature, and characterizes more than 130 carbonate-bearing formations, divided at the finest stratigraphic resolution made possible by available sources. *Microstrat* includes tabulations of feature occurrence, thickness, sedimentological, mineralogical, and paleoenvironmental data.

The sedimentological characteristics of Precambrian carbonate rocks provide an informative and under-explored record of ocean oxygenation, seawater chemistry, and interactions between life and its environments. Although metamorphism can obscure the physical sedimentology and textures of carbonate rocks, these features are more robust than geochemical characteristics through burial, deformation, and exhumation. The sedimentology of carbonate rocks thus provides an independent line of evidence for changes in Earth's surface environments—one that can be compared with geochemical, paleobiological, and molecular records. *Microstrat* benefits from the long study of Precambrian rocks by many researchers. It integrates observations and interpretations of carbonate texture and physical sedimentology across many authors, time periods, and continents. We hope that the first version of *Microstrat*, described here, inspires conversations among sedimentologists about data collection, management, and sharing, to improve future versions of this dataset and other efforts to develop large, powerful sedimentological datasets. While we focus in the first instance on broad patterns at a relatively coarse temporal scale, we envision an evolving community tool that will address local, regional and global patterns with increasingly fine time resolution.

1.1. A brief history of Precambrian carbonate studies

Modern field investigations of Archean and Proterozoic carbonates began in the 1960s and 1970s as part of a broader interest in the Precambrian sedimentary record (e.g., Hoffman, 1969; Cloud and Semikhatov, 1969; Cloud et al., 1969). At the same time, investigations of modern carbonates in the Bahamas, the Persian Gulf, and elsewhere began to provide a mechanistic basis for interpreting this ancient record (e.g., (Cloud, 1962; Gebelein, 1969; Shinn et al., 1969; Bathurst, 1972). Beyond linking observable processes to the textures in carbonate rocks, principal drivers of the mounting interest in Archean and Proterozoic carbonate rocks included the desire to understand ancient tectonics and biology. For example, at a time when understanding of plate tectonics was in its infancy, Hoffman (1969) demonstrated that facies relationships of Paleoproterozoic carbonates from Great Slave Lake, Canada, support the hypothesis that plate tectonics governed basin development two billion years ago. Biological interest was stoked by Tyler and Barghoorn's (1954); Barghoorn and Tyler, 1965) discovery of microfossils more than a billion years older than the most ancient animal fossils. Spurred by pioneering studies by Soviet stratigraphers, studies of Precambrian carbonate sedimentology and paleobiology began to coalesce through mutual interest in stromatolites. Reconnaissance mapping of thick Proterozoic platform carbonates in Siberia showed that stromatolites were major constituents of these rocks, displaying a common pattern of stratigraphic succession across multiple basins (Semikhatov et al., 1973). In the absence of other markers, stromatolites gained prominence in stratigraphic correlation (Bertrand-Sarfati and Trompette, 1976; Preiss, 1977; Bertrand-Sarfati and Walter, 1981), and, by analogy to the stratigraphic succession of animal fossils in younger deposits, observed changes in stromatolite morphology through time were first ascribed to microbial evolution (Cloud and Semikhatov, 1969), and later, at least in part, to environmental change (Grotzinger and Knoll, 1999).

In a key contribution, Grotzinger (1989) argued that the distribution of carbonates in Archean and Proterozoic basins documents tectonic and (in part related) sea-level controls on carbonate sequence development comparable to those in operation today. Other features, however, suggest that processes without modern analogues also helped to shape Archean and Proterozoic carbonates (Sumner and Grotzinger, 1986, 1993; Sumner, 1997; Grotzinger and James, 2000). Precambrian carbonates were hardly a uniform whole: important physical and chemical features of carbonates changed through the three billion years they record.

Grotzinger and James (2000) summarized some of these perceived variations, including a long-term decline in the abundance and distribution of seafloor precipitate textures (Plate 1, A, E); the restriction of molar tooth structures (Plate 2 B, C Shields, 2002; Pollock et al., 2006; James et al., 2012) to Archean (Bishop and Sumner, 2006) through earlier Neoproterozoic rocks; the occurrence of giant ooids in Neoproterozoic platform successions (Plate 2, E, F); and the increased abundance of thrombolites near the Proterozoic-Cambrian boundary (Plate 3, A). Other suggested changes include variation in stromatolite abundance and morphology (Plate 4, C, D; Walter and Heys, 1985; Semikhatov and Raaben, 1996, summarized by Grotzinger and Knoll, 1999), and changes through time in the nature and abundance of dolomite (Tucker, 1977, 1982, 1984; Zempolich et al., 1988; Burdett et al., 1990; Knoll and Swett, 1990; Zempolich and Baker, 1993; Wright, 2000; Kah, 2000; Corsetti et al., 2006; van Smeerdijk Hood et al., 2011; Wood et al., 2017; van Smeerdijk Hood and Wallace, 2018). Post-Marinoan cap carbonates, with their distinctive textural features, geochemistry, and bedforms, have been advanced as sedimentary evidence for global change associated with Snowball deglaciation (e.g., Hoffman et al., 2007; Le Hir et al., 2009; Lamb et al., 2012; Creveling et al., 2016). In general, then, decades of observations have resulted in a number of hypothesized changes in the carbonate record. *Microstrat* enables us to integrate observations across researchers, study locations, and time intervals to test these perceived temporal trends quantitatively.

1.2. Processes driving variations in Earth's carbonate record

This long study of Precambrian carbonate strata has suggested significant, time-bound changes in the nature of the carbonate record. Drivers for this variation may include other important changes in Earth's surface environments over the same interval.

The growth of cratons, changes in their configuration, and associated increases in weathering and sediment influx may have influenced the distribution and occurrence of carbonate platforms. In modern settings, carbonate platforms are typically (although not exclusively) associated with the passive margins of continents, especially at low to middle latitudes; however, carbonate platforms within epeiric seas and continental seaways are also well-represented in the ancient record. Changes in the size, stability, configuration, and flooding of continents may impact the global deposition of carbonate platforms, and these

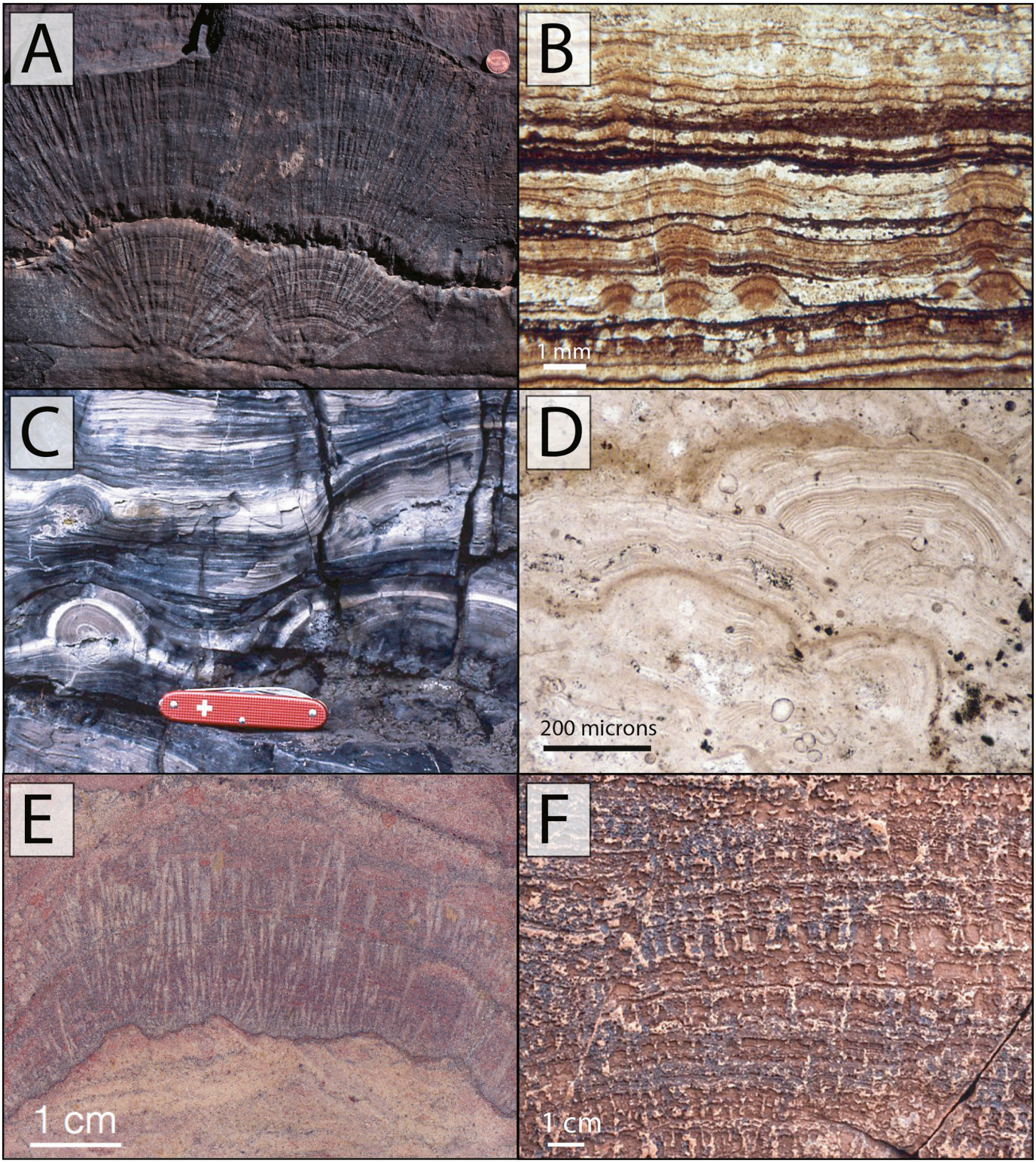

Plate 1. Precipitation at the sediment-water interface was an important component of the pre-Tonian carbonate record.
A Crystal fans growing from the sediment-water interface. Upper Archean Campbellrand Subgroup, Transvaal Supergroup, South Africa. *Photo: John Grotzinger*
B Millimeter-scale precipitates in silicified peritidal microbial carbonates. Lower Mesoproterozoic Kotuikan Fm, Siberia. *Photo: A. Knoll*
C Peritidal, precipitated stromatolites from the Upper Mesoproterozoic Narssârssuk Fm, Greenland. *Photo: A. Knoll*
D Micron-scale precipitated laminae from the peritidal Kotuikan Fm, Lower Mesoproterozoic. Siberia. *Photo: A. Knoll*
E Crystal fans from the Ediacaran Rainstorm Member are closely associated with iron and manganese-rich heavy mineral lag deposits. Johnnie Fm, Death Valley. *Photo: K. Bergmann*
F Peritidal, digitate microprecipitates. 1850 Ma Duck Creek Fm, Australia. *Photo: A. Knoll*

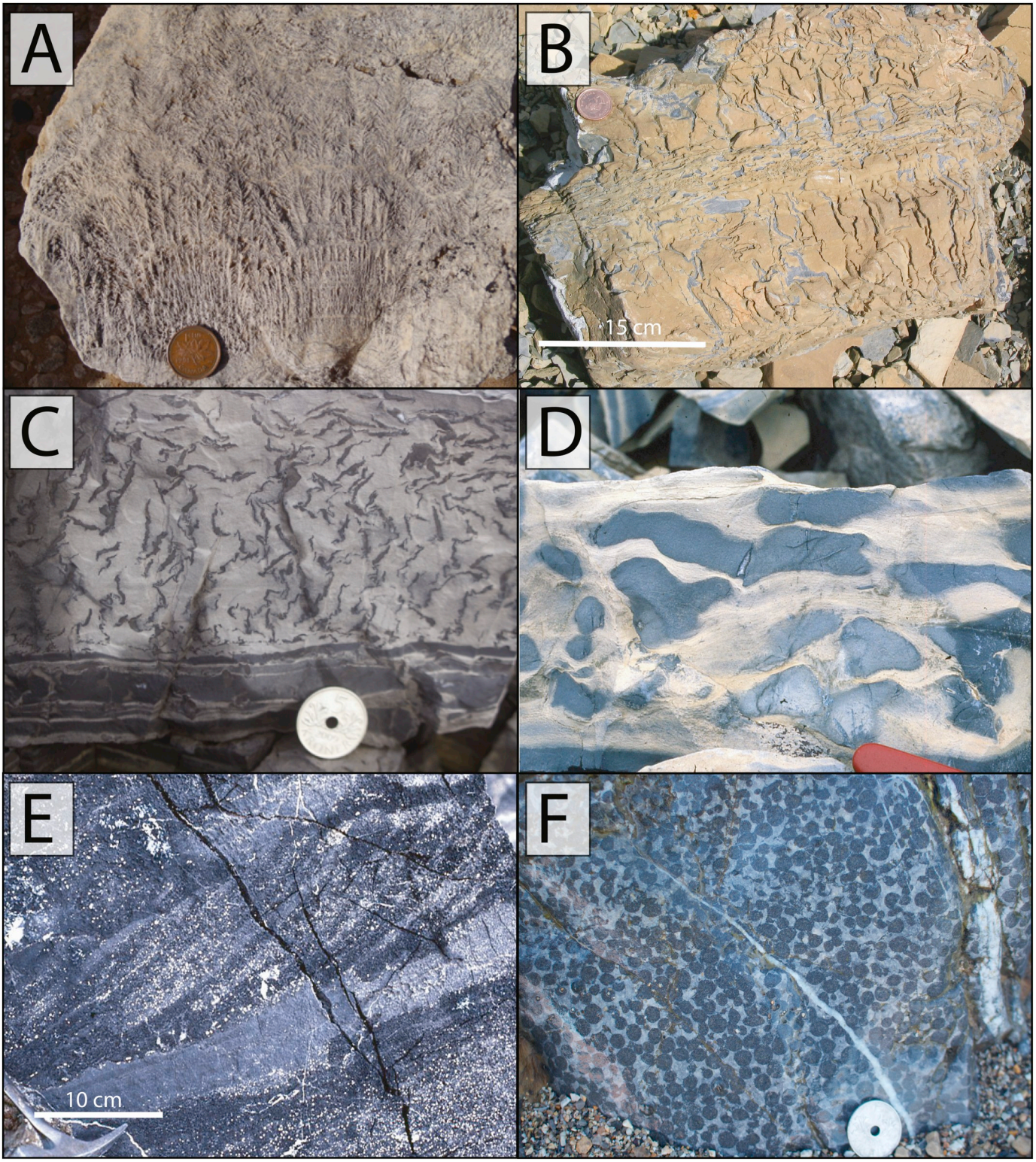

Plate 2. The Neoproterozoic and Cambrian intervals saw secular changes in the locus of carbonate precipitation.
A Tufa. Ediacaran Buah to Ara Fm. transition. Sultanate of Oman. *Photo: K. Bergmann*
B Molar tooth cement. Lower Mesoproterozoic Helena Fm, correlative to the Wallace Fm included in the database. Belt Supergroup, Montana. *Photo: A. Knoll*
C Molar tooth cements, Tonian Svanbergfjellet Fm, Svalbard. These calcite cements formed within a dolomitic matrix. Diameter of Norwegian 5 kroner coin is 26 mm. *Photo: K. Bergmann*
D Mottled carbonate. These carbonates, which show penecontemporaneous formation of limestone nodules (and later dolomitization around them), are seen in Tonian formations globally. Grusdievbreen Fm, Svalbard. *Photo: A. Knoll*
E Cross-bedded oolite of giant ooids. Backlundtoppen Fm, Ny Friesland, Svalbard. *Photo: A. Knoll*
F Giant ooids. Backlundtoppen Fm, Ny Friesland, Svalbard. Diameter of Norwegian 5 kroner coin is 26 mm. *Photo: K. Bergmann*

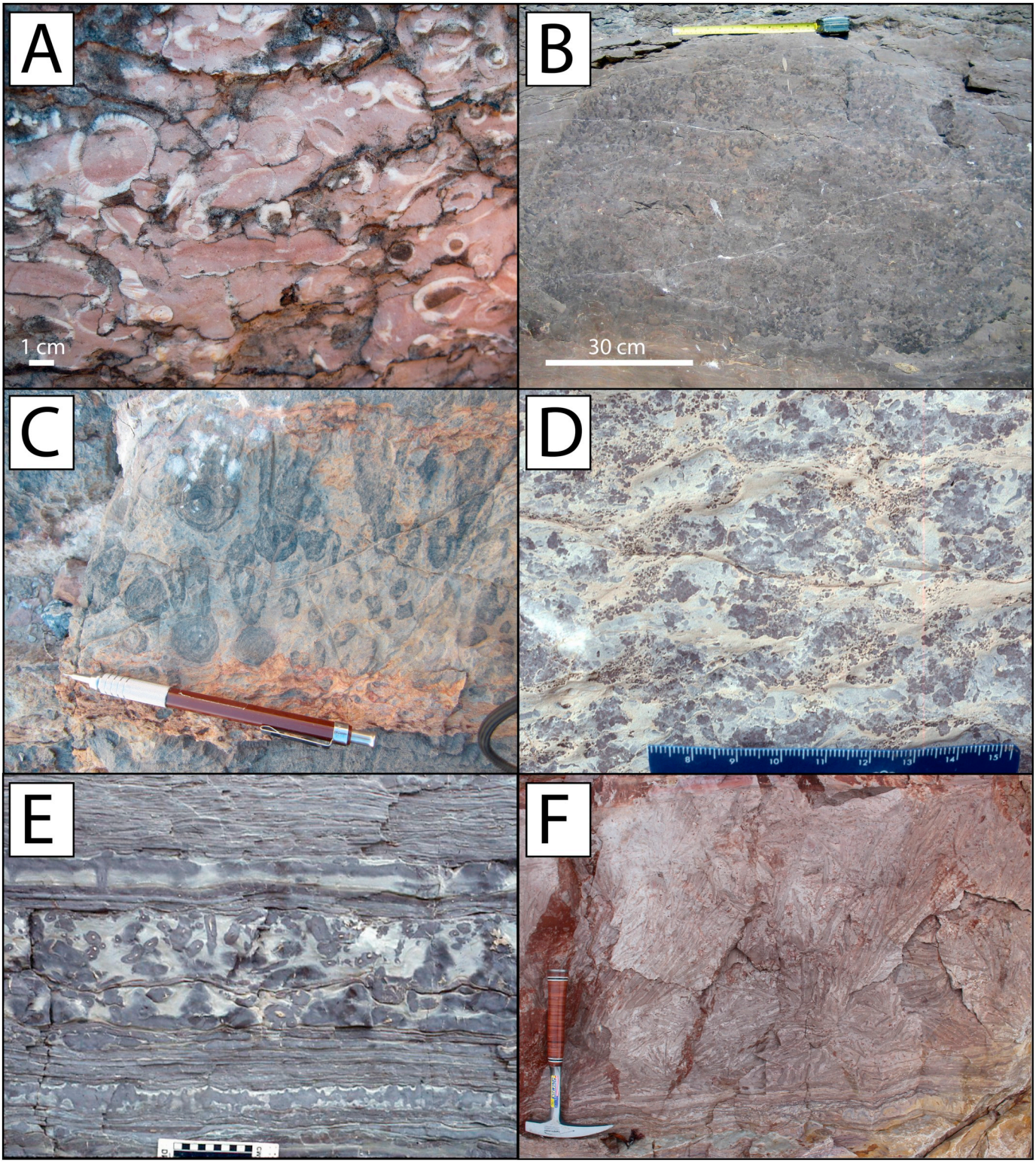

Plate 3. New interactions between metazoans and sediments and the abundance and co-association of thrombolites and oncoids characterize Cambrian carbonates.
A Archaeocyathid skeletal material in reef flank mud. Arroyo Pedroche Fm, Spain. Photo: *A. Knoll*
B Thrombolite, Lower Ordovician Boat Harbor Fm., Port au Port Group, Newfoundland. Ordovician stratigraphy is not yet included in the database; this image illustrates thrombolites of this type which are included in Cambrian stratigraphy within the database. *Photo: A. Knoll*
C Digitate thrombolites grow upward from exceptionally large oncoids. Carrara Fm, Death Valley. *Photo: K. Bergmann*
D Thrombolitic texture, Manykai Fm, Siberia. *Photo: A. Knoll*
E Basal Cambrian burrows in carbonate mud, showing penecontemporaneous cementation around burrows. Manykai Fm, Siberia. *Photo: A. Knoll*
F Edgewise intraclast conglomerate. Upper Cambrian (Furongian) Berry Head Fm, Port au Port Group, Newfoundland, *Photo: K. Bergmann*

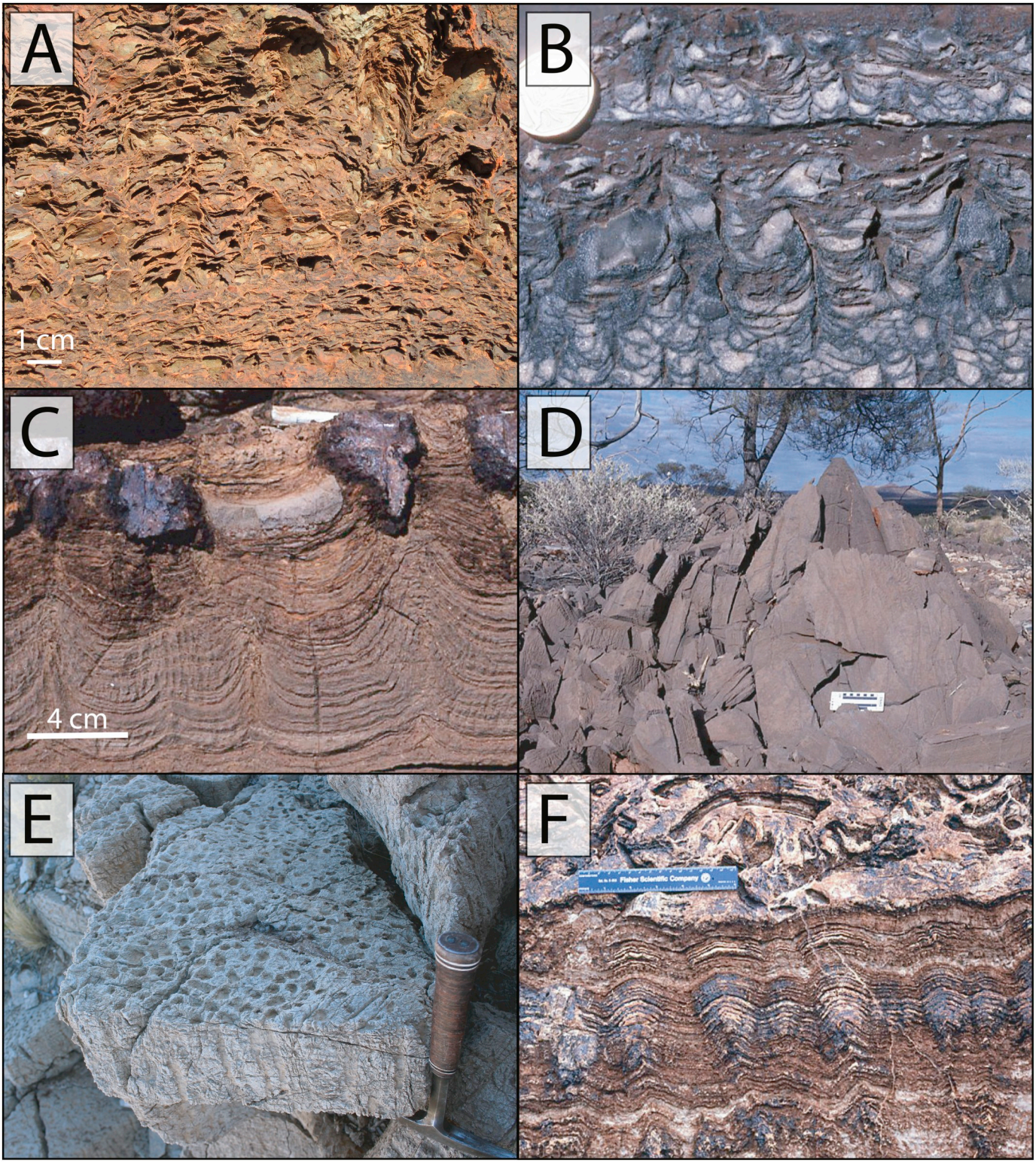

Plate 4. The direct precipitation of carbonate plays a major role in defining stromatolite morphologies.
A Fenestrate stromatolites from the 2200-2400 Ma Kazput Fm, Australia. *Photo: A. Knoll*
B Fenestrate stromatolites from the Archean Transvaal Supergroup. *Photo: A. Knoll*
C Peritidal conical stromatolites, Lower Mesoproterzoic Bangemall Group, Australia. *Photo: A. Knoll*
D Basinal *Conophyton*. Lower Mesoproterozoic Bangemall Group, Australia. *Photo: A. Knoll*
E "Tubestone" stromatolites from the Ediacaran Noonday Fm, Nevada. *Photo: K. Bergmann*
F Peritidal precipitated laminae with intraformational conglomerate above. 1850 Ma Duck Creek Fm, Australia. *Photo: A. Knoll*

have certainly influenced their preservation. Aspects of the initiation of plate tectonics and the growth of continental crust may be recorded by Archean carbonates, whereas Proterozoic carbonates may reflect, at least in part, the assembly and breakup of supercontinents, including Nuna and Rodinia (Li et al., 2008; Cawood et al., 2013; Lee et al., 2016; Merdith et al., 2017). In addition to the distribution of passive margins and epicratonic seas, riverine delivery of cations, anions and siliciclastic sediment to the ocean varies as a function of continental configuration and weathering. Freeboard, or the exposure of continents above sea level, is also dependent on the volume of ancient oceans and the isostatically-controlled distribution of continental elevation; estimates suggest freeboard has varied within a narrow range since at least the early Proterozoic (Wise, 1974; Windley, 1977; Galer, 1991; Eriksson, 1999; Korenaga et al., 2017) following large-scale emergence of continents (Bindeman et al., 2018).

Geochemical measurements and mineralogical observations of sedimentary rocks indicate that seawater chemistry has changed through Earth's history. The most significant change, the oxygenation of Earth's atmosphere and surface environments, was first discerned from geological observations (summarized in Holland, 1999), including the temporal distribution of iron formation and the presence of pyrite and uranite as detrital grains in Archean alluvial sediments. Geochemical studies, including constraints from the temporal distribution of mass-independent fractionation of sulfur and description and iron speciation data, suggest that environmental oxygen concentrations rose markedly twice in the deep past (Farquhar et al., 2000; Holland, 2006; Kump, 2008; Lyons et al., 2014). During the Great Oxygenation Event, c. 2400 Ma, oxygen in the atmosphere and surface oceans first accumulated to physiologically significant levels, while beginning in the later Neoproterozoic Era, atmospheric oxygen levels climbed again. Some evidence suggests additional complexity in this record, reporting geochemical evidence consistent with a Mesoproterozoic rise in oxygen (Kah et al., 1999, 2004; Johnston et al., 2005); these subtleties call for additional testing as evolving datasets are refined. The Neoproterozoic rise in oxygen may have been critical for the evolution of macroscopic, mobile animal life, dependent on diatomic oxygen to fuel both locomotion and digestion (Canfield et al., 2007; Sperling et al., 2013). A consensus is further developing that deeper ocean environments (below storm wave base) remained anoxic well into the Paleozoic Era (Dahl et al., 2010; Gill et al., 2011; Thompson and Kah, 2012; van Smeerdijk Hood and Wallace, 2015; Saltzman et al., 2015; Sperling et al., 2015; Wood et al., 2018; Halverson et al., 2018; Krause et al., 2018; Stolper and Keller, 2018; Hammarlund et al., 2019; Tostevin et al., 2019).

Aspects of seawater chemistry that directly impact the precipitation of carbonates have changed through time, as well. Many modern surface ocean settings are saturated or supersaturated with respect to aragonite, calcite, and dolomite, but precipitation of dolomite in particular, is not favored kinetically. The abundance of peritidal and shallow subtidal marine dolomite and limestone through the Archean and Proterozoic Eons indicates that shallow seawater was consistently supersaturated with regard to calcium carbonate minerals, yet key controls on the carbonate system likely did not remain static through that interval (Baker and Kastner, 1981; Kastner, 1983). The ratio of and concentrations of magnesium and calcium in the Precambrian ocean likely varied through time as a function of ocean crust production and riverine cation delivery (Hardie, 2003).

Other key controls on the Precambrian marine carbonate system are poorly constrained, including temperature, alkalinity, and pCO_2. Several authors (Ronov, 1968, 1984; Kempe and Degens, 1985; Grotzinger and Kasting, 1993) have suggested that the alkalinity of Precambrian oceans was higher than that of today's, promoting carbonate precipitation; in turn, Halevy and Bachan (2017) suggested that the pH of seawater has increased through time, with early Archean values between 6.5 to 7.0, and Proterozoic values likely as high as 7.75. Low seawater pH often correlates with low carbonate saturation state and carbonate dissolution, though alkalinity and dissolved inorganic carbon can counterbalance this. The temperature history of the Precambrian Eon has also long been debated (e.g., (Burdett et al., 1990; Knauth, 2005; Gaucher et al., 2008; Hren et al., 2009; Blake et al., 2010; Pope et al., 2012; Hoffman et al., 2017 and references therein). As a primary control on chemical equilibria, precipitation rate, and evaporation, temperature plays a key role in the formation, distribution, and textural character of carbonates. The period from 2250 Ma to 719 Ma lacks sedimentological evidence for widespread, synchronous glaciation across multiple localities, although paleomagnetic and sedimentological evidence consistent with low-latitude, near sea-level glaciation at c. 1800 Ma has been reported from Australia's Kimberley Basin (Williams, 2005; Schmidt and Williams, 2008). This lack of evidence for widespread glaciation is consistent with relatively warm temperatures during this interval. The sedimentology of Snowball Earth deposits, in turn, shows that substantially colder periods with widespread glaciation book-ended this relatively clement interval (Hoffman et al., 2017 and references therein). Warm temperatures returned in association with Snowball deglaciations (Pierrehumbert, 2005).

Beyond the components directly involved in the carbonate system, seawater contains other ions that affect the precipitation and growth of carbonate minerals from seawater. Changes in temperature, pH, and dissolved oxygen would also affect the speciation of other ions in the ocean, altering kinetic inhibition associated with carbonate precipitation and the chemical consequences of microbial respiratory metabolisms. For example, at times sulfide, reduced iron, and manganese would have been more common relative to iron and manganese oxides and (Sumner and Grotzinger, 1996; Canfield and Farquhar, 2009; Blättler et al., 2018). Silica concentrations in Precambrian seawater were high relative to Phanerozoic oceans (Siever, 1992; Tosca et al., 2016) making primary and early diagenetic chert a common chemical sediment in carbonate-rich environments.

Microbial processes and redox conditions can have a direct effect on carbonate saturation state (Ω). Aerobic respiration disrupts carbonate precipitation because of its effects on pH; however, a host of anaerobic microbial metabolisms as well as oxygenic photosynthesis can promote carbonate precipitation through the production of alkalinity and/or pH increase (Soetaert et al., 2007; Higgins et al., 2009; Bergmann et al., 2013). For this reason, changes in the oxygenation of the ocean may have influenced styles of carbonate precipitation via the shifting location of the oxic-anoxic interface.

Though the broad division of redox history into intervals of "no", "some" and "a lot" of O_2 seems reasonable, resolving the oxygenation history of Earth's environments at a finer spatial and temporal resolution remains challenging. Carbonate precipitation may be helpful: the style and location of carbonate precipitation is redox-sensitive, because aerobic and anaerobic metabolisms affect the carbonate system in different ways (Higgins et al., 2009; Bergmann et al., 2013). Thus, changes in the style and loci of carbonate precipitation, tracked through depositional environments and integrated across time, provide an independent constraint on changing redox conditions on the early Earth.

In part related to redox history, biological innovation has been a continuing influence on Earth's physical environment. For example, oxygen production by photosynthesizing cyanobacteria was key to the Great Oxygenation Event (Johnson et al., 2013; Lyons et al., 2014; Fischer et al., 2015, 2016; Knoll et al., 2016). Molecular clocks suggest that cyanobacteria continued to diversify through the Proterozoic Eon (Schirrmeister et al., 2016; Sánchez-Baracaldo et al., 2017), potentially influencing the character of stromatolites, although no empirical evidence from Proterozoic rocks informs this possibility (Grotzinger and Knoll, 1999). Eukaryotic organisms evolved early in the Proterozoic Eon and radiated in Neoproterozoic oceans (Parfrey et al., 2011; Cohen and Macdonald, 2015; Knoll, 2015). By the Ediacaran Period, eukaryotic diversity included complex multicellular organisms, both animals and algae (Knoll, 2011). New interactions between these organisms and their environment created changes in the carbonate system. For example, bioturbation began during the late Ediacaran Period and

expanded into the Cambrian (Buatois et al., 2009; Tarhan et al., 2015; Mángano and Buatois, 2016; Tarhan, 2018b), profoundly altering the geochemistry of surficial sediments and permitting new ecological associations on and within the seafloor (Meysman et al., 2006; Erwin, 2008; Erwin et al., 2011). These changes are coincident with the first appearance of carbonate-mineralized skeletons in the latest Ediacaran and predate a shift to skeletal carbonate as the dominant mode of carbonate precipitation in the middle Ordovician (Pruss et al., 2010a; Creveling et al., 2013). These and other changes provide constraints on time-variant interactions between life and environment.

1.3. The power and potential of large sedimentological datasets

How could these variations, documented by researchers across broad swathes of Earth's history and surface, be captured, pooled, compared, and used to advance our understanding of the Precambrian Earth? Paleontologists and geochemists have made informed use of databases to carry out paleontological and biogeochemical studies of the Precambrian Earth, documenting changes through time in both life (e.g., Knoll et al., 2016; Knoll et al., 2006; Butterfield, 1995, 2009; Cohen and Macdonald, 2015; Schopf and Klein, 1992) and environments (e.g., Lyons et al., 2014; Canfield, 2004; Wei et al., 2018; Sperling et al., 2015; Reinhard et al., 2013). Earlier efforts to harness the power and possibility of large sedimentological datasets have also met with promising success.

Alexander Ronov, a pioneering Soviet geologist who generated global volumetric analyses of sedimentary rocks through time (Ronov, 1968, 1982, 1985; Ronov et al., 1980, 1981, 1982), was among the first to explore the possibilities of these datasets. Ronov's work indicated a tectonically-driven cyclicity in the volume of sedimentary deposits, suggesting relationships among volcanic outgassing, carbonate volume, and the chemistry of seawater and sedimentary rocks. More recently, a group led by Shanan Peters at the University of Wisconsin has built *Macrostrat*, a database that integrates much of the published stratigraphic literature into a searchable, quantitative record of sedimentary rocks at the formation scale in North America and elsewhere, first described in Peters (2006). *Macrostrat* has enabled the quantitative testing of hypotheses about causal linkages in Earth history, including the relationships among sea level, erosion, and biodiversity (Hannisdal and Peters, 2011; Peters and Gaines, 2012), and the rise of atmospheric oxygen as mediated by sedimentary storage of organic carbon (Husson and Peters, 2017; Peters and Husson, 2017). By developing a tool, *GeoDeepDive*, to harvest "dark data" in literature, this group has also explored primary controls on the temporal distribution of stromatolites (Peters et al., 2017).

A third approach focused on analysis of various specific sedimentary facies through time has also yielded useful results. Flat-pebble conglomerates and hardgrounds are two carbonate features both formed by the early cementation and lithification of marine sediments. Analysis of their temporal distribution in early Phanerozoic carbonate successions suggests feedback between carbonate cementation and biodiversity (Wright and Cherns, 2016). The declining abundance of sole marks (erosional and deformational features preserved at the sole of a bed) throughout the Phanerozoic Eon reflects changes in the rheology of the Phanerozoic seafloor during the expansion of bioturbation (Tarhan, 2018a). Petrographic analysis of the internal textures of temporally diverse Phanerozoic ooids (concentrically coated carbonate grains) provides insight into the ratio of Ca and Mg in seawater through time (Pigott, 1981; Mackenzie and Pigott, 1982; Hardie, 2003). These works demonstrate the explanatory potential of large sedimentological datasets focused on one or a few features in developing and testing hypotheses about the co-evolution of Earth and life. Large sedimentological datasets that track a wider range of features and structures while tracking their co-occurrence may provide additional insights.

1.4. Challenges of working with sedimentological data

These attempts to tabulate and quantify the sedimentological record have succeeded despite the variable practices of data reporting among sedimentologists and stratigraphers. Sedimentological data, typically recorded as a part of stratigraphic columns, are more idiosyncratic and difficult to compare than either quantitative geochemical data or the paleontological presence or absence of a genus or species. Comparing results across workers or field areas magnifies this difficulty. Integrating sedimentological data—and analyzing it in a meaningful way—is no small task. However, the potential power of a dataset that integrates fine-scale stratigraphic and sedimentological observations across globally and temporally distributed formations provides a tantalizing reward.

Here, we present the first version of *Microstrat*, a global, high-resolution, sedimentological database with a current focus on Archean through Cambrian carbonate strata. We describe these carbonate rocks, layer by layer, at the finest scale possible by drawing from available sources, primarily published literature and theses. We quantify the thickness, sedimentological character, and depositional environment of > 75 kilometers of stratigraphic sections that range from shallowest (subaerial to peritidal environments, or above fair-weather wave base) to shallow (above storm wave base) to deep water (below storm wave base), including more than 47 kilometers of carbonate stratigraphy, of which 46,452 meters are marine (the ~28 kilometers of stratigraphy with non-carbonate lithologies are not included in analyses here). The median thickness of a carbonate layer within the database is 0.8 m. The high resolution of this dataset, and its focus on capturing the details of all beds recorded within a stratigraphic column, allows us to test hypotheses regarding the spatial and environmental relationships among facies. Integration over time further enables quantitative tests of hypotheses concerning patterns of facies variation in pre-skeletal carbonate rocks.

We first test the results of our dataset to see if it replicates previous observations about the Precambrian carbonate record. This offers an initial test of our methods constructing and analyzing the database. We then identify and explore relationships between several carbonate structures, textures, and features and their depositional environment, and temporal distribution. *Microstrat* offers a dataset that can be used to generate, develop, and test old and new hypotheses about the nature of the carbonate record. In particular, we examine the influence of changing redox conditions and animal evolution on the nature of carbonate deposits through time.

2. Methods

2.1. Building the current database

To build this first iteration of a Precambrian to Cambrian carbonate database, we compiled sedimentological data from stratigraphic columns. We prioritize stratigraphy from long-lived, spatially expansive platforms in environments where carbonate precipitation occurred (rather than in some downslope environments where reworked carbonate material may have accumulated but was not generated). Both purely carbonate and mixed siliciclastic-carbonate systems are included, though only the carbonate components of mixed systems—beds or layers which have a dominant carbonate lithology as indicated by the primary authors—are included in the analyses here. Where multiple columns by different authors were available for a formation, we preferred columns that recorded stratigraphy at the finest scale, and selected columns that sampled across depositional environments. Not surprisingly, more recent time intervals boast many more preserved platforms and formations than older intervals. In older cases, we endeavored to tabulate the majority of known formations and platforms; in younger cases with much more abundant stratigraphic information, we aimed to sample broadly to assemble a globally and

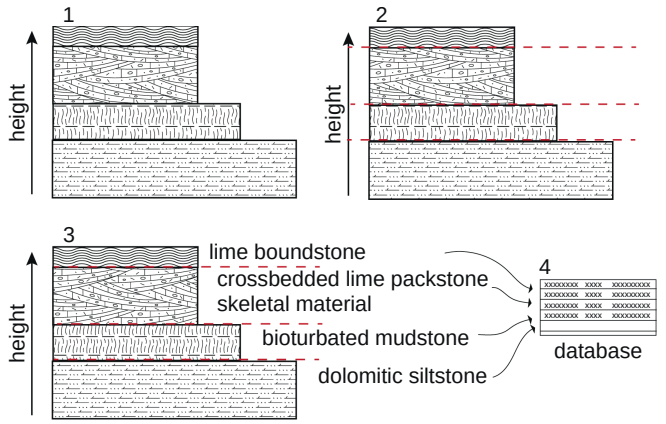

Fig. 1. Workflow for incorporating stratigraphy into *Microstrat*. 1) A stratigraphic column is identified; to date, stratigraphy has come mostly from theses appendices and published literature, with some from unpublished field notes or government agency reports. 2) The stratigraphic column is divided at the finest resolution possible. 3) Intervals are tagged with a range of identifiers. 4) Each interval is represented as an entry in the database.

environmentally diverse sample. Though we include early Archean formations in the database, they are not included in most analyses shown here because the record is so limited: only 107 total vertical meters of carbonate stratigraphy from the Strelley Pool Chert (Allwood et al., 2006, 2007) and the Buck Reef Chert (Tice, 2005).

Fig. 1 describes our methodology for incorporating stratigraphy into our database. After identifying and selecting stratigraphic columns from the literature, we divided columns into the finest layers made possible by the resolution of the observations recorded within the columns. We then tagged each layer with a range of characteristics, including mineralogy, Dunham classification, sedimentary structures, and depositional environment; the full list of tracked features is given in Table 1. Primary authors present specific interpretations of depositional environment, which we use to assign each bed to broad depositional environment categories, including the deep subtidal (all environments below storm wave base); shallow subtidal environments (environments between storm and fair-weather wave base); and shallowest marine environments (environments above fair-weather wave base, including tidal and peritidal environments). Other categories include terrestrial, lacustrine, and fluvial environments, but intervals from these depositional environments are excluded from the analyses presented here as they represent less than one kilometer of total stratigraphy in *Microstrat*. Environmental assignments are based on the interpretation of the primary author(s), facies association information, and other published works in ambiguous or disputed cases.

Age constraints on our data are in some cases quite broad, with the depositional ages of several formations only constrained by the age of underlying basement and intruding dikes. We expect that geochronologists will continue to identify and refine depositional ages for many of these formations and anticipate that better-resolved age models for these strata will enhance the utility of the database. At present, we assign a coarse age interval (Early Archean, Late Archean, Paleoproterozoic, Mesoproterozoic, Tonian, Cryogenian, Ediacaran, Early Cambrian, Middle Cambrian, Late Cambrian) to each layer using ages from published literature. While not shown in the analyses here, *Microstrat* also includes numerical age constraints (minimum age, maximum age, and "best" or preferred age) within its structure; this provides opportunities for further refinement and analyses of higher-resolution time bins.

In this study, we identify changes in the carbonate record across these fairly coarse age and environmental divisions. This allows us to test the accuracy of the database using known and long-described patterns. *Microstrat* currently spans 170 stratigraphic columns representing 166 formations and > 60 platforms from early Archean to late Cambrian time. Throughout this paper, we consider only marine carbonate intervals from the database: this results in a record of 143 formations and 46,452 total meters of stratigraphy. The spatial and temporal coverage of the marine carbonate strata in our database is shown in Fig. 2. Table 2 shows the total thickness (which includes interbedded intervals with a dominant non-carbonate lithology) and the carbonate thickness of all formations included in the database. Some of the formations included in the database are short siliciclastic formations interbedded with carbonate-bearing formations; they are recorded in the database to preserve stratigraphic relationships, but they do not contribute to our analysis of carbonate strata and their total carbonate thickness in Table 2 is given as 0.

The median thickness of a marine carbonate layer in the database is 0.8 m; the thinnest layer is 0.002 m and the thickest is 547 meters thick. The thickness of a layer within *Microstrat* corresponds with the resolution of the stratigraphic column from which the layer originates. It does not necessarily have a relationship to bed or bedset thickness. Median layer thickness should be interpreted only as an indicator to the relative resolution of the parent stratigraphic column. Layer thickness varies between different stratigraphic columns because authors publish stratigraphic columns at a range of resolutions. Some of the analyses presented in this paper rely on measurements of thickness and are therefore influenced by the resolution of stratigraphic columns. We include average layer thickness for each formation in Table 2 so readers can identify which formations are recorded at relatively fine or coarse resolution.

Throughout our analyses, we use the Dunham classification (Dunham, 1962) to describe the grain size and texture of carbonate rocks. We also include additions to the Dunham schema made by Embry and Klovan (1971) (e.g., rudstone).We use this system because it prioritizes sedimentological information relevant for the interpretation of depositional environments. However, the Dunham classification system was developed to describe Phanerozoic carbonate sediments, which are often texturally distinct from their Precambrian antecedents. Phanerozoic carbonate rocks often contain volumetrically abundant skeletal material or evidence of bioturbation; by contrast, Precambrian carbonate strata largely lack these features and host others, such as seafloor crystal fans or molar tooth structures, which are rare or absent in the Phanerozoic record. For this reason, we have added additional categories (e.g., macroprecipitate) to the traditional Dunham schema (Table 1) to more fully describe the textures of Precambrian carbonates. The Dunham classifications of "packstones" and "wackestones," which refer to carbonate rocks made of a mixture of mud and grains, deserve special consideration when applied to Precambrian carbonate rocks. Grains, granules, and clasts in Phanerozoic carbonates are often skeletal in origin. In the Precambrian record, they may be cement, coated grains, or ripped-up and resedimented carbonate material.

2.2. Metrics used and the limits of interpretation

The analyses presented here focus primarily on the abundance and temporal and environmental distribution of carbonate structures, textures, and features across the preserved record. Designing meaningful metrics to discuss the abundance and distribution of carbonate features is not straightforward and is complicated not only by the preservation of the rock record but also our limited understanding of the sedimentology of Precambrian carbonate facies. The absence of animal fossils and the presence of carbonate facies very different from modern facies make it challenging to interpret the origin of Precambrian carbonates. Additionally, interpretations of Precambrian carbonate successions rely on far fewer examples than Phanerozoic or modern studies. A specific example of how the serendipity of the record affects our dataset is that late Archean deep-water carbonate rocks are mostly represented by the Agouron GKP01 core from South Africa, diminishing confidence in the global interpretation of these carbonate strata (see

Table 1
Features tracked within the database.

Category	Descriptor	Notes
Platform geometry		
	Rimmed shelf	
	Ramp	
	Unknown	
Tectonic setting		
	Passive margin	
	Plume-related	E.g., greenstone belt-related carbonates
	Continental arc	
	Rift basin	
	Fault-controlled basin	
	Intracratonic basin	
	Unknown	
Region		
	Australia	
	North America	
	South America	
	Russia	
	Asia	
	Africa	
	Europe	
	India	
Time period		
	Early Archean	4000-3200 Ma
	Late Archean	3200-2500 Ma
	Paleoproterozoic	2500-1600 Ma
	Mesoproterozoic	1600-1000 Ma
	Tonian	1000-717 Ma
	Cryogenian	717-635 Ma
	Ediacaran	635-539 Ma
	Early Cambrian	539-509 Ma
	Middle Cambrian	509-497 Ma
	Late Cambrian	497-485 Ma
Dominant lithology		
	Carbonate	
	Siliciclastic	
	Volcanic	
	Chert	
	Iron formation	
	Paleosol	
	Talc	
	Covered interval	Interval is not exposed
	Unknown	Lithology not described
Grain size		
	Mud	Silt to clay-sized particles (< 125 microns)
	Sand	Sand sized particles (> 125 microns - < 250 microns)
	Heterogenous (not further specified)	Heterogenous grain size
	Heterogenous (small)	Grains include sand-sized particles and smaller
	Heterogenous (large)	Grains are heterogenous in size, and include some clasts larger than sand (> 250 microns)
	Silt	63-125 microns; used for siliciclastic intervals
	Crystalline	Interval has a crystalline or sparry fabric in which the component grain size cannot be determined or is not relevant
	Unknown	
Carbonate lithology		
	Limestone	Primarily or entirely calcite, $CaCO_3$
	Dolomite	Primarily or entirely dolomite, $CaMg(CO_3)_2$
	Not relevant	
	Magnesian carbonate	Primarily or entirely $MgCO_3$
Bedding and lamination		
	Cross-stratified	Layering at an angle to the bedding plane, formed by deposition of grains on the inclined surfaces of bedforms
	Heterolithic bedding	May range from flaser to lenticular bedding
	Massive or no bedding	Massively bedded or with no bedding
	Wavy, crinkly or tufted; microbial influence	Laminations reflect microbial influence
	Planar lamination	Flat-lying laminations
	Isopachous lamination	Very fine, isopachous laminae associated with stromatolites
	Contorted	Disrupted by soft sediment deformation or slumping
	Bioturbated	Disrupted by burrowing
	Wavy laminated	No microbial influence necessarily implied

(*continued on next page*)

Table 1 (*continued*)

Category	Descriptor	Notes
Modified Dunham classification		
	mudstone	Composed of carbonate mud particles < 125 microns (silt and clay-sized particles)
	pack- or wackestone	Mixture of mud- and grain-sized particles
	grainstone	Composed of grains with no mud
	boundstone	Carbonate rock originally bound by encrusting or reef-building organisms; within this study, typically microbial
	rudstone	Carbonate rock containing clasts > 2mm in size
	macroprecipitate	Formed by in situ precipitation of calcium carbonate at the sediment-water interface (e.g., seafloor precipitate textures, crystal fans)
	primary texture not preserved	No primary texture can be discerned
Microbial features		
	Microbial lamination	Flat microbial laminations
	Low domal stromatolites	Small stromatolites with relatively low synoptic relief.
	Columnar and/or branching stromatolites	Used very broadly here to refer to any type of stromatolite with a columnar and/or branching habit. Synoptic relief may be small or large.
	Conical stromatolites	Stromatolite with conical morphology, e.g., *Conophyton*
	Thrombolites	Microbial carbonate dominated by clotted internal texture
	Giant stromatolites	Very large (meters tall) stromatolites; size of individual stromatolites not always clear from stratigraphic column, so this designation is likely less frequently used in the database than it could be, and very large stromatolites may be tagged with other features
	Cuspate/fenestrate stromatolites	Microbial fabric characterized by horizontal microbial elements drape vertical growth structures, resulting in a tented morphology.
	Oncoids	Coated grain formed by the microbial trapping and binding of sediment around a nucleus
	Roll-up structures	Disrupted microbial laminae
	Microdigitate stromatolites	Stromatolite with small, closely spaced columns; dominated by
Sedimentary structures and miscellaneous		
Coated grains, cements, and associated features		
	Ooids	Concentrically coated carbonate grains
	Peloids	Coated carbonate grain
	Pisoid	Refers here to marine pisoids, large (> 2 mm) coated grain, formed in arid peritidal settings. Some references use this term for large coated grains better described as giant ooids; the database uses this terminology.
	Giant ooids	Ooids larger than 2 mm; some sources refer to these as “pisoids”
	Herringbone calcite	Carbonate cement and seafloor precipitate characterized by dark and light crenulated bands; first described by Sumner and Grotzinger, 1996
	Seafloor precipitate	Carbonate precipitated at the seafloor as cements, including seafloor crystal fans, microprecipitate, and herringbone calcite
	Molar tooth structure	Calcite microspar-filled voids and rents within sediments
	Tufa	We are using tufa to describe micritic, dendritic morphologies formed in tidal flats and evaporitic environments (sensu Pope and Grotzinger, 2000); hydrothermal or lacustrine settings not implied.
	Microprecipitate	Cement precipitated near the seafloor with small crystal size.
	Intraclast	Partially lithified and remobilized sediment.
	Edgewise conglomerate	A characteristic texture of some intraclast conglomerates in which intraclasts are imbricated into “rosette” polygons.
	Skeletal material	Grains of skeletal material
Disruption features		
	Tepees	Buckled and broken crusts formed in carbonate sediments when cements exert pressure during growth. Associated with cycles of wetting and drying in peritidal settings. Appear as dish-shaped polygons in planview and as broken, antiformal features in cross section.
	Mudcracks	Formed during the subaerial exposure and drying of (usually siliciclastic) sediments
	Karst or dissolution surfaces	Carbonate fabric created by subaerial exposure and interaction with meteoric fluids
	Diastasis cracks	Cracks generated by differential behavior of sediments during loading; resemble mudcracks, but do not result from drying
	Soft sediment deformation	Disruption of beds prior to lithification
	Bioturbation	Disruption of bedding by burrowing
	Ball and pillow structure	Soft sediment disruption feature in heterogenous, multilayered strata
	Breccia or debris flow	Heterogenous unit with a range of grain sizes, defined broadly
	Turbidite	Sedimentary gravity flow deposit created by turbidity current
Cross stratification		
	Cross stratification	Cross stratification not otherwise specified
	Ripple cross stratification	Cross stratification due to ripple bedforms
	Trough cross stratification	Cross stratification associated with dune migration
	Hummocky cross stratification	Cross stratification associated with formation by storm waves
	Planar tabular cross stratification	Cross stratification formed by migration of straight-crested bedforms
	Dune	Preserved dune
Miscellaneous		
	Glauconite	Authigenic mica mineral associated with low-oxygen conditions
	Hardgrounds	Synsedimentarily cemented seafloor; typically used in Phanerozoic successions
	Nodular texture	Rock texture characterized by packed nodules
	Fenestrae or vugs	“Windows” or small cavities within rocksn
	Evaporite	Mineral precipitated during evaporation of seawater (e.g., halite, anhydrite)
	Tuff	Rock formed by consolidation of volcanic ash
	Stylolites	Surface within rock created by pressure dissolution
	Sulfate minerals	Minerals containing sulfate, e.g., anhydrite, gypsum; associated with evaporitic conditions
	Pyrite	Pyrite noted within unit
	Detrital pyrite	Transported pyrite noted within unit
	Chert or silicification	Presence of chert or silificiation within unit

(*continued on next page*)

Table 1 (*continued*)

Category	Descriptor	Notes
	Significant siliciclastic component in carbonate unit	Carbonate unit contains substantial siliciclastic component
	Significant carbonate component in siliciclastic unit	Siliciclastic unit contains substantial carbonate component
	Iron concretions	Iron concretions present
Siliciclastic lithology		
	Quartz	
	Arkosic	
	Unspecified	

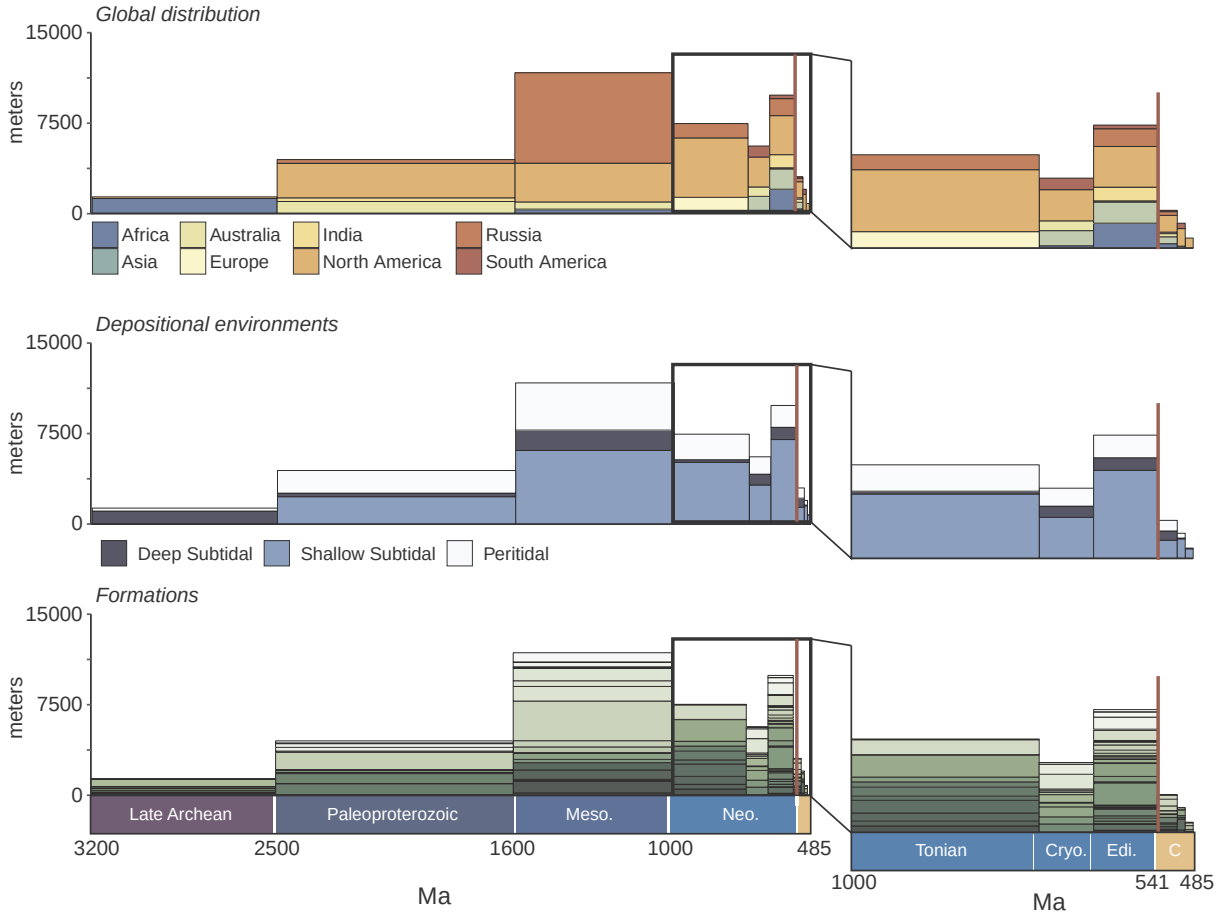

Fig. 2. Spatial and temporal coverage of the database (top); environmental and temporal coverage (middle); and the contribution of individual formations to the database (bottom; each box represents one formation).

Supplementary Figs. S12-S17 for analyses presented without GKP01). In other analyses, we focus on the percent of formations within a time interval that bear a particular feature. Feature occurrence at the formation level through time is a simple way to understand the occurrence of sedimentary structures, as each formation unites a temporally and spatially related set of depositional environments. Because of the resolution of observation typically reported in published sedimentological studies, these formation-level metrics may hold more explanatory power than finer-scale metrics. However, this metric is also sensitive to the total number of formations and the span of each formation within a time interval. The same sedimentary succession with the same set of sedimentary features would give different results using this metric, depending on whether the succession were defined as one thick formation or divided into multiple thinner formations. This bias is a concern when comparing older and younger stratigraphic successions, because thick stratigraphic intervals are usually finely divided into more formations in younger (Neoproterozoic and Phanerozoic) stratigraphy but can be quite coarsely divided in older stratigraphy. These issues are fundamental to ongoing efforts to quantify the sedimentary rock record. We address them by showing trends in our data using a range of metrics, including:

- The percent of formations within a particular interval which display a particular feature.
- The total thickness of beds within an interval which display a particular feature. A single carbonate bed may contain multiple features of the same type; for example, a single bed might contain both low domal stromatolites and microbial laminites, two types of

Table 2
Formations included within the complete database, including their total thickness (including all siliciclastic layers), average layer thickness, total carbonate thickness, and total marine carbonate thickness. Interbedded siliciclastic formations with a total carbonate thickness of zero have been logged and included in the database, but do not contribute to analyses presented herein.

	Time period	Total thickness included in database (m)	Average interval thickness of source (m)	Total carbonate thickness (m)	Total marine carbonate thickness (m)	Citation
Buck Reef Chert	Early Archean	241	16	96	96	Tice, 2005
Strelley Pool Chert	Early Archean	23	2	11	11	Allwood et al., 2007, 2006
Ball Assemblage of Red Lake Greenstone Belt	Late Archean	110	1	83	83	McIntyre and Fralick, 2017
Boomplaas	Late Archean	95	47	95	95	Knoll and Beukes, 2009
Cheshire	Late Archean	111	0	63	63	Hofmann et al., 2004
Chobeni Fm	Late Archean	45	0	26	26	Siahi et al., 2017
Frisco	Late Archean	191	1	138	138	Saylor, 1996
Gamohaan	Late Archean	202	1	174	174	Saylor, 1996
Klein Naute	Late Archean	53	27	18	18	Saylor, 1996
Klein Naute, Kuruman	Late Archean	99	99	0	0	Saylor, 1996
Lokammona	Late Archean	40	20	25	25	Knoll and Beukes, 2009
Monteville	Late Archean	102	51	102	102	Knoll and Beukes, 2009
Nauga	Late Archean	623	19	586	586	Saylor, 1996
Tumbiana Fm	Late Archean	95	2	31	0	Coffey et al., 2013
Vryburg	Late Archean	118	29	0	0	Knoll and Beukes, 2009
Wallace Lake Assemblage of the Wallace Lake Greenstone Belt	Late Archean	110	18	54	54	McIntyre and Fralick, 2017
Beechey	Paleoproterozoic	36	6	11	11	Grotzinger et al., 1987
Blanchet	Paleoproterozoic	212	16	42	42	Hoffman, 1968
Denault Fm	Paleoproterozoic	1016	7	935	898	Zentmyer et al., 2011
Douglas Peninsula	Paleoproterozoic	18	6	18	18	Hoffman, 1968
Duck Creek Dolomite	Paleoproterozoic	966	42	816	816	Wilson et al., 2010
Hearne Fm	Paleoproterozoic	91	15	91	91	Hoffman, 1968
McLean	Paleoproterozoic	96	32	0	0	Hoffman, 1968
Pekanatui Point	Paleoproterozoic	104	8	80	80	Hoffman, 1968
Rocknest Fm	Paleoproterozoic	1564	3	1410	1410	Grotzinger, 1985
Stark Fm	Paleoproterozoic	256	37	108	108	Hoffman, 1968
Taltheilei Fm	Paleoproterozoic	119	1	119	0	Hoffman, 1968
Tulomozero Fm	Paleoproterozoic	413	2	323	306	Melezhik et al., 2013
Utsingi Fm	Paleoproterozoic	64	7	52	0	Hoffman, 1968
Vempalle Fm	Paleoproterozoic	313	3	306	306	Chakrabarti et al., 2014
Wildbread Fm	Paleoproterozoic	60	5	59	59	Hoffman, 1968
Wooly Dolomite	Paleoproterozoic	267	2	167	167	Krapez et al., 2015
Allamoore Fm	Mesoproterozoic	334	2	196	196	Unpublished field notes, K.D. Bergmann
Angmaat Fm	Mesoproterozoic	1210	3	970	970	Kah, 1997; Turner, 2009
Aouinet Ould Bou Derbala	Mesoproterozoic	63	2	46	46	Kah et al., 2012
Aouinet Ould Bou Derbala Fm Unit I-9	Mesoproterozoic	64	2	43	43	Kah et al., 2012
Atar Fm	Mesoproterozoic	128	7	101	101	Kah et al., 2012
Atar Fm (Unit I-5)	Mesoproterozoic	128	6	104	104	Kah et al., 2012
Avzyan Fm	Mesoproterozoic	1125	31	769	769	Bartley et al., 2007
Bangemall Group	Mesoproterozoic	2569	143	601	601	Buick et al., 1995
Iqqittuq Fm	Mesoproterozoic	403	5	267	267	Kah, 1997; Turner, 2009
Kazput Fm	Mesoproterozoic	172	2	159	159	Martindale et al., 2015
Kotuikan Fm	Mesoproterozoic	554	25	528	528	Sergeev et al., 1995
Ksar Torchane	Mesoproterozoic	20	2	10	10	Kah et al., 2012
Ksar Torchane (Unit I-4)	Mesoproterozoic	20	2	9	9	Kah et al., 2012
Mukun Fm	Mesoproterozoic	5	5	0	0	Sergeev et al., 1995
Oued Tarioufet	Mesoproterozoic	94	5	30	30	Kah et al., 2012
Oued Tarioufet (Unit I-6)	Mesoproterozoic	89	6	24	24	Kah et al., 2012
Pass Mountain Fm	Mesoproterozoic	509	9	465	465	Medig et al., 2016
Rubble Creek Fm	Mesoproterozoic	591	17	513	513	Medig et al., 2016
Satka Fm	Mesoproterozoic	4810	107	3259	3259	Semikhatov et al., 2009
Sukhaya Tunguska Fm	Mesoproterozoic	1230	51	1201	1201	Sergeev et al., 1997
Sulky Fm	Mesoproterozoic	497	7	468	468	Kearns, 1982; Kah et al., 2006
Suran Fm	Mesoproterozoic	2566	151	1015	1015	Petrov and Semikhatov, 2009
Tawaz	Mesoproterozoic	67	4	67	67	Kah et al., 2012
Tawaz Fm (Unit I-7)	Mesoproterozoic	73	3	73	73	Kah et al., 2012
Touiderguilt	Mesoproterozoic	44	9	42	42	Kah et al., 2012
Ust'-ll'ya Fm	Mesoproterozoic	146	3	18	18	Sergeev et al., 1995
Wallace Fm	Mesoproterozoic	1894	0	357	357	Grotzinger, 1981
Wumishan Fm	Mesoproterozoic	43	1	43	43	Tang et al., 2013; Dongjie et al., 2013; Tang et al., 2014

(*continued on next page*)

Table 2 (*continued*)

	Time period	Total thickness included in database (m)	Average interval thickness of source (m)	Total carbonate thickness (m)	Total marine carbonate thickness (m)	Citation
Yusmatakh Fm	Mesoproterozoic	798	80	756	756	Sergeev et al., 1995
Andree Land Group	Tonian	996	24	667	667	Klaebe et al., 2018
Backlundtoppen Fm	Tonian	412	1	392	392	Fairchild et al., 1991
Beck Springs Dolomite	Tonian	687	7	652	652	Harwood, 2013
Boot Inlet Fm	Tonian	1063	89	1015	1015	Jones et al., 2010
Callison Lake	Tonian	412	5	337	337	Strauss, 2015
Coppercap Fm	Tonian	788	14	724	724	Aitken et al., 2019
Draken Fm	Tonian	472	4	417	417	Fairchild et al., 1991
Fort Collins Fm	Tonian	185	93	0	0	Jones et al., 2010
Grassy Point Fm	Tonian	240	240	0	0	Jones et al., 2010
Killian Fm	Tonian	474	3	391	391	Rainbird, 1991
Little Dal Group	Tonian	2302	9	1784	1784	Turner, 1999; Aitken, 1988
Natkusiak	Tonian	36	7	14	14	Rainbird, 1991
Redstone River Fm	Tonian	2	2	2	2	Aitken et al., 2019
Shorikha Fm	Tonian	1217	18	1196	1196	Petrov and Semikhatov, 2009
Thundercloud Fm	Tonian	28	2	28	28	Aitken et al., 2019
Tindir Group	Tonian	2423	22	804	804	Young, 1982
Wynniat	Tonian	16	3	16	16	Rainbird, 1991
Altungol Fm	Cryogenian	642	20	28	28	Xiao et al., 2004
Bayisi Fm	Cryogenian	347	19	0	0	Xiao et al., 2004
Elatina Fm	Cryogenian	134	5	0	0	Rose, 2012
Enorama Fm	Cryogenian	188	47	0	0	Rose, 2012
Etina Fm	Cryogenian	1212	4	643	643	Rose, 2012
Khongor Fm	Cryogenian	18	18	0	0	Bold et al., 2016
Lapa Fm	Cryogenian	960	120	803	803	Azmy et al., 2006
Macho Fm	Cryogenian	575	96	310	310	Stewart et al., 2002
Mina el Mezquite Fm	Cryogenian	297	50	134	54	Stewart et al., 2002
Monteso Fm	Cryogenian	885	38	700	619	Stewart et al., 2002
Ombaatjie Fm	Cryogenian	193	6	193	193	Hoffman et al., 1999
Sete Lagoas Fm	Cryogenian	122	4	122	122	Babinski et al., 2007
Sierra Chiltepin Fm	Cryogenian	1092	38	134	134	Stewart, 1970
Taishir Fm	Cryogenian	1349	13	1184	1184	Bold et al., 2016
Terekeen Fm	Cryogenian	2353	107	1	1	Xiao et al., 2004
Trezona Fm	Cryogenian	442	3	138	138	Rose, 2012
Yaltipena Fm	Cryogenian	78	6	2	2	Rose, 2012
Zhaobishan Fm	Cryogenian	381	13	0	0	Xiao et al., 2004
Katakturuk Dolomite	Cryogenian, Ediacaran	2479	23	2479	2349	Clough and Goldhammer, 2000
Ara Group	Ediacaran	49	< 1	45	44	Bergmann, 2013
Buah Fm	Ediacaran	637	1	489	471	Bergmann, 2013
Cerradinho	Ediacaran	55	9	0	0	Gaucher, 2000
Clemente Fm	Ediacaran	145	29	2	2	Stewart et al., 2002
Dengying Fm	Ediacaran	61	4	61	61	Jiang et al., 2007
Doushantuo Fm	Ediacaran	356	2	207	207	Jiang et al., 2007
El Arpa and Caborica Fms	Ediacaran	399	50	227	227	Stewart et al., 2002
Elandshoek Fm	Ediacaran	189	3	189	189	Hoffman et al., 1999
Ella Bay Fm	Ediacaran	685	20	526	526	Dewing et al., 2004
Gamuz and Papaiote Fms	Ediacaran	159	32	113	113	Stewart et al., 2002
Hankalchough Fm	Ediacaran	316	79	4	4	Xiao et al., 2004
Huns Fm	Ediacaran	80	3	51	51	Saylor, 1996
Infra Krol Fm	Ediacaran	162	13	39	39	Jiang et al., 2002, 2003
Johnnie Fm	Ediacaran	600	3	116	116	Summa, 1993
Kaines Fm	Ediacaran	47	5	0	0	Saylor, 1996
Kane Basin Fm	Ediacaran	130	22	18	18	Dewing et al., 2004
Kennedy Channel Fm	Ediacaran	653	18	91	91	Dewing et al., 2004
Khufai Fm	Ediacaran	493	3	432	432	Osburn et al., 2014
Kliphoek Fm	Ediacaran	80	5	0	0	Saylor, 1996
Krol Fm	Ediacaran	1168	38	1080	1055	Jiang et al., 2002
Liuchapo Fm	Ediacaran	41	10	40	40	Jiang et al., 2007
Maieberg Fm	Ediacaran	275	92	275	275	Hoffman et al., 1999
Mara Fm	Ediacaran	37	3	27	27	Saylor, 1996
Mooifontein Fm	Ediacaran	23	2	15	15	Saylor, 1996
Noonday Fm	Ediacaran	237	3	158	158	Creveling et al., 2016
Nuccaleena Fm	Ediacaran	106	4	93	93	Rose, 2012
Ol Fm	Ediacaran	199	12	193	193	Bold et al., 2016
Polanco	Ediacaran	252	6	252	252	Gaucher, 2000
Rawlings Bay Fm	Ediacaran	276	25	0	0	Dewing et al., 2004
Schwarzrand Subgroup	Ediacaran	643	3	414	414	Saylor, 1996
Scorseby Bay Fm	Ediacaran	232	77	232	232	Dewing et al., 2004
Shuiquan Fm	Ediacaran	204	19	47	47	Xiao et al., 2004
Shuram Fm	Ediacaran	516	3	82	82	Bergmann, 2013

(*continued on next page*)

Table 2 (*continued*)

	Time period	Total thickness included in database (m)	Average interval thickness of source (m)	Total carbonate thickness (m)	Total marine carbonate thickness (m)	Citation
Shuurgat Fm	Ediacaran	884	10	836	822	Bold et al., 2016
Staraya Rechka	Ediacaran	43	1	42	31	Vorob'eva and Petrov, 2014
Tamengo	Ediacaran	43	3	41	41	Gaucher, 2000
Tecolote Quartzite	Ediacaran	40	13	0	0	Stewart et al., 2002
Vapol Fm	Ediacaran	967	138	967	967	Vorob'eva et al., 2006
Yerbal Fm	Ediacaran	608	11	0	0	Gaucher, 2000
Yshkemes Fm	Ediacaran	1016	145	422	422	Vorob'eva et al., 2006
Yukkengol Fm	Ediacaran	166	55	0	0	Xiao et al., 2004
Zhamoketi Fm	Ediacaran	855	9	13	13	Xiao et al., 2004
Zuun-Arts Fm	Ediacaran	197	4	170	170	Smith, 2015
Adoudouian Fm, Tifnout Member	Early Cambrian	140	2	133	133	Maloof et al., 2010b
Arthurs Creek Fm	Early Cambrian	211	105	211	211	Creveling et al., 2013
Bueha Fm	Early Cambrian	67	34	8	8	Stewart et al., 2002
Cerro Victoria	Early Cambrian	128	10	106	106	Gaucher, 2000
Dodo Creek Fm	Early Cambrian	522	8	432	432	Strauss, 2015
Hartshill	Early Cambrian	19	1	8	8	Brasier et al., 1978
Lie de Vin Fm	Early Cambrian	407	3	226	226	Maloof et al., 2010b
Manykai Fm	Early Cambrian	88	3	66	66	Kaufman et al., 1996
Pedroche	Early Cambrian	195	3	112	112	Creveling et al., 2014
Platonovskaya Fm	Early Cambrian	321	4	235	235	Bartley et al., 1998
Proveedora Fm	Early Cambrian	40	40	0	0	Stewart et al., 2002
Puerto Blanco Fm	Early Cambrian	325	41	20	20	Stewart et al., 2002
Salaagol Fm	Early Cambrian	514	7	372	372	Smith, 2015
Sewki Fm	Early Cambrian	840	4	547	538	Dilliard, 2006
Shady Dolomite	Early Cambrian	354	6	329	329	Pfeil and Read, 1980
Thorntonia Limestone	Early Cambrian	49	5	43	43	Creveling et al., 2013
Xishanblaq Fm	Early Cambrian	6	6	0	0	Xiao et al., 2004
Bayangol Fm	Early Cambrian, Ediacaran	537	4	304	304	Smith, 2015
Carrara Fm	Early Cambrian, Middle Cambrian	446	2	169	145	Adams, 1993
Arrojos Fm	Middle Cambrian	320	46	192	192	Stewart et al., 2002
Bonanza King	Middle Cambrian	864	1	851	851	Montanez and Osleger, 1993
Cerro Prieto Fm	Middle Cambrian	13	7	5	5	Stewart et al., 2002
Chaomidian	Middle Cambrian	192	1	163	163	Chough et al., 2010
La Laja	Middle Cambrian	485	3	429	429	Gomez and Astini, 2015
Maryville Limestone	Middle Cambrian	210	7	103	103	Srinivasan and Walker, 1993
Tren Fm	Middle Cambrian	120	20	120	120	Stewart et al., 2002
Dunderberg Fm	Late Cambrian	72	3	72	72	Baker, 2008
Emigrant Springs Fm	Late Cambrian	175	7	167	167	Baker, 2008
Orr Fm	Late Cambrian	341	3	303	303	Baker, 2008
Port au Port Group	Late Cambrian	270	1	225	224	Cowan, 1992
Whipple Cave Fm	Late Cambrian	54	7	45	45	Baker, 2008

microbially-influenced carbonate textures tracked in our database. In some of our analyses, we would consider the thickness of such a bed in both the microbial laminite and low domal stromatolite categories. We call this metric "concatenated thickness" throughout the figures associated with this text.

- The total proportional thickness per time interval is shown for features for which each layer is assigned one and only one identifier.
- The pairwise analysis of features.

When trends are consistent across a range of metrics, we place more confidence in them. We augment our observations of trends in the database with observations from field and petrographic studies. Fig. 2 shows the temporal and spatial coverage of the formations included in the database, and Table 2 lists the formations included. In the Supplement, we include a set of analyses identical to the ones presented here, but with the two thickest formations from each time interval removed (Supplementary Figs. S5–S11) to investigate if trends remain robust with the removal of thick formations. We test this because thick formations are often logged at coarse resolution and have the greatest potential to distort thickness metrics within our analysis.

We also track feature co-occurrence using a ratio of observed feature co-occurrence to expected feature co-occurrence, calculated under the assumption that co-occurrence is random. The presence or absence of selected features within each formation is noted, yielding a binary presence/absence table at the formation level. For every pair of features, the total observed number of co-occurrences at the formation level is tallied and compared against the expected number of co-occurrences, if the distribution of each feature is random and independent. The ratio of these two numbers gives insight into how much more or less frequently than expected two features occur together, with ratios much greater than 1 suggesting more frequent co-occurrence than would be expected if feature distribution were random, and ratios much less than 1 indicating significant anti-correlation. This approach is inspired by and uses tools from probabilistic species co-occurrence analysis (Griffith et al., 2016).

A limit of the (expanded) Dunham classification scheme is that it does not always quantitatively describe the grain size of all elements within a sample. While some Dunham classifications, like "mudstone" or "rudstone," do provide grain size information, the classification "boundstone" provides no explicit grain size information. The Dunham classification scheme also provides little information about the composition of grains or clasts within sediments. For example, an interval

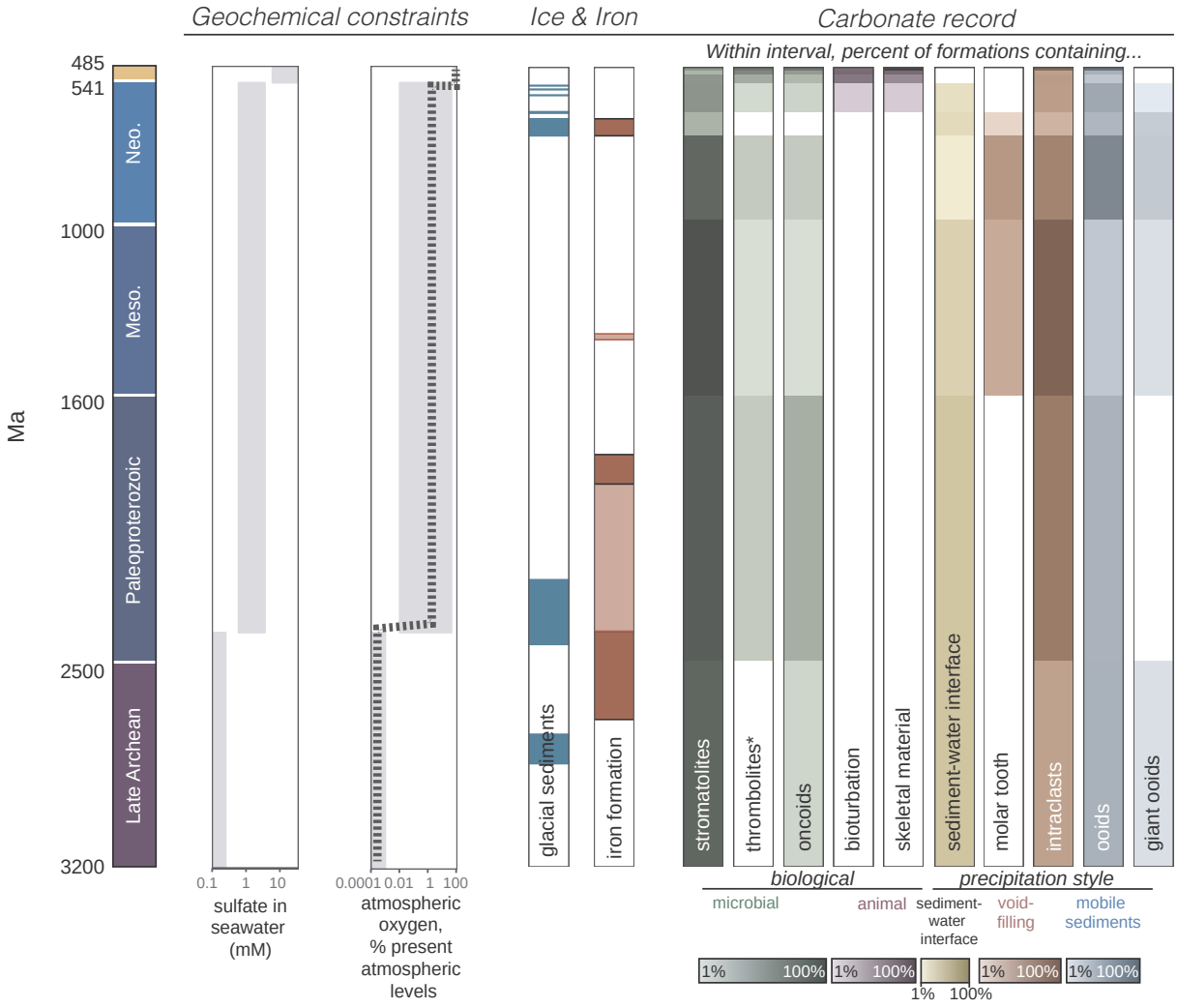

Fig. 3. Geochemical trends over Earth history are shown alongside trends in the carbonate record. The colored strips on the right side are divided into time intervals running from the Late Archean to Late Cambrian. Each interval within a strip is colored according to the percentage of formations within that interval that exhibit a particular feature. The category "sediment-water interface" includes crystal fans, tufas, microdigitate stromatolites, and microprecipitates. We use the term "thrombolite" broadly here to describe any microbially influenced carbonate with a clotted internal texture, without implying uniformity through time in the generation of such fabrics; Cambrian thrombolites are distinct from earlier structures. This figure incorporates additional data from Canfield and Farquhar, 2009; Kump, 2008; Lyons et al., 2014; Posth et al., 2011; Young et al., 2009; Xiao et al., 2004; Campanha et al., 2008; Vernhet et al., 2011; Hoffman, 2013; Hofmann et al., 2014; Rooney et al., 2015; Pu et al., 2016). (For interpretation of the references to color in this figure legend, the reader is referred to the web version of this article.)

with mud intraclasts in a mud matrix would be considered a rudstone, and the fact that all of the components in this material are made of mud will not be represented without added detail. The expanded Dunham classification scheme identifies the grain size of the larger components as the relevant detail for the texture of the unit and does not describe the grain size of the components within clasts. Dunham classifications within *Microstrat* thus underestimate the amount of fine-grained material present in an interval. More broadly, throughout the literature, for both carbonate and siliciclastic intervals, grain size is rarely reported quantitatively and often not reported explicitly. Where it is not been reported, we have interpreted likely grain size classifications, but assert more confidence in the accuracy of expanded Dunham classifications.

Not all intervals of Earth history are equally well represented by carbonate rocks; our record is fragmentary. Tectonic forces and the erosion of continents both modulate the deposition and preservation of carbonate sediments, while primary changes in the carbonate factory itself shape the carbonate sedimentary record (Liu et al., 2017; Peters and Husson, 2017; Husson and Peters, 2018). Some regions of the world (e.g., North America, Australia, Russia) are well-represented in our database relative to others (e.g., South America) because of the scope of available literature and outcrop exposure. To avoid the possibility that the analyses reported here simply reflect preservational biases of the rock record or the biases of particularly fine or coarse resolution within stratigraphic columns, we quantify results in a number of ways, including the true thickness of the rock units; the relative thickness of carbonate rocks of a particular type or age; and the total number of formations that exhibit a particular feature.

Another area of concern in *Microstrat* is the assignment of depositional ages and the representation of change through time. As discussed above, age constraints on many successions are coarse. As radiometric ages are proliferated through Precambrian carbonate successions, and age models are built for these successions, *Microstrat* will be able to resolve changes in these successions through time at finer scale. Because the database currently ends at the late Cambrian Period, it does not capture the mid-Ordovician radiation and reorganization of marine ecosystems or the subsequent changes in marine carbonates, including changes in substrate and the beginning of skeletal material as a

volumetrically significant component of the carbonate record (Droser and Finnegan, 2003; Harper, 2006; Pruss et al., 2010b; Pruss and Clemente, 2011; Mángano et al., 2016; Tarhan, 2018a).

Data presented in this paper have been translated by primary authors from rock to published stratigraphic column, and again to our own database entry. This database integrates and attempts to cast the work of these many scientists into similar, standardized terms, yet must certainly do so imperfectly in some cases; these errors are our own. We believe that the broader temporal and environmental trends described in this work, many of which are consistent with previous hypotheses based on less comprehensive datasets, are robust to translation errors. The broad time intervals used for analysis are expected to smooth imposed errors present in any of the relatively narrow stratigraphic interval any one succession describes. This work would not be possible without the exacting and exhausting field campaigns of several generations of scientists working to understand the Precambrian and Cambrian outcrop and core record; we are indebted to them and grateful for their efforts.

2.3. Building upon the database

The sedimentary rock archive is our best chronicle of Earth's past surface environments, and intense interest in Earth's past and future motivates many investigations into this record. This effort is put forward to demonstrate the power and potential of large physical sedimentological datasets in answering these questions. Yet this effort, though comprising a great deal of stratigraphy, is incomplete and limited. Building a larger and sustainable database at high resolution will require buy-in and commitment from the sedimentological community at large, as well as caretakers who can seek out, perform quality control on, and disseminate the dataset. We take encouragement from other parts of the Earth science community that have built large, community datasets in fields from paleontology to petrology, and look forward to continuing conversations with the community about building, expanding, and developing this record. A template for generating sedimentological data in a format consistent with *Microstrat* is included in the Supplementary Materials to this work; we encourage interested parties to reach out to the corresponding and first authors with questions, comments, and stratigraphic information.

3. Results

In constructing our database, we build on decades of studies of Precambrian and Cambrian carbonate strata. These studies provide not only the raw data for our analyses, but also hypotheses about how the carbonate record has changed. We use these hypotheses as benchmarks for our initial results and data entry methods and as case studies of changes in carbonate stratigraphy through time. Our results highlight a number of changes through time in the nature of carbonate sedimentation (Fig. 3; figure incorporates data from Canfield and Farquhar, 2009; Kump, 2008; Lyons et al., 2014; Posth et al., 2011; Young et al., 2009; Xiao et al., 2004; Campanha et al., 2008; Vernhet et al., 2011; Hoffman, 2013; Hofmann et al., 2014; Rooney et al., 2015; Pu et al., 2016). We also identify, describe, and contextualize several observed patterns. From the global deposition of cap carbonates following Cryogenian glaciations to the longer-term evolution of characteristic features, the carbonate record of our planet is marked by substantial textural variation.

3.1. Time-bound styles of carbonate precipitation

In the modern era, carbonate is predominantly precipitated enzymatically, on and within organic matrices, rather than by either inorganic or microbially influenced precipitation as in Archean and Proterozoic oceans. In addition to enzymatic precipitation during biomineralization, primary carbonate precipitation can occur at the sediment-water interface, within voids or pore space in shallow sediments, on the surfaces of individual coated grains that can be transported (e.g., ooids, peloids), or in the water column. These non-enzymatic modes of carbonate precipitation dominate the Precambrian and even the Cambrian carbonate records (Pruss et al., 2010a; Creveling et al., 2013). Changes in the location and style of carbonate precipitation suggest that, even in the absence of biomineralizing organisms, large-scale reorganizations of the carbonate system occurred through this interval. Here, we describe long-standing observations about the shifts in the balance between these loci through the Precambrian Era and compare their predictions to results from our database. First, we focus on the temporal distribution of crystal fans, molar tooth structures, and giant ooids: three intensely studied carbonate fabrics which are time-bound to some degree.

Crystal fans (Photo Plate 1A) are formed by the precipitation of carbonate at the sediment-water interface to form bladed, upward-growing structures. Crystal fans are often associated with post-Marinoan cap carbonates where they can be spectacularly preserved (Grotzinger and James, 2000; Sumner and Grotzinger, 2000; James et al., 2001; Hoffman and Schrag, 2002; Corsetti et al., 2004; Babinski et al., 2007; Pruss et al., 2008). However, Ediacaran occurrences represent a rare and transient re-establishment of this fabric, which is more frequently observed in Archean and Paleoproterozoic successions (Grotzinger and Read, 1983; Hofmann and Jackson, 1987; Kah and Grotzinger, 1992; Kah and Knoll, 1996; Sumner and Grotzinger, 1996; Grotzinger and James, 2000; Higgins et al., 2009; Bergmann et al., 2013). Seafloor precipitate textures continue into the Meso- and Neoproterozoic, but decrease markedly in size, abundance, and environmental distribution, until expanding again briefly but globally following the Marinoan glaciation, and with rare occurrences thereafter. Taken together, these observations indicate that although the sediment-water interface was a favorable location for carbonate precipitation during the Archean and Paleoproterozoic, carbonate precipitation generally shifted away from this location through time.

Molar tooth structures, calcite microspar ribbons and blobs within crack-like voids in cohesive but unlithified sediments, demonstrate the precipitation of carbonate within the pore or void spaces of shallow sediments (Bishop and Sumner, 2006; Pollock et al., 2006). While molar tooth structures occur in carbonate sediments from the Archean to the Ediacaran, they are most abundant in Mesoproterozoic and Tonian carbonates (James et al., 1998; Grotzinger and James, 2000; Shields, 2002; Bishop and Sumner, 2006; Hodgskiss et al., 2018).

Ooids are concentrically coated carbonate grains. They may be mobile during their growth, transported in bedload or in suspension. Giant ooids (ooids larger than 2 mm in diameter) occur throughout the carbonate record, but are believed to be particularly abundant in Neoproterozoic successions (Zempolich et al., 1988; Knoll and Swett, 1990; Sumner and Grotzinger, 1993). The abundance and size of ooids (some up to 16 mm in diameter; Knoll and Swett, 1990) both increase during the Neoproterozoic Era, when the total thickness of ooid-bearing layers is substantial.

Results from the first version of *Microstrat* are consistent with previous observations regarding these distinctive carbonate textures. Crystal fans are most abundant in Archean and Paleoproterozoic successions and then decline in abundance, re-expanding transiently in post-Marinoan cap carbonates (Fig. 4). Molar tooth structures first appear as minor features of late Archean carbonates, but expand to maximum abundance ($>$ 40 % of all formations) in the Tonian Period after which they are not present within *Microstrat* (two Ediacaran occurrences have been noted but are not represented within the database; Hodgskiss et al., 2018). Ooids and giant ooids are most abundant during the Neoproterozoic Era.

These results from *Microstrat* support observations from previous researchers, showing that this database can replicate previous observations and encouraging a search for additional patterns. For example, we note the changing abundance of intraclasts, reworked clasts

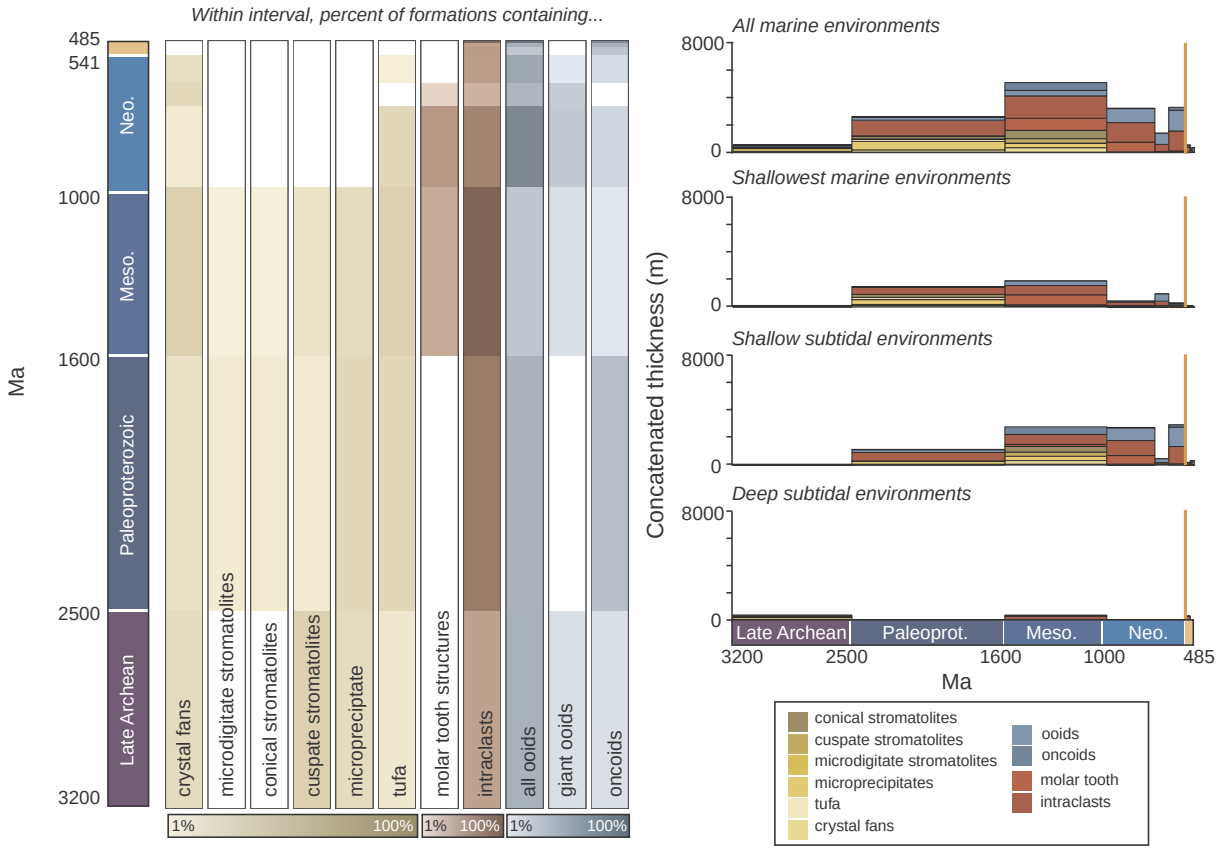

Fig. 4. Trends in the locus of carbonate precipitation through time. Precipitation moves from the sediment-water interface into shallow sediments and mobile sediments as the sediment-water interface becomes oxic. The colored strips on the left side are divided into time intervals running from the Late Archean to Late Cambrian. Each interval within a strip is colored according to the percentage of formations within that interval that exhibit a particular feature. See the text for a discussion of the "concatenated thickness" metric. (For interpretation of the references to color in this figure legend, the reader is referred to the web version of this article.)

of lithified carbonate seafloor, through the Precambrian Era. They are most abundant in the Mesoproterozoic Era, when they occur in more than 80% of all formations within the database—a frequency seen again only in the late Cambrian Period (Fig. 4). We explore the shifts between loci of carbonate precipitation in greater detail and its connection to other changes in the Earth system in the Discussion.

3.2. Secular change in the morphologies and environmental distributions of boundstones

Boundstones are growth structures in which carbonate sediment is trapped and bound as it accretes, in the Precambrian and Cambrian largely represented by stromatolites and thrombolites. The internal and external morphologies and environmental distribution of boundstones vary systematically through Earth history. Previous tabulations, based largely on stromatolite diversity as judged by quasi-Linnean binomial nomenclature (Walter and Heys, 1985; Semikhatov and Raaben, 1996), note that dominant stromatolite morphologies change through time. For example, conical stromatolites show distinct temporal variation, peaking in the Mesoproterozoic Era (Walter and Heys, 1985). Semikhatov and Raaben (1996) noted a Neoproterozoic diversity peak in branching columnar stromatolites. *Microstrat* reproduces these observations (Fig. 5). *Microstrat* also adds numerical heft to some previous observations. For example, although conical stromatolites do reach their greatest abundances during the Mesoproterozoic Era, they do not contribute a great deal of stratigraphic thickness to the Mesoproterozoic carbonate record.

A marked change in both the abundance and character of boundstones across the Proterozoic-Cambrian transition has been long-known (Awramik, 1971; Walter and Heys, 1985; Kennard and James, 1986). Stromatolites and laminites (Plate 5), which are characterized by smooth, crinkly, or pustular internal laminations, declined in favor of internally clotted thrombolites (Plate 3, B). Thrombolites *sensu lato* are not restricted to the Cambrian Period; they also occur in Proterozoic rocks (e.g., Dongjie et al., 2013; Kah and Grotzinger, 1992; Harwood, 2013). Note, however, that we use the term "thrombolite" broadly here to describe any boundstone with a clotted internal texture, without implying uniformity through time in the mechanism of construction of such fabrics. *Microstrat* replicates this transition in the internal character of boundstones (Fig. 5). *Microstrat*'s success in reproducing long-known changes in the morphology and internal textures of boundstones suggests that our methodology in translating these features to the database is successful.

Microstrat further indicates a temporal and spatial co-association of thrombolites and oncoids (Plate 3 B, C), grains formed by microbial growth, trapping and binding of sediment around a nucleus during transport (Peryt, 1983). Like thrombolites, oncoids increase in abundance across the Proterozoic-Cambrian transition, although they first occur in much older rocks (Fig. 5). At the formation scale, thrombolites and oncoids co-occur more frequently than would be expected if their distribution were random and independent (Fig. 9). These observations are consistent with shared processes driving, or at least permitting, the formation of these features.

3.3. Skeletons and bioturbation track the environmental expansion of animals

The dominance of enzymatic precipitation of carbonate minerals

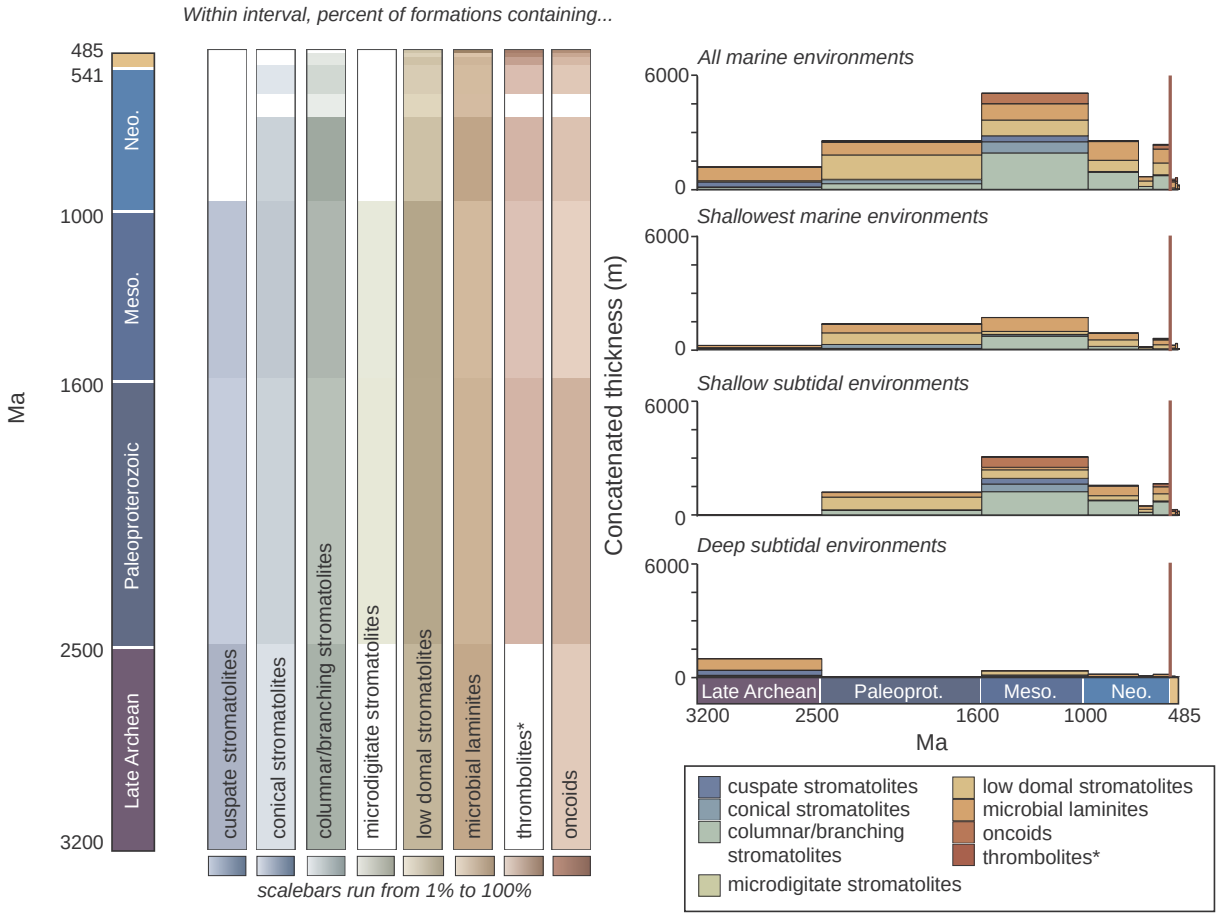

Fig. 5. Trends in the character and abundance of stromatolites, thrombolites, and oncoids. Changes in their abundance and morphology correspond to changes in clastic sediment transport, the locus of carbonate precipitation, and the rise of eukaryotic communities. We use the term "thrombolite" broadly here to describe any microbially influenced carbonate with a clotted internal texture, without implying uniformity through time in the generation of such fabrics; Cambrian thrombolites are distinct from earlier structures. The colored strips on the left side are divided into time intervals running from the Late Archean to Late Cambrian. Each interval within a strip is colored according to the percentage of formations within that interval that exhibit a particular feature. See the text for a discussion of the "concatenated thickness" metric. (For interpretation of the references to color in this figure legend, the reader is referred to the web version of this article.)

began late in the Ediacaran Period with the first appearance of lightly skeletonized animals of uncertain taxonomic affiliation, and it accelerated with the Cambrian diversification of sponges, cnidarians, and bilaterian metazoans (e.g., Knoll, 2003; Maloof et al., 2010a; Wood, 2018; Plate 3). Although all primary mechanisms of skeletonization appeared in the Cambrian Period (Thomas and Reif, 1993), field observations suggest that skeletal material did not become a volumetrically significant component of carbonate sediments until the Ordovician radiation (Pruss et al., 2010b; Creveling et al., 2014). Within our database, skeletal material occurs in no more than 25% of carbonate layers in the Cambrian Period (Fig. 6). Within layers in which skeletal material does occur, it is often a small component by volume, though stratigraphic columns do not always, and *Microstrat* does not currently, track the volumetric contributions of various grain types to individual beds.

Although these components are volumetrically small parts of the Ediacaran and Cambrian rock record, skeletal material and bioturbation track animal activity. Their environmental expansion serves as a proxy for the expansion of animal diversity and habitats. *Microstrat* is consistent (Fig. 6) with other studies which note that both bioturbation and skeletal material appear first in shallow subtidal environments before expanding into shallower and deeper marine environments in the Paleozoic Era (Buatois et al., 2009, 2016; Peters and Gaines, 2012; Tarhan et al., 2015). Predictably, bioturbation and skeletal material also co-occur together at ratios much higher than would be expected if their distribution were random and independent (Fig. 7).

3.4. Environmental and temporal distribution of carbonate mud

The source of carbonate mud has been a topic of active research for decades (Lowenstam and Epstein, 1957; Cloud, 1962; Bathurst, 1972; Neumann and Land, 1975; Shinn et al., 1989; MacIntyre and Reid, 1992; Robbins and Blackwelder, 1992; Milliman, 1993; Milliman et al., 1993; Yates and Robbins, 1998; Morse et al., 2007; Trower et al., 2019). *Microstrat* indicates that carbonate mudstone makes up a substantial component of the preserved Proterozoic record in all time intervals and environments (Fig. 8). Deep subtidal environments experience the most variation in relative mudstone thickness through time.

3.5. Precambrian dolomite is quantitatively and qualitatively different from Phanerozoic dolomite

Today, dolomite (calcium magnesium carbonate, $CaMg(CO_3)_2$) rarely precipitates as a primary chemical sediment from surface waters. The sheer volume of dolomite in the rock record compared with the paucity of modern dolomite, leads to an apparent paradox, the "dolomite problem" (Van Tuyl, 1915; Fairbridge, 1957; Hsu, 1966; Hsu and Siegenthaler, 1969; Given and Wilkinson, 1987; Arvidson and Mackenzie, 1999; Holland and Zimmermann, 2000). Observations of when and where modern dolomite does form—in low oxygen and low sulfate environments, associated with organic material or microbial activity (De Deckker and Last, 1988; Vasconcelos and Mckenzie, 1997; Warthmann et al., 2000; Wright, 2000; Roberts et al., 2013)—led to the

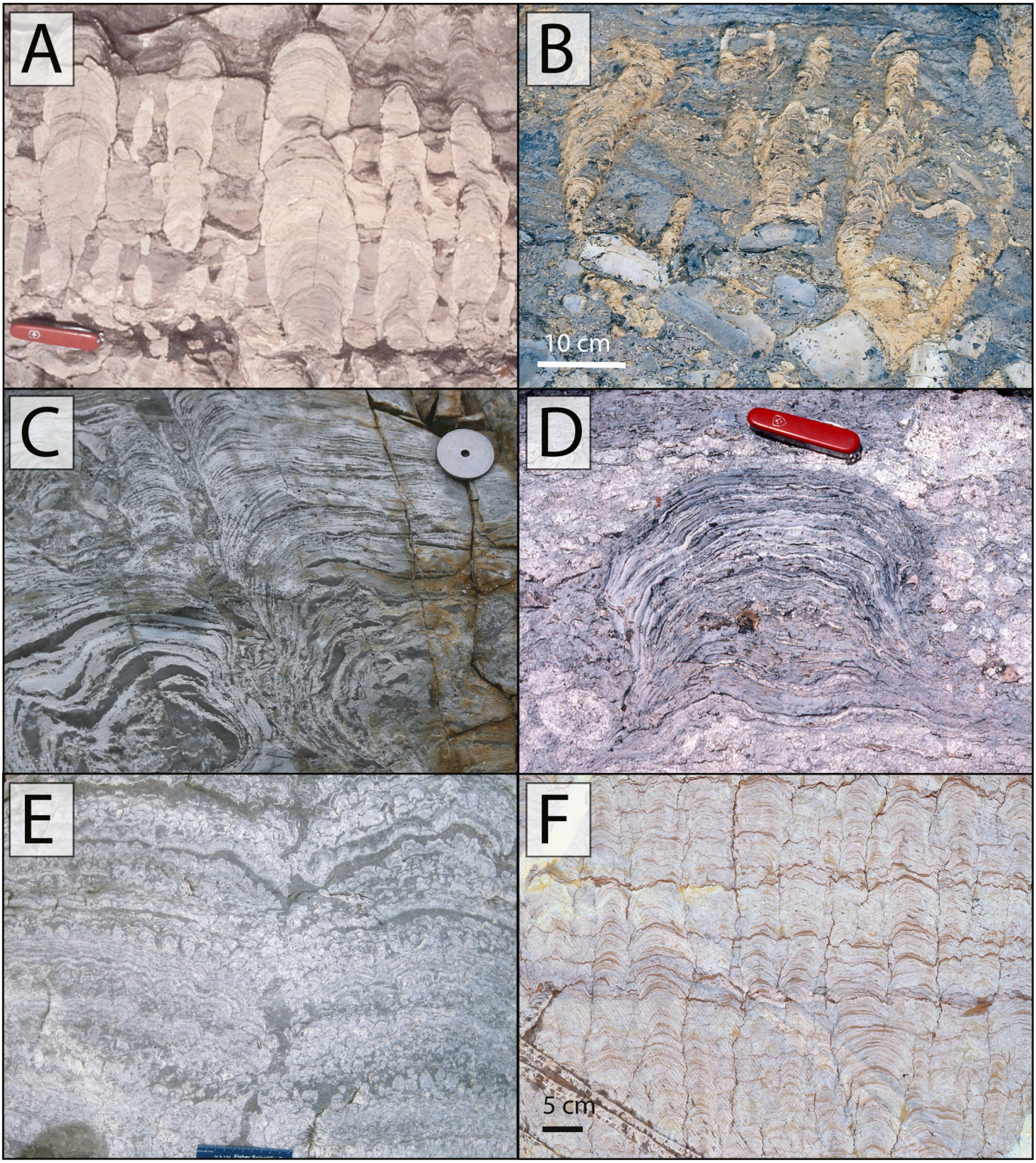

Plate 5. TaB Strom Plate.
pan Fm stromatolites, Siberia. *Photo: A. Knoll*
B Tonian Upper Eleonore Bay Group stromatolites nucleated on cobbles. Greenland. *Photo: A. Knoll*
C Svanberfjellet Fm, Ny Friesland, Svalbard. *Photo: K. Bergmann*
D Domal stromatolite from Tonian Grusdievbreen Fm, Svalbard. *Photo: A. Knoll*
E Cambrian (Furongian) Petite Jardin Fm stromatolites, Port au Port Group, Newfoundland. *Photo: A. Knoll*
F Tonian stromatolites, Inzer Fm., Ural Mountains, Russia. The Inzer Fm is not currently included in the database because sufficiently detailed stratigraphy is not available at time of publication. *Photo: A. Knoll*

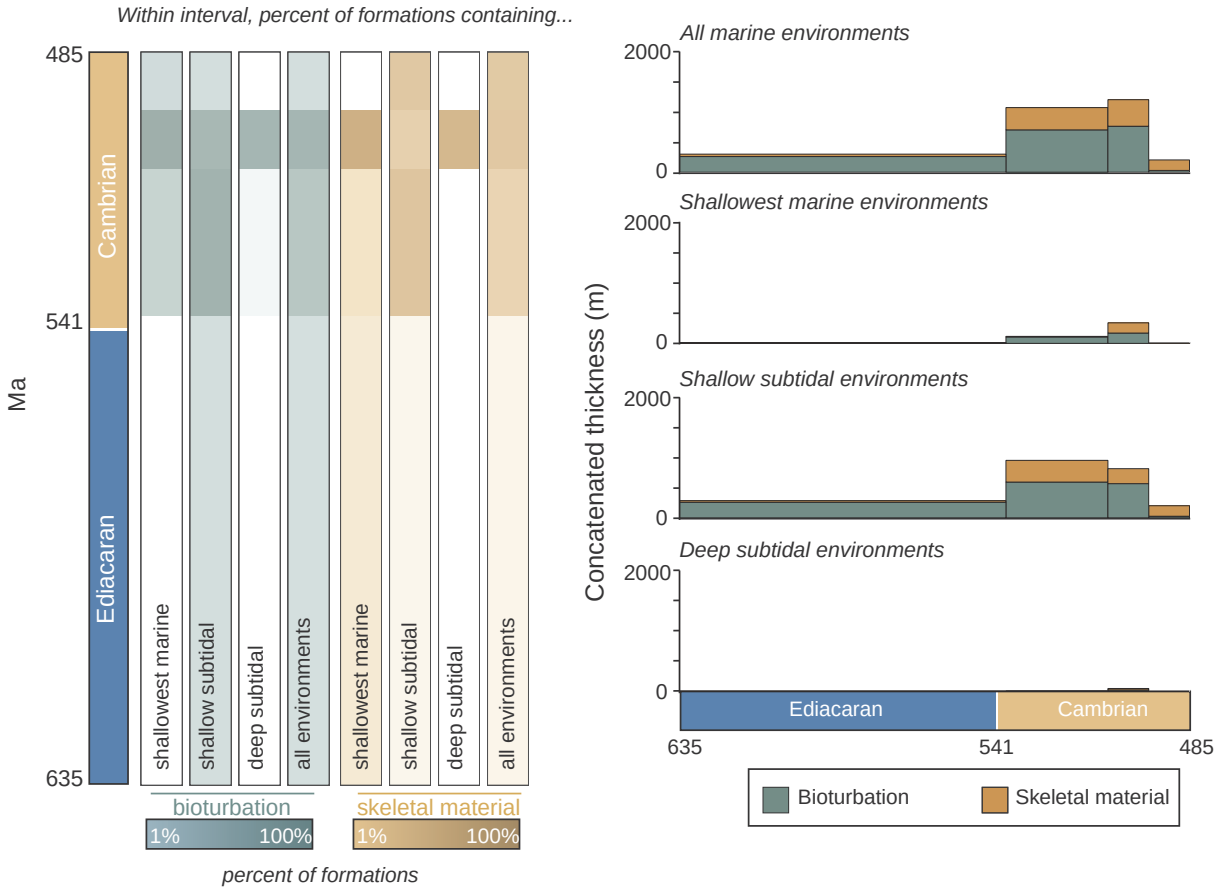

Fig. 6. Trends in the environmental distribution of animals through the Ediacaran Period and into the Cambrian. Consistent with a persistent anoxic deep subtidal zone, evidence for animals first appears in shallow subtidal environments and later appears in a more limited way in deep subtidal environments. The thickness of the bars indicating Ediacaran bioturbation span the entire Ediacaran period, but note that this feature only occurs in late Ediacaran formations. The colored strips on the left side are divided into time intervals running from the Ediacaran to Late Cambrian. Each interval within a strip is colored according to the percentage of formations within that interval that exhibit a particular feature. See the text for a discussion of the "concatenated thickness" metric. (For interpretation of the references to color in this figure legend, the reader is referred to the web version of this article.)

suggestion that substantially different seawater chemistry during the Archean and Proterozoic eons allowed precipitation of dolomite as a primary or early secondary chemical sediment (Fairchild, 1980; Baker and Kastner, 1981; Kastner, 1983; Fairchild et al., 1991; Burns et al., 2000; van Smeerdijk Hood and Wallace, 2018). Supporting this suggestion, many workers have observed that the character of some Precambrian dolomite is distinct from most Phanerozoic counterparts (Plate 6, Fig. 8). Precambrian dolomite can be exquisitely fabric-retentive (also called "mimetic dolomite"), commonly preserving early marine fibrous cements, radial oolitic fabrics, spherulites precipitated in stromatolite laminae, filamentous microfossils, and even fine mudstones with gypsum swallowtails (Plate 6, B, D, E, F); Phanerozoic dolomite, by contrast, often exhibits coarse fabrics characterized by coarse, interlocking, rhombohedral crystals, evidence of dissolution and reprecipitation. (Tucker, 1977, 1982, 1984; Zempolich et al., 1988; Burdett et al., 1990; Knoll and Swett, 1990; Sibley, 1991; Zempolich and Baker, 1993; Knoll and Semikhatov, 1998; Wright, 2000; Corsetti et al., 2006). Our results replicate these textural observations to a limited degree (Fig. S1) although we note that high-resolution, petrographic studies of Precambrian and Phanerozoic dolomite are better suited to describe dolomitic fabric than *Microstrat*, which focuses on larger-scale facies.

Nonetheless, *Microstrat* reproduces observations about the changing temporal distribution of dolomite (Daly, 1909; Ronov, 1968; Holland and Zimmermann, 2000; Warren, 2000) and the concentration of dolomite in shallow-water environments (Fairbridge, 1957; Warren, 2000). Results from *Microstrat* show that both older carbonate successions and carbonate rocks deposited in shallower water contain more dolomite than younger strata or rocks deposited in deeper environments (Fig. 9). The abundance, nature, and environmental distribution of dolomite, however, change most notably across the Proterozoic-Phanerozoic transition. In peritidal environments, more than 90% of Precambrian carbonate strata are dolomitic. Similar abundances persist into the Ediacaran Period, but by the mid-Cambrian, dolomite characterizes only 50% of peritidal carbonate rocks. As skeletal animals came to dominate carbonate precipitation, the probability of carbonate deposition in peritidal environments itself declined (Knoll and Swett, 1990). Dolomite makes up approximately 75% of shallow subtidal carbonate rocks in the Tonian Period and then diminishes to approximately 10% in Cambrian successions. Limestone is relatively abundant (50% of recorded thickness) in deep subtidal facies through most of the Proterozoic Eon, but increases to nearly 100% in the Cambrian Period.

4. Discussion

Several broad and potentially coordinated changes in carbonate sedimentation are evident from *Microstrat*. Some of these changes quantify changes previously proposed, as reviewed above. Seafloor precipitate textures decline through time in size and abundance and become restricted to shallow facies. Intraclasts and molar tooth structures, rare in older strata, reach Mesoproterozoic and Tonian apogees, respectively, before declining. Over the same interval, ooids and

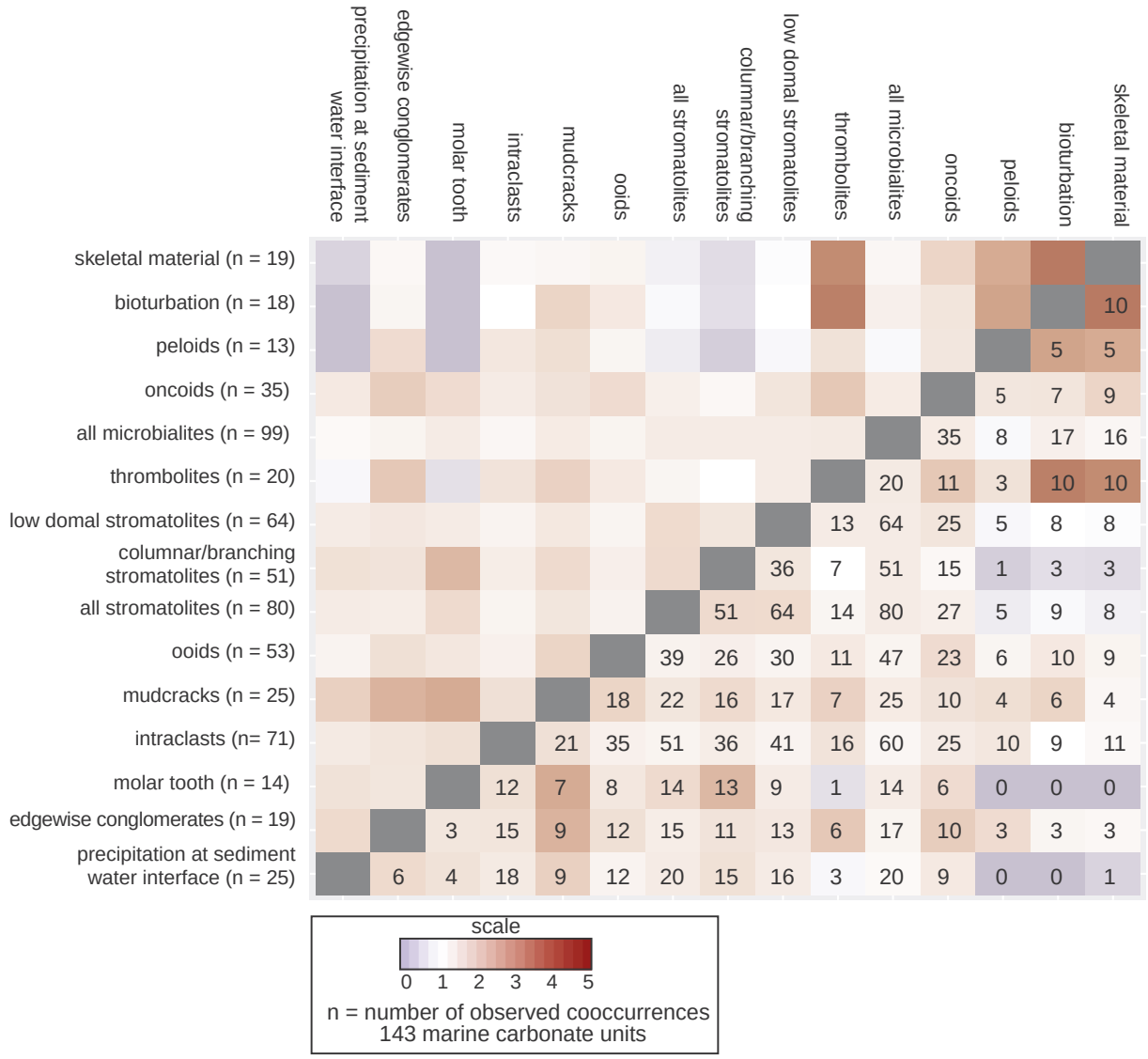

Fig. 7. Relationships between pairs of carbonate features tracked in the database. The presence or absence of each feature within each formation is noted. For every pair of features, the total observed number of co-occurrences at the formation level is tallied and compared against the expected number of co-occurrences, if distribution is random. The ratio of these two numbers gives some insight into how much more or less frequently than expected two features occur together, with ratios much greater than 1 suggesting much more frequent co-occurrence and ratios less than one indicated less frequent co-occurrence.

columnar stromatolites become more prevalent. Dolomite abundance decreases across all environments from Tonian to Cambrian, and its petrologic character changes markedly. Across the Proterozoic-Phanerozoic transition, skeletons and trace fossils, not yet volumetrically significant components of carbonate rocks, begin to appear and thrombolites become the predominant microbialites in shallow subtidal settings. We graphically summarize some of these most important changes in Fig. 10. Here, we consider these observed patterns in relation to potential sources of variation in the ancient carbonate record.

4.1. Changing carbonate textures reflect shifts in microbial communities caused by oxygenation

Determining the high-resolution redox history of Earth's surface—when different environments became oxygenated—is critical to understanding geochemical cycles and the evolution of biological diversity. Aspects of the redox record are difficult to resolve, with post-depositional processes or natural variability within depositional environments complicating proxy geochemical records (e.g., Albut et al., 2018), but the carbonate textural record is more robust to post-depositional overprinting. Previous work has suggested that changes in carbonate textures through time track the saturation of calcium carbonate in seawater and the size of the dissolved inorganic carbon pool in the ocean (Ronov, 1968, 1984; Kempe and Degens, 1985; Grotzinger and Kasting, 1993; Higgins et al., 2009). We suggest that the oxygenation of different environments and, more directly, the replacement of anaerobic heterotrophy with oxygen-dependent metabolisms also impacted carbonate textures through Earth history by changing the timing and shifting between loci of precipitation.

Microbial metabolisms change the carbonate saturation state, Ω, by altering local seawater or porewater chemistry. The stoichiometry of key metabolisms, and their effects on carbonate chemistry, are summarized in Fig. 11, (Bergmann et al., 2013). We hypothesize that shifts in the dominant microbial metabolisms operating within carbonate-precipitating environments, caused by the environmental expansion of oxygenation, are reflected in Precambrian carbonate textures. This makes the carbonate textural record, at least in part, a chronicle of environmental oxygenation.

Anaerobic metabolisms making use of iron reduction and manganese reduction dramatically increase the carbonate ion saturation state,

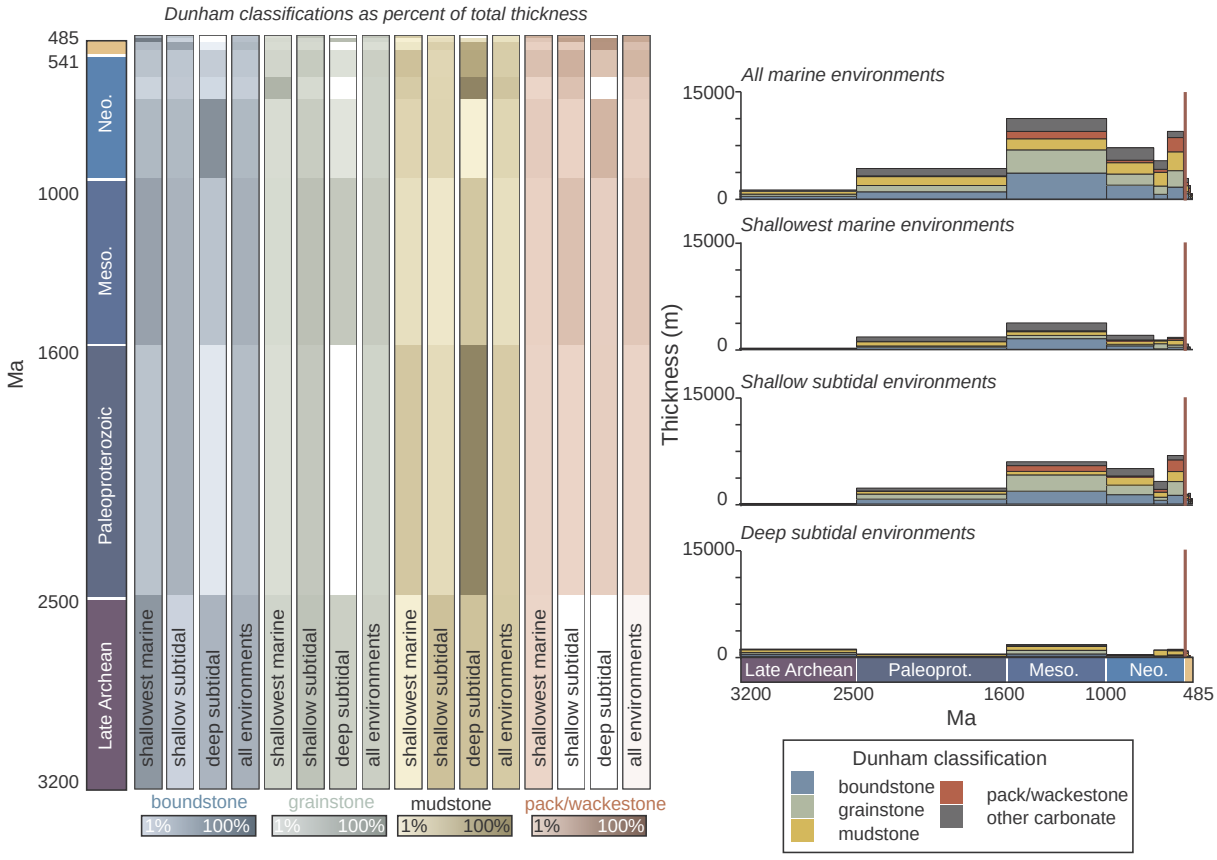

Fig. 8. Trends in the textures of carbonates as described by their Dunham classification. The colored strips on the left side are divided into time intervals running from the Late Archean to Late Cambrian. Each interval within a strip is colored according to the fractional thickness of carbonate stratigraphy within a time interval that is described by a Dunham category—a different metric than similar figures use through this analysis. (For interpretation of the references to color in this figure legend, the reader is referred to the web version of this article.)

Ω, by increasing alkalinity and the concentration of dissolved inorganic carbon (Kuivila and Murray, 1984; Lovley, 1987; Sigg et al., 1991; Nealson and Myers, 1992; Hendry, 1993; Chen and Wang, 1999; Hulth et al., 1999; Bergmann et al., 2013). Iron and manganese reducing microbial metabolisms have been linked to the occurrence of crystal fans at the sediment-water interface (Bergmann et al., 2013). Iron reduction predominated in most Archean and many Proterozoic anoxic settings (Craddock and Dauphas, 2011; Kunzmann et al., 2017). Before the widespread oxidation of Earth's surface environments, these metabolisms made use of oxidized iron or manganese generated by biotic (Garrels et al., 1973; Widdel et al., 1993; Konhauser et al., 2002, 2007; Kappler et al., 2005; Crowe et al., 2008; Johnson et al., 2013) or abiotic (Cairns-Smith, 1978; Braterman et al., 1983; Kurzweil et al., 2016) processes that operated in the absence of molecular oxygen.

In contrast, metabolisms which require molecular oxygen, either directly, as in aerobic respiration, or indirectly, for example, sulfate reduction (which requires oxic environments in which substantial amounts of sulfate can be produced), do not promote carbonate precipitation to the same degree (Fig. 11, Bergmann et al., 2013). Sulfate reduction results in only a modest increase in Ω, although this depends on molecular substrate (Gallagher et al., 2012), and decreases pH to a minimum point of no change (6.7); aerobic respiration decreases both Ω and pH, promoting carbonate dissolution (Walter and Burton, 1990; Hu and Burdige, 2008; Higgins et al., 2009; Bergmann et al., 2013).

Not only did the dominant microbial metabolisms responsible for the respiration of organic matter change through time, but the environmental distribution of metabolisms also shifted. As surface environments became oxygenated, metabolisms dependent on oxygen (either directly or indirectly) such as aerobic respiration and sulfate reduction replaced anaerobic pathways in newly oxygenated environments. These anaerobic metabolisms, including iron reduction, manganese reduction, and elemental sulfur reduction, continued in anaerobic settings, including anaerobic zones within shallow and very shallow sedimentary substrate.

We hypothesize that the replacement of Ω-increasing (anaerobic) with Ω-decreasing (aerobic or otherwise oxygen-dependent) metabolisms leaves a signature in the carbonate textural record. Consistent with earlier reports (Grotzinger and Read, 1983; Hofmann and Jackson, 1987; Kah and Grotzinger, 1992; Sumner and Grotzinger, 1996; Kah and Knoll, 1996; Semikhatov and Raaben, 1996; Knoll and Semikhatov, 1998; Grotzinger and Knoll, 1999; Grotzinger and James, 2000; Higgins et al., 2009; Bergmann et al., 2013), *Microstrat* shows that seafloor macro- and micro-precipitates are abundant in Archean and Paleoproterozoic carbonate deposits across the observed depth gradient, but are uncommon thereafter. We suggest that the abundance of seafloor precipitate textures is consistent with the presence of precipitation-promoting anaerobic metabolisms dominating an anoxic sediment-water interface during the Archean and Paleoproterozoic intervals. The frequency of seafloor precipitate textures declines through time, beginning in the Paleoproterozoic Era. We connect this trend to the environmental expansion of aerobic respiration that accompanied the Great Oxygenation Event. We hypothesize that as oxygen-producing cyanobacteria spread across the seafloor, they oxygenated the sediment-water interface, leading to the replacement of anaerobic metabolisms with aerobic respiration and decrease of Ω at the seafloor. As aerobic respiration became a major metabolism active at the seafloor, we hypothesize that the sediment-water interface became unsuitable for carbonate nucleation due to the effects of aerobic respiration on carbonate saturation

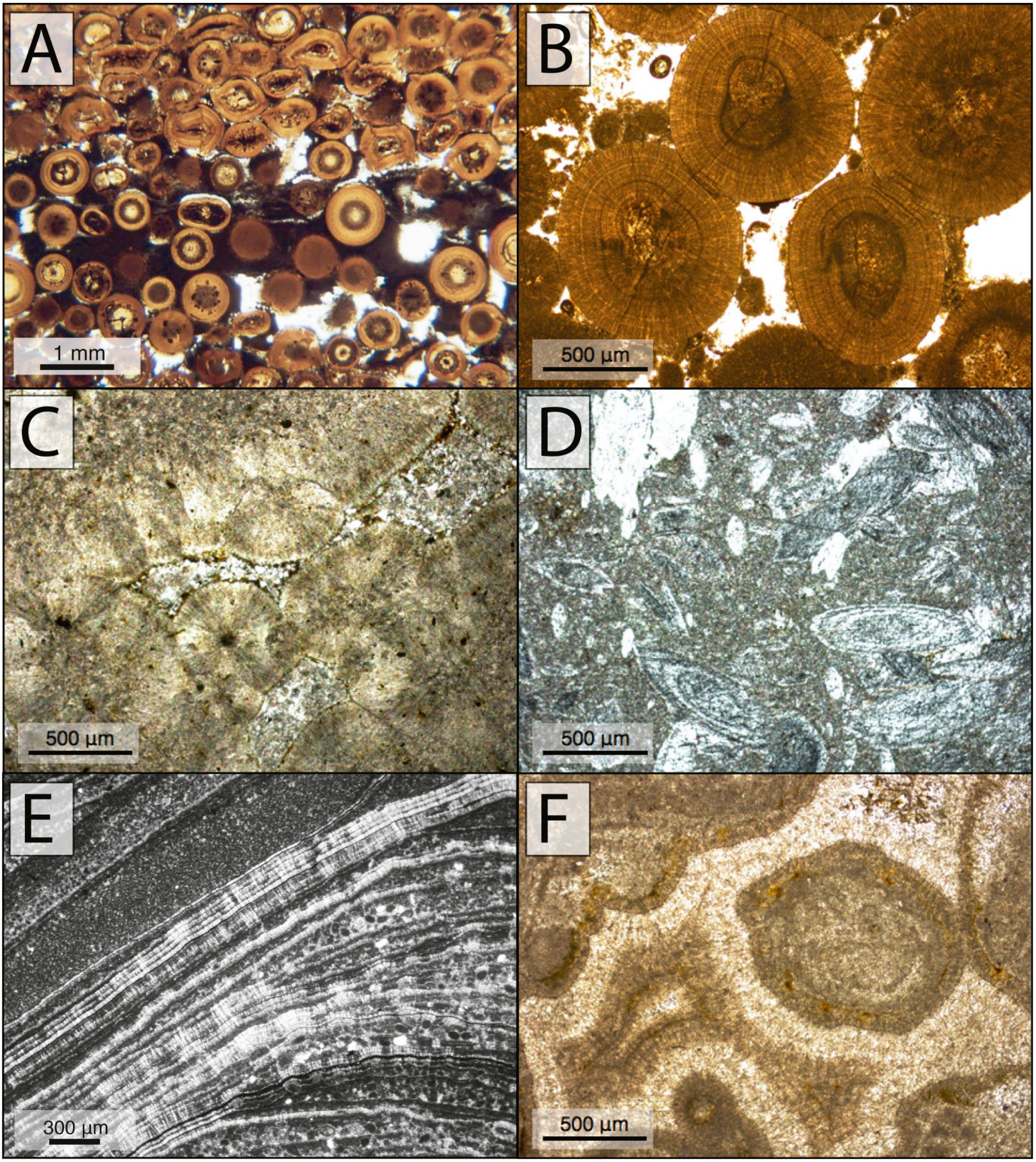

Plate 6. A Silicified ooids. Lower Mesoproterozoic, Yusmastakh Fm, Siberia. *Photo: A. Knoll*
B Mimetic dolomite ooids, Ediacaran Khufai Fm, Sultanate of Oman. *Photo: K. Bergmann*
C Mimetic dolomite spherulitic texture with maltese crosses in an Ediacaran *Conophyton* reef. Buah Fm, Sultanate of Oman. *Photo: K. Bergmann*
D Mimetic dolomite preserving white gypsum pseudomorphs with swallowtail morphologies and oval features. Buah Fm, Sultanate of Oman. *Photo: K. Bergmann*
E Microprecipitates in Lower Mesoproterozoic *Gongyolina* stromatolites, Kyutingda Fm, Siberia. The Kyutingda Fm is not included within the database because sufficiently detailed stratigraphy is not available at time of publication. *Photo: A. Knoll*
F Pisoids and early marine cements preserved as mimetic dolomite. Ara Group, Sultanate of Oman. *Photo: K. Bergmann*

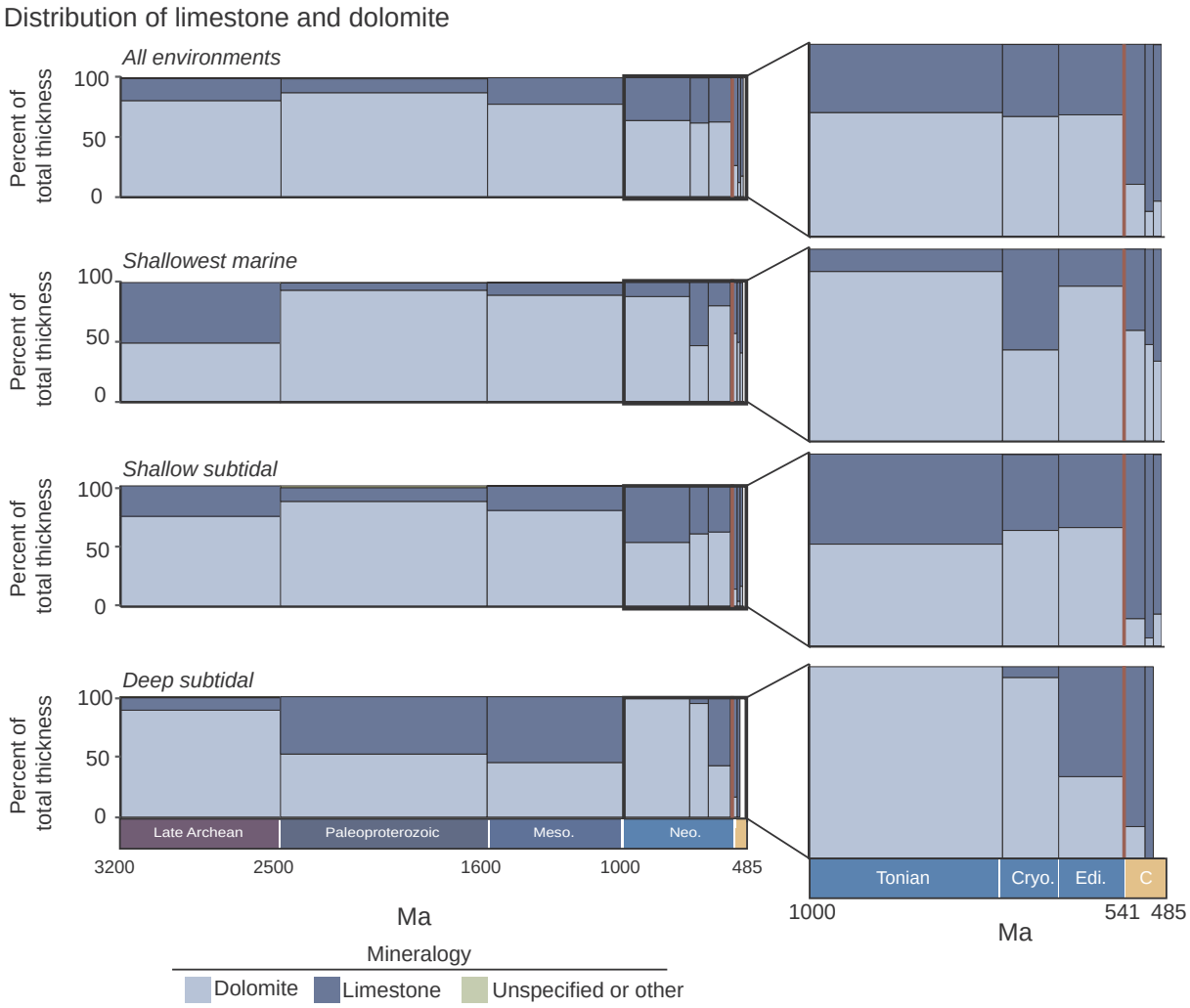

Fig. 9. The temporal and environmental distribution of limestones and dolomites. In the Phanerozoic Eon, dolomite becomes much less common.

state, leading to a great reduction in the abundance and environmental distribution of macroscopic crystal fans extending above the sediment-water interface. Millimeter-scale crystal fans continued to form in peritidal environments, but at least in some cases, one can demonstrate that nucleation occurred within sedimentary substrate (Bartley et al., 2000).

Co-occurring with this reduction in precipitation at the sediment-water interface, molar tooth structures and intraclasts become more abundant. Intraclasts derive from a rapidly lithified, brittle substrate, cemented by the precipitation of carbonate within pore spaces rapidly after deposition (penecontemporaneous cementation). Molar tooth structures (Plate 2B, C) formed when microspar precipitated within voids created by gas (Pollock et al., 2006; Hodgskiss et al., 2018). Pressure from gas generated by microbial heterotrophs is thought to have formed the voids in the sediments (Furniss et al., 1998), and anaerobic microbial metabolism, specifically iron reduction, has been implicated in cement precipitation (Hodgskiss et al., 2018). The substrate was still ductile when molar tooth structures formed, and the geometries of molar tooth structures reflect the production of gas and the deformation of ductile sediments by gas expansion and propagation. Therefore, full lithification in molar tooth-bearing units occurred somewhat later than in intraclast-bearing intervals. However, both structures require precipitation within the sediment rather than directly at the sediment-water interface. We suggest that the increase in both these features along with the decline of crystal fans is consistent with the retreat of carbonate precipitation to pore spaces below the sediment-water interface following the oxygenation of the interface. In some cases, such as conditions leading to the formation of intraclasts, this precipitation could be rapid. Petrographic evidence for rapid precipitation within pore spaces includes tufts of cyanobacterial filaments, preserved in vertical orientation (e.g., Knoll et al., 2013, Fig. 2E) as well as by preserved voids where cell clusters decayed, indicating cementation on the time scale of cell degradation (Sergeev et al., 1994). Based on the abundance of intraclasts and other petrographic evidence, we suggest that penecontemporaneous cementation—precipitation within the pore spaces of shallow sediments rapidly following deposition—was a hallmark of the Mesoproterozoic Era.

Widespread penecontemporaneous cementation would have rapidly immobilized detrital sediment. This hypothesis thus makes the prediction that features that require regular sediment transport should be less abundant in the Mesoproterozoic Era. Oolitic barchan dunes in the Mesoproterozoic Angmaat Formation, show that although ooids formed in this Mesoproterozoic basin, they often became cemented to the seafloor and immobilized, producing conditions of sediment starvation (Kah, 1997)Though the mechanisms that govern ooid formation, growth, and size remain an active area of research (Sumner and Grotzinger, 1993; Pacton et al., 2012; Diaz et al., 2015; O'Reilly et al., 2017; Trower et al., 2018), ooids are unlikely to form in rapidly lithifying environments where incipient grains are cemented to the seafloor and immobilized. Actively growing ooids in present-day environments are linked to turbulent, energetic shoal environments (e.g., Trower et al., 2018). By analogy, oncoids, which grow by the microbial

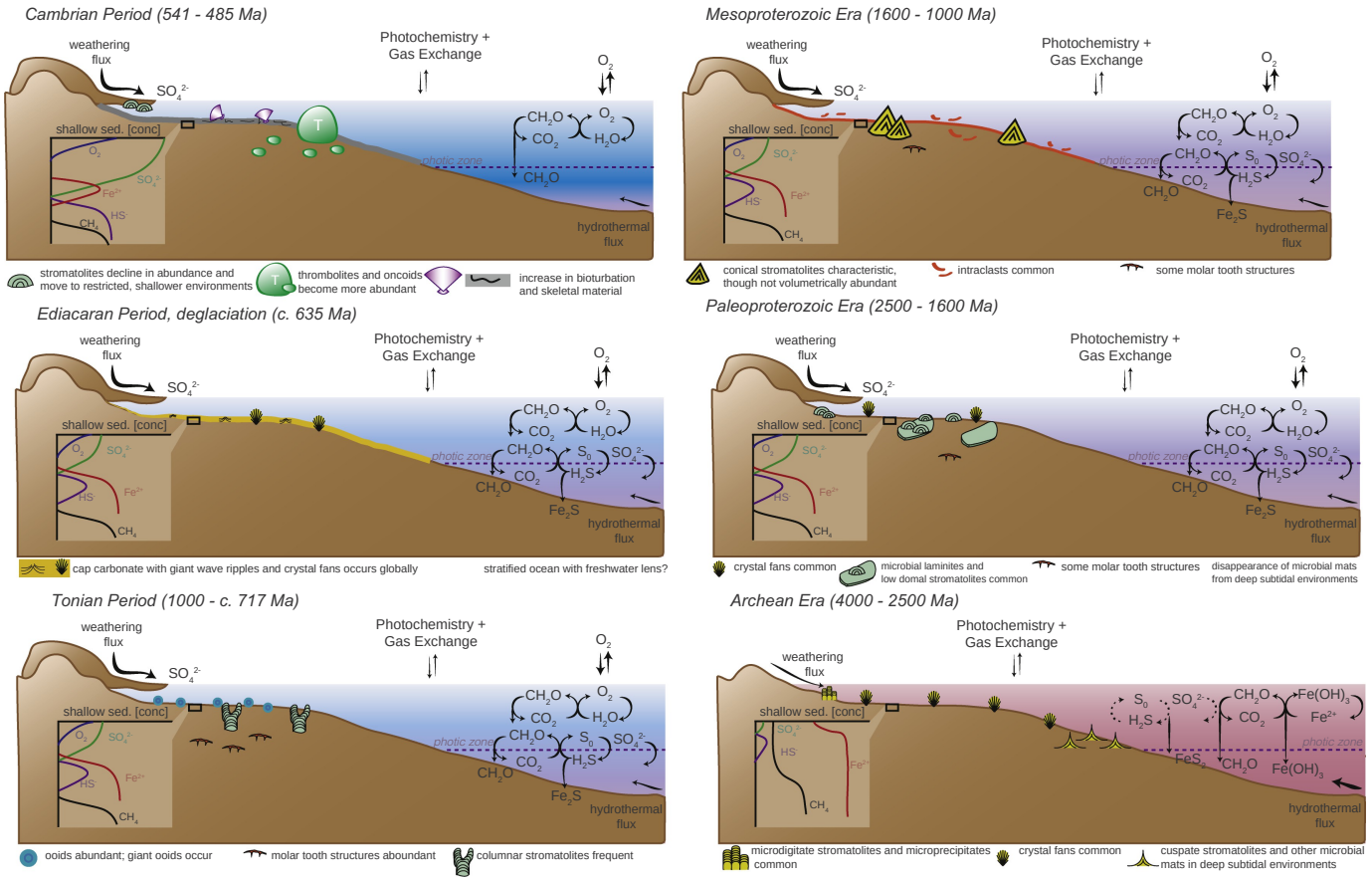

Fig. 10. These platform diagrams visualize some of the most characteristic changes in the abundance and texture of Precambrian carbonates.

trapping and binding of sediment in addition to the precipitation of carbonate, should also require regular movement to continue growing as a discrete oncoid rather than as an immobile stromatolite. Indeed, ooids occur in < 25% of Mesoproterozoic formations within the database—the lowest proportion for any interval in the database—and oncoids are also quite uncommon, though stromatolites are especially abundant (Fig. 3), perhaps due to rapid precipitation enhancing stromatolitic accretion.

Ooids are found in marine strata as old as the Archean (e.g., Barley et al., 1979), but are volumetrically most significant in the Neoproterozoic Era (Fig. 4). The Neoproterozoic increase in ooid volume, therefore, suggests a change in the character of carbonate-precipitating environments. The Mesoproterozic seafloor, dominated by penecontemporaneous cementation and rapid lithification, was like a "papier-mâché" substrate, on which mobile sediment could rapidly become affixed; in comparison, carbonate grains were more often transported, continuing to grow over extended periods, on the Neoproterozoic seafloor. Changes in the geometry and tectonic settings of carbonate platforms may have contributed to this change. The origin and occurrences of giant ooids, also associated with the Neoproterozoic Era, remain active areas of research (Sumner and Grotzinger, 1993; Trower and Grotzinger, 2010; Tang et al., 2015). Hypotheses for their large size have included a lack of nuclei leading to dramatic growth on fewer grains; a change in carbonate chemistry leading to rapid precipitation; or a change in environmental agitation and grain mobility (Sumner and Grotzinger, 1993). We suggest that as penecontemporaneous precipitation declined in very shallow sediments due to the expansion of aerobic respiration, shifting into deeper sediment pore spaces or the water column, carbonate grains were more likely to form and remain in traction load, promoting ooid formation. This change in Neoproterozoic carbonate precipitation, from shallowly buried sediments to the surfaces of mobile grains like ooids, may result from a combination of factors impacting the carbonate system, including climate, increasing seafloor oxidation, or changes in tectonic activity during the Neoproterozoic Era. From the late Archean to the Neoproterozoic, the shifting styles of carbonate precipitation can be interpreted as sedimentological evidence for changes in environmental oxygenation and carbonate chemistry.

4.2. Animal habitat expansion tracks depth-dependent oxygenation of the ocean

We note that evidence for animal influences in carbonate depositional environments—skeletal material and bioturbation—originate in shallow subtidal environments before expanding to both deeper subtidal and shallower coastal environments. In terms of thickness, most deep subtidal evidence for animals in the database comes from skeletal material. Because skeletal material can be transported into deeper environments following organism death, it is not necessarily evidence of a widespread presence of skeletal animals in the deep subtidal environment. We interpret this trend as consistent with attenuated oxygenation of the deep subtidal environment in the Cambrian Period, and the depth-dependent expansion of animal habitats. Once again, this conforms with observations made from the body and trace fossil records (Buatois et al., 2009, 2016; Tarhan et al., 2015), suggesting that both the processes for bringing data into *Microstrat* faithfully replicate sedimentological, paleontological and environmental assignments, and that carbonate data complement canonical paleontological archives.

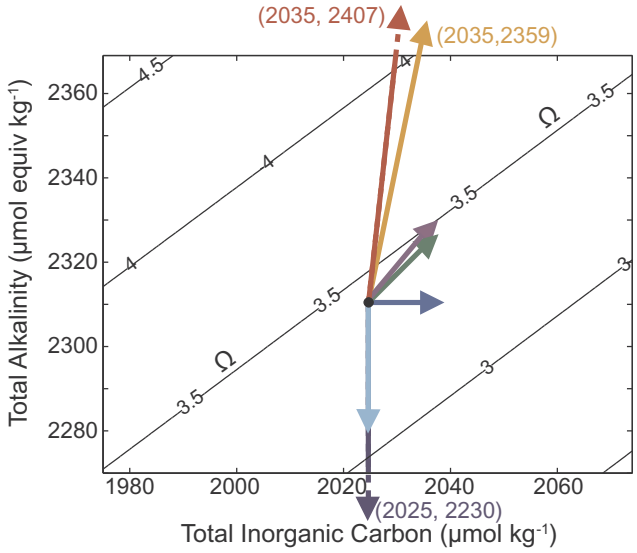

REACTION	STOICHIOMETRY	ΔDIC	ΔALK	pH	
aerobic respiration	$4\ C_{106}H_{175}O_{42} + 515\ O_2 \rightarrow 424\ CO_2 + 350\ H_2O$	1	0	5.18	
denitrification	$2\ C_{106}H_{175}O_{42} + 206\ NO_3^- + 206\ H^+ \rightarrow 212\ CO_2 + 103\ N_2 + 278\ H_2O$	1	1.0	6.78	
manganese reduction	$2\ C_{106}H_{175}O_{42} + 515\ MnO_2 + 1030\ H^+ \rightarrow 212\ CO_2 + 515\ Mn^{2+} + 690\ H_2O$	1	4.9	+	
iron reduction	$2\ C_{106}H_{175}O_{42} + 515\ Fe_2O_3 + 2060\ H^+ \rightarrow 212\ CO_2 + 1030\ Fe^{2+} + 1205\ H_2O$	1	9.7	+	
sulfate reduction	$8\ C_{106}H_{175}O_{42} + 515\ SO_4^{2-} + 1030\ H^+ \rightarrow 848\ CO_2 + 515\ H_2S + 700\ H_2O$	1	1.2	6.72	
methanogenesis	$8\ C_{106}H_{175}O_{42} + 330\ H_2O \rightarrow 333\ CO_2 + 515\ CH_4$	1	0	5.56	
AOM	$8\ C_{106}H_{175}O_{42} + 515\ SO_4^{2-} + 1030\ H^+ \rightarrow 848\ CO_2 + 515\ H_2S + 700\ H_2O$	1	1.2	7.88	
sulfide oxidation	$1\ H_2S + 2\ O_2 \rightarrow SO_4^{2-} + 2\ H^+$	0	-2	-	
iron oxidation	$4\ Fe^{2+} + 4\ H_2O + O_2 \rightarrow 2\ Fe_2O_3 + 8\ H^+$	0	-8	-	

Fig. 11. The stoichiometry and effects on carbonate chemistry of key metabolisms are shown. Modified from Bergmann et al. (2013).

4.3. Microbialite morphologies reflect evolutionary and environmental changes

The success of stromatolite stratigraphy in the broad correlation of Proterozoic sedimentary successions and the evident facies relationships of stromatolite forms within individual basins indicate that the morphologies of these boundstones vary spatially and temporally in Precambrian carbonate successions (Cloud and Semikhatov, 1969; Bertrand-Sarfati and Trompette, 1976; Walter, 1976; Bertrand-Sarfati and Moussine-Pouchkine, 1988; Knoll and Semikhatov, 1998; Kah et al., 2006, 2009; Murphy and Sumner, 2008). Our database corroborates these broad changes in stromatolite morphologies (Fig. 4); we hypothesize that these changes are explained by changes in the style and loci of carbonate precipitation.

We start by noting the critical roles that both carbonate precipitation and microbial trapping and binding of sediment can play, to varying degrees, in the development and growth of stromatolites (Fairchild, 1991; Grotzinger and Knoll, 1999). The central role of carbonate precipitation in some stromatolite morphologies results in isopachous cement laminae, steep angles of repose, and/or internal void space (Plate 1, B, C, D, F Grotzinger and Knoll, 1999; Pope et al., 2000; Riding, 2011). Precipitated stromatolites can form with or without the templating influence of microbial mats, and precipitated structures in Precambrian successions have provoked debate about biogenicity for decades (Grotzinger and Rothman, 1996; Allwood et al., 2009; Wacey et al., 2016). Most (but not all; Pope and Grotzinger, 2000; Pope et al., 2000) Proterozoic and younger stromatolites also show evidence of microbial influence both in the trapping and binding of fine particles and in metabolically induced precipitation of carbonate cements (Grotzinger and Knoll, 1999). Local physical conditions, including light, water depth, tidal currents, and sediment flux, also shape stromatolite morphologies (Gebelein, 1969; Hofmann, 1973; Serebryakov and Semikhatov, 1974; Horodyski, 1976, 1977; Semikhatov et al., 1979; Grotzinger, 1989; Kah and Knoll, 1996; Narbonne and James, 1996; Bartley et al., 2000; Dupraz et al., 2007; Allwood et al., 2009; Riding, 2011; reviewed by Grotzinger and Knoll (1999). We interpret the secular changes in stromatolite morphology seen over the Precambrian Eon to be primarily driven by changes in carbonate precipitation.

For example, cuspate stromatolites–peaked stromatolites marked by large primary void space–are particularly conspicuous in later Archean and early Paleoproterozoic successions (Sumner, 1997, 2000; Murphy and Sumner, 2008), although younger examples have been reported

(e.g., Kah, 1997; Wallace et al., 2014; Bartley et al., 2015). Formation of at least void-rich cuspate stromatolites requires penecontemporaneous cement precipitation at the sediment-water interface to preserve void space geometries (e.g., Bartley et al., 2015; Martindale et al., 2015). Cuspate stromatolites were most common in times and environments where seafloor carbonate precipitation was most common, declining in abundance and distribution as the broader pattern of carbonate precipitation changed. This pattern is especially pronounced in deep water stromatolites, whose absolute thickness and morphological diversity diminishes after the Archean Era. To determine if this trend were merely the result of improved sampling in Archean deep-water facies, thanks to the > 1000 meter GKP01 core which targeted deep-water facies of the upper Archean Transvaal Supergroup (Knoll and Beukes, 2009), we examine these trends without this core in Supplementary Figs.s S12–S17. The trends remain stable, suggesting that it is not merely the result of improved sampling in Archean deep-water environments.

Studies of modern cuspate stromatolites in quiet water environments show that their complex morphology becomes muted as siliciclastic mud influx increases (Mackey et al., 2017). We hypothesize that the dramatic decline in cuspate stromatolites after the Archean Eon could be connected to an increased influx of siliciclastic mud to deeper marine environments from enhanced continental emergence or tectonic uplift near the Archean-Proterozoic boundary (Bindeman et al., 2018). We also note that even later occurrences of cuspate stromatolites in the Iqqituq, Angmaat, and Dismal Lakes units occur in environments with little detrital input (Kearns, 1983; Kah, 1997; Turner, 2009; Bartley et al., 2014).

The decline of penecontemporaneous cementation at the sediment-water interface also resulted in the decline of morphologies (e.g., cuspate and microdigitate stromatolites) in which rapid precipitation within microbial layers is critical to building or maintaining stromatolite structure (Sumner, 1997; Murphy and Sumner, 2008). Such forms make up a relatively small component of peritidal facies in Mesoproterozoic successions (e.g., Bartley et al., 2000), but microprecipitate textures and microdigitate stromatolites still occur. Though we have categorized the latter morphologies as exhibiting precipitation at the sediment-water interface, these stromatolite morphologies are also influenced by the precipitation of carbonate within pore space within a broadly evaporative setting (Grotzinger and Knoll, 1999).

Conical stromatolites do not contribute much total volume to the rock record, but consistently occur across time intervals and depositional environments where clastic influx is low. We note that many of the conical stromatolites described in our compilation accreted on transgressive surfaces, potentially when and where stromatolite growth dominated by carbonate precipitation could outpace growth by trapping and binding of sediment because total clastic sedimentation rate was low. Petrographic investigation of conical stromatolites reveals that spherulitic or fan-like precipitate textures are often within these structures (Kearns, 1983; Kah et al., 2006, 2009; Bergmann, 2013) (Plate 4, C, D; Plate 6C). Conversely, columnar stromatolites, both branched and unbranched, become more abundant and widely distributed as seafloor precipitation wanes. The spacing and branching of columns are commonly (although not always) governed by clastic sediment movement, which inhibits mat growth in synoptic lows between adjacent columns (Serebryakov and Semikhatov, 1974; Swett and Knoll, 1985). Thus, the abundance of grainstones in general, and the abundance of ooids in particular, in Tonian formations provides a mechanistic explanation for the abundance of columnar and branching stromatolites.

Various explanations for the end-Proterozoic expansion of thrombolites have been suggested. One group of hypotheses attributes thrombolite expansion to increasing animal influences, citing the timing of thrombolite expansion, the disruptive effects of grazers and bioturbation on microbial mats, and the frequent association between thrombolites and skeletal debris (Awramik, 1971; Walter and Heys, 1985; Planavsky and Ginsburg, 2009). However, modern bioturbated stromatolites can lack thrombolitic clotted textures (Planavsky and Ginsburg, 2009). In Cambro-Ordovician rocks from the Great Basin, thrombolitic fabrics are bioturbated, but bioturbation is not the source of thrombolitic clots (Harwood Theisen and Sumner, 2016). Skeletal debris produced by (non-grazing) sessile benthos and thrombolites covary positively in space (Sprinkle and Guensburg, 1995; Sumrall et al., 1997; Pruss and Knoll, 2017). Thrombolites (*sensu lato*) predate evidence for animal activity (Kennard and James, 1986; Kah and Grotzinger, 1992; Turner et al., 2000; Harwood and Sumner, 2011, 2012).

Taken together, this evidence suggests that the animal activity hypothesis has limited explanatory power. The growth of non-filamentous mats and calcimicrobes, mat colonization by eukaryotes, rapid carbonate precipitation, alteration by diagenesis and decomposition of organic matter have also been proposed as alternate explanations for the appearance of thrombolites (Kah and Grotzinger, 1992; Turner et al., 2000; Harwood Theisen and Sumner, 2016; Pruss and Knoll, 2017). In particular, Feldmann and McKenzie (1998) noted that on the modern Bahama Platform, thrombolite textures are associated with subtidal microbial mounds festooned by fleshy algae. Algal hypotheses for later Neoproterozoic and Cambrian thrombolitic fabric development are consistent with the distribution of thrombolites in time and space and can account for both the clotted character of thrombolites and their association with sessile benthic invertebrates (Sprinkle and Guensburg, 1995; Sumrall et al., 1997; Pruss and Knoll, 2017).

Algal hypotheses are unlikely to account for early thrombolites (*sensu lato*); molecular clock estimates place the origin of algae between 900–1900 Ma (Sánchez-Baracaldo et al., 2017), but the diversification of algae and their rise to ecological prominence as primary producers did not occur until the Cryogenian and Ediacaran periods (Brocks et al., 2017; Hoshino et al., 2017). Algal remains are not seen in detailed petrographic studies of the Little Dal Formation, which contains massive Neoproterozoic thrombolite reefs, although a taphonomic cause for this absence is possible (Turner et al., 2000). In general, before the rise of widespread benthic algal communities, the disruptive mechanisms that produced thrombolitic textures may have included localized crystal growth, and taphonomic processes, among others.

The co-occurrence of thrombolites and oncoids within formations is an intriguing feature of our dataset (Fig. 7, Fig. S4), suggesting that similar conditions promote or permit the formation of both textures. In the absence of early lithification at the seafloor, fabric-disrupting processes during either deposition or diagenesis can generate clotted thrombolitic textures. Under these conditions, mat fragments can become oncoids; slow cementation permits their continued mobility and growth. Rapid, penecontemporaneous cementation, as in the Mesoproterozoic, might suppress the occurrence of both thrombolites and oncoids. During the same interval, stromatolites, which may be enhanced by rapid penecontemporaneous cementation, are abundant (Fig. 4). During the Neoproterozoic and Cambrian, penecontemporaneous cementation wanes and both thrombolites and oncoids become more common.

4.4. Non-uniformitarian model for Precambrian vs Phanerozoic dolomite

Dolomite is common in the Precambrian rock record but rare in modern sedimentary environments. The frequency of dolomite occurrence increases with depositional age, a trend which could be explained if carbonate rocks are simply more likely to experience dolomitization with time, although this suggestion is not well-supported (Given and Wilkinson, 1987). However, we and others observe a shift in both the proportion (Fig. 8), and style of dolomitization (Tucker, 1982, 1983; Kah, 2000; Corsetti et al., 2006; Kah et al., 2006; van Smeerdijk Hood and Wallace, 2018) across the Precambrian-Cambrian boundary, suggesting that dolomite was once more common in depositional and early diagenetic settings.

In the Phanerozoic Eon, dolomitization frequently occurs as a fluid-flushing diagenetic process which obscures petrographic detail and results in coarse, rhombohedral replacement textures (e.g., Wallace, 1990; Sibley, 1991; Warren, 2000; Corsetti et al., 2006). Tabulations of the Phanerozoic rock record have noted increases in the rate of dolomite formation co-occurring with periods of continental flooding (Given and Wilkinson, 1987) and the global extent of evaporitic and lagoonal basins (Sun, 2003) because these settings provide the right hydrological conditions for Mg-rich seawater to flush through carbonate rocks during diagenesis. Dolomitization under these conditions is influenced by paleoclimate, tectonic configuration, and eustasy (Given and Wilkinson, 1987; Sun, 2003), and occurs during diagenesis and shallow burial. Phanerozoic dolomite more frequently shows a lack of primary fabrics, consistent with fabric-destructive diagenetic dolomitization, and occurs less frequently across all environments (Tucker, 1982, 1983; Corsetti et al., 2006) when compared to Precambrian dolomite. *Microstrat* shows that Precambrian dolomite is common in all environments, though most common in shallow marine environments. Precambrian dolomite also is distinct from Phanerozoic dolomite in that it often preserves fine petrographic detail (Photo Plate 6; B, C, D, F). These changes in abundance, environmental distribution (Fig. 9), and character (Plate 6, Tucker, 1982, 1983; Corsetti et al., 2006) of Precambrian dolomite are consistent with the suggestion that a different set of processes drove Precambrian dolomite formation than Phanerozoic dolomitization. Within individual Precambrian carbonate samples, the petrographic relationships of limestone and dolomite often show that dolomite formed early and was not associated with fabric-destructive dolomitization (e.g., Plate 2C, 2D).

Observations indicate that dolomite formed as an early marine cement during Precambrian time, especially in restricted environments (Fairchild et al., 1991; van Smeerdijk Hood et al., 2011; Wood et al., 2017). Geochemical records, models, and stratigraphy provide additional support for the suggestion that Precambrian seawater chemistry produced dolomite as an abundant, early mineral. For much of the Precambrian Eon, seawater sulfate concentrations were far less than modern (Canfield and Teske, 1996; Canfield, 2004; Kah et al., 2004; Hurtgen et al., 2006; Canfield and Farquhar, 2009; Osburn et al., 2015; Blättler et al., 2018), which is important in part because sulfate is an inhibitor of dolomite formation (Baker and Kastner, 1981; Kastner, 1983). Precambrian microbial communities may also have promoted dolomite formation. Abundant microbial biofilms may have provided nucleation sites for dolomite formation, and likely played a critical role in concentrating Mg so that dolomite could form (Wang et al., 2009). High concentrations of iron and manganese in early marine dolomite cements (van Smeerdijk Hood et al., 2011) are consistent with the anaerobic metabolisms hypothesized by Burns et al. (2000) and Kah (2000) to enhance dolomite formation, as well as the iron- and manganese-reducing metabolisms which drive carbonate precipitation through the creation of alkalinity (Kah, 2000; Bergmann et al., 2013). Models, stratigraphy, and fluid inclusions suggest that Mg/Ca ratios were relatively high in Precambrian seawater and decreased across the Proterozoic-Cambrian transition (Hardie, 2003; Brennan et al., 2004; Peters and Gaines, 2012), offering a source for the required Mg. We attribute the observed changes in the environmental abundance and distribution of dolomite in the Precambrian and the Phanerozoic intervals to changes in redox state and seawater chemistry, not as age-dependent artifacts of diagenetic processes operating continuously on buried carbonate successions.

In addition to hypothesizing different chemical conditions in Precambrian oceans, we note that rare occurrences of fabric-retentive dolomite in Phanerozoic rocks may be helpful in identifying which other processes contributed to the textural difference between the Precambrian and Phanerozoic dolomite records. During the Cenozoic Era, the diminished frequency and magnitude of eustatic sea-level variation may have driven more time-limited contact between carbonate rocks and dolomitizing fluids, resulting in fabric-retentive dolomite (Sibley, 1991). In a warmer Precambrian world with no evidence for glaciation from c. 2400 to 717 Ma, fabric-retentive dolomite could be more common because of a lack of eustatic sea-level variation driving fabric-destructive dolomitization. The record is unclear: Snowball Earth episodes may be associated with fabric-destructive dolomitization, as in Mongolia (Bold et al., 2016), or with widespread, global dolomitization (Ahm et al., 2019), though certainly not all dolomite associated with Cryogenian glacial deposits is the result of fabric-destructive dolomitization processes (e.g., Fairchild, 1983). This hypothesis could be tested by comparing occurrences of Precambrian fabric-retentive dolomite with high-resolution stratigraphic records of sea-level change.

4.5. Carbonate mud is a substantial component of the Proterozoic carbonate record

Hypotheses for the genesis of carbonate mud generally fall into one of three categories: carbonate mud precipitates directly from seawater as whitings, perhaps aided by primary planktonic production in the shallow ocean (Cloud, 1962; Shinn et al., 1989; MacIntyre and Reid, 1992; Milliman et al., 1993; Morse et al., 2003); muds are produced by the biological activities of animals and benthic algae (e.g., fecal pellets, or the decomposition of calcareous algal skeletons) (Lowenstam and Epstein, 1957; Adjas et al., 1990; Gischler and Zingeler, 2002; Gischler et al., 2013; O'Connell and James, 2015); and/or muds reflect the abrasion of carbonate grains (Van Ee and Wanless, 2008; Trower et al., 2019). All these processes can generate carbonate mud. Changes in seawater chemistry, biological activity, and/or sediment transport could result in changes in the volumetric contribution of any individual process, with consequences for the ultimate sedimentary volume and environmental location of carbonate mud.

Our data shows substantial volumes of carbonate mudstone in the Proterozoic Eon, demonstrating that skeletal decomposition is not required to produce volumetrically significant amounts of micrite. Fig. 6 shows at best limited variation in the relative thickness of carbonate muds among time intervals, providing little support in favor of hypotheses for secular variation in the global probability of whiting precipitation. Petrographic analysis of silicified carbonate clasts suggests that some grains and coarser clasts themselves formed from lithified muds, along with stromatolites that trapped and bound mud (Knoll and Swett, 1990); our Dunham classification-based analysis thus likely underestimates total Precambrian mud production.

4.6. Do periods of glaciation, oxidation, and sedimentation leave similar imprints in the carbonate record?

Twice in Earth history, a similar series of events occurred: global oxidation, glaciation, and sedimentation, first in the early Paleoproterozoic Era, and then during the Neoproterozoic Era. The similarity of these two intervals has been noted before (e.g. Kirschvink et al., 2000; Young, 2013). In both cases, the oxygenation of Earth's atmosphere may have been modulated by the burial of organic carbon in sedimentary rocks (Husson and Peters, 2017), and increased oxidative weathering may have led to CO_2 drawdown and glaciation. Because carbonate rocks are a major sink for inorganic carbon, they are tied to perturbations in the carbon cycle, and changes in Earth's climate state. Are the carbonate textures associated with these two periods similar?

Textural similarities between the two intervals include less evidence of penecontemporaneous cementation (lower abundances of intraclasts, higher abundances of ooids) and boundstone textures consistent with disturbance of microbial laminae before lithification (oncoids and thrombolites). These textures may suggest that these periods of oxygenation leave similar imprints in the carbonate rock record, as penecontemporaneous cementation within shallow or very shallow pore spaces and precipitation at the sediment water interface are muted by increased aerobic respiration. The percentage of shallow subtidal

depositional environments increases in our database in the Paleoproterozoic, the Tonian, and the Cambrian intervals (Fig. 8, Fig. S4). In the Cambrian Period and Paleoproterozoic Era, perhaps this subtidal expansion is tied to significant transgression following glaciation. Such a relationship between the Great Unconformity and the Cryogenian glaciations has been proposed (Peters and Gaines, 2012; Keller et al., 2019). These observations from *Microstrat* are consistent with the suggestion that these periods of glaciation and oxygenation may result in similar carbonate textures and changes in carbonate environments. Evaluating this hypothesis may require tighter age constraints, especially in the Paleoproterozoic Era, on carbonate successions associated with these events.

4.7. Tectonic signatures in the carbonate record

The style, abundance, and distribution of carbonate features are functions not only of ocean chemistry, biology, and environments, but also of continental configuration, basin distribution, and platform architecture, and thus of tectonics. Changes we observe in carbonate structures, textures and features may be explained by changes in tectonically-controlled drivers (e.g., the number of shallow, intracratonic basins, or the abundance of shallow-marine environments in the tropics) in addition to changes in carbonate chemistry or biological drivers. At the scale of our time bins, we do not observe a clear trend in platform geometry through time, which suggests that the trends we observe depend on other allochthonous factors (Fig. S3). The correspondence between observed trends in the carbonate record and the broader redox history of the planet support our conclusion that many of these trends are primarily driven by changes in the oxygenation of Earth's surface environments (Fig. 3), a change linked to biological and potentially geological or tectonic drivers (e.g., Kump et al., 2001; Campbell and Allen, 2008; Lyons et al., 2014; Husson and Peters, 2017). We also note that the onset and intensification of oxidative weathering on the continents through the Precambrian has moved carbon dioxide from the atmosphere into the oceans and, ultimately, into the sedimentary reservoir (Walker et al., 1981; Berner, 1992; Kump et al., 2000).

All areas included in the database have received detailed sedimentological study, but in many cases, their tectonic context remains unclear, complicated by limited depositional age control and the complex geometries of continent amalgamation and rifting. Supercontinent cycles might be reflected in the carbonate record. Earth's "middle age" has been described as an interval of lithospheric and environmental stability resulting from a stable continental configuration, initiated during assembly of the supercontinent Nuna and which persisted to the breakup of Rodinia (Cawood and Hawkesworth, 2014). Distinctive aspects of the Mesoproterozoic carbonate record (e.g., widespread penecontemporaneous precipitation, abundance of intraclasts) are perhaps the result of shallow epeiric seas, intracratonic basins, or continental seaways dominating this period of the carbonate record.

4.8. Sharing stratigraphic data will create large datasets with great potential

Large stratigraphic datasets have enormous explanatory potential, but current difficulties in pooling and comparing these data across locations and workers and through time prevent their full observational power from being realized. Figures in theses or published literature commonly abbreviate and abridge the full level of detail recorded during field study. It is our hope that this paper, along with the efforts of others, highlights this potential and promotes a community movement towards reporting stratigraphic and sedimentological data in a format that facilitates the creation of large, multi-contributor datasets. As other parts of the geosciences community move towards creating large, searchable archives of data (e.g., EarthChem, iSamples), the sedimentology and stratigraphy communities have an opportunity to establish a similar database. A simple spreadsheet noting stratigraphic height, mineralogy, grain size, Dunham classification, major components, and sedimentary structures, generated from stratigraphic columns, is straightforward and could potentially transmit more original field observations to other workers. In the Supplemental Materials, we provide a template compatible with *Microstrat*; we also solicit contributions and a continuing community conversation about the creation of a more complete high-resolution database effort of both carbonate and siliciclastic strata through Earth history.

5. Conclusion

By tracking carbonate features through time and environment, we gain a richer picture of Precambrian time and strata, and the Precambrian-Cambrian transition in detail. The ability to collect and parse multiple observations of physical sedimentology across time, space, and worker allows the generation of new hypotheses, some of which have been explored here. The coupled effects of evolutionary events, changing environmental conditions, and carbonate precipitation yield a dynamic and rich record with the power to resolve important changes in the Earth and ocean systems at high resolution. We identify the development of a shallow seafloor surface unsuitable for carbonate precipitation in the Neoproterozoic Era, and suggest that it is the result of aerobic respiration, demonstrating the usefulness of carbonate sedimentology as a tracker of redox state. We also note changes in the morphology of boundstones, and suggest that the nature and extent of Precambrian dolomite is consistent with a very different ocean chemistry. We close by noting the power and potential of pooled, large datasets, and look forward to joining the community in developing robust digital repositories for sharing hard-won sedimentological and stratigraphic data.

Supplementary data to this article can be found online at https://doi.org/10.1016/j.earscirev.2019.103065.

Declaration of Competing Interest

The authors declare that they have no known competing financial interests or personal relationships that could have appeared to influence the work reported in this paper.

Acknowledgements

Thanks to members of the Bergmann research group and others for their thoughtful comments on this manuscript and analyses presented herein. Thoughtful reviews by Galen Halverson and Linda Kah improved the manuscript. We also thank Henry Barker for his help digitizing sections. MDC was supported by a National Defense Science and Engineering Graduate Fellowship and the Hugh Hampton Young Fellowship (MIT). KDB acknowledges support from the MIT node of the NASA Astrobiology Institute (NNA13AA90A), the MIT Ally of Nature and Wade funds, and the Packard Fellowship. AHK acknowledges support from the W.M. Keck Foundation. The authors declare no competing interests.

References

Adams, R., 1993. Sequence stratigraphic analysis of mixed carbonate siliciclastic Cambrian sediments. In: Carrara Formation, southwest Basin and Range. Massachusetts Institute of Technology, California and Nevada.

Adjas, A., Masse, J.P., Montaggioni, L.F., 1990. Fine-grained carbonates in nearly closed reef environments: Mataiva and Takapoto atolls. Central Pacific Ocean 67, 115–132. https://doi.org/10.1016/0037-0738(90)90030-W.

Ahm, A.S.C., Maloof, A.C., Macdonald, F.A., Hoffman, P.F., Bjerrum, C.J., Bold, U., Rose, C.V., Strauss, J.V., Higgins, J.A., 2019. An early diagenetic deglacial origin for basal Ediacaran "cap dolostones". Earth Planet. Sci. Lett. 506, 292–307. https://doi.org/10.1016/j.epsl.2018.10.046.

Aitken, J.D., 1988. Giant "algal" reefs, Middle/Upper Proterozoic Little Dal Group (> 770, < 1200 Ma), Mackenzie Mountains, N.W.T., Canada: Reefs. Canada and

Adjacent Areas 13, 13–23.
Aitken, J., Turner, E.C., MacNaughton, R., 2019. Thirty-six archival stratigraphic sections in the Katherine, Little Dal, Coates Lake, and Rapitan groups (Neoproterozoic), Mackenzie Mountains, Northwest Territories. Geological Survey of Canada Open File 6391.
Albut, G., Babechuk, M.G., Kleinhanns, I.C., Benger, M., Beukes, N.J., Steinhilber, B., Smith, A.J.B., Kruger, S.J., Schoenberg, R., 2018. Modern rather than Mesoarchean oxidative weathering responsible for the heavy stable Cr isotopic signatures of the 2.95 Ga old Ijermijn iron formation (South Africa). Geochimica et Cosmochimica Acta 228, 157–158.
Allwood, A.C., Walter, M.R., Kamber, B.S., Marshall, C.P., Burch, I.W., 2006. Stromatolite reef from the Early Archaean era of Australia. Nature 441, 714–718. https://doi.org/10.1038/nature04764.
Allwood, A.C., Walter, M.R., Burch, I.W., Kamber, B.S., 2007. 3.43 billion-year-old stromatolite reef from the Pilbara Craton of Western Australia: Ecosystem-scale insights to early life on Earth. Precambrian Res. 158, 198–227. https://doi.org/10.1016/j.precamres.2007.04.013.
Allwood, A.C., Grotzinger, J.P., Knoll, A.H., Burch, I.W., Anderson, M.S., Coleman, M.L., Kanik, I., 2009. Controls on development and diversity of Early Archean stromatolites. Proc. Natl. Acad. Sci. 106, 9548–9555. https://doi.org/10.1073/pnas.0903323106.
Arvidson, R.S., Mackenzie, F.T., 1999. The dolomite problem: control of precipitation kinetics by temperature and saturation state. Am. J. Sci. 299, 257–288. https://doi.org/10.2475/ajs.299.4.257.
Awramik, S.M., 1971. Precambrian Columnar Stromatolite Diversity: Reflection of Metazoan Appearance. Science 174.
Azmy, K., Kaufman, A.J., Misi, A., de Oliveira, T.F., 2006. Isotope stratigraphy of the Lapa Formation, Sao Francisco Basin, Brazil: Implications for Late Neoproterozoic glacial events in South America. Precambrian Res. 149, 231–248. https://doi.org/10.1016/j.precamres.2006.07.001.
Babinski, M., Vieira, L.C., Trindade, R.I.F., 2007. Direct dating of the Sete Lagoas cap carbonate (Bambuí Group, Brazil) and implications for the Neoproterozoic glacial events. Terra Nova 19, 401–406. https://doi.org/10.1111/j.1365-3121.2007.00764.x.
Baker, J.L., 2008. Carbon Isotopic Fractionation Across a Late Cambrian Carbonate Platform: A Regional Response to the SPICE Event as Recorded in the Great Basin. Weber State University, United States.
Baker, P.A., Kastner, M., 1981. Constraints on the formation of sedimentary dolomite. Science 213, 214–216. https://doi.org/10.1126/science.213.4504.214.
Barghoorn, E.S., Tyler, S.A., 1965. Microorganisms from the Gunflint Chert. 147. pp. 563–577.
Barley, M.E., Dunlop, J.S.R., Glover, J.E., Grovesm, D.I., 1979. Sedimentary evidence for an Archaean shallow-water sedimentary facies, eastern Pilbara block, Western Australia. Earth Planet. Sci. Lett. 43, 74–84. https://doi.org/10.1016/S0167-4137(07)80004-7.
Bartley, J.K., Pope Knoll, A.H., Semikhatov, M.A., Petrov, P.Y., 1998. A Vendian-Cambrian boundary succession from the northwestern margin of the Siberian Platform: stratigraphy, palaeontology, chemostratigraphy and correlation. Geol. Mag. 135, 473–494. https://doi.org/10.1017/S0016756898008772.
Bartley, J.K., Knoll, A.H., Grotzinger, J.P., Sergeev, V.N.V.N., 2000. Timing of early marine lithification and stromatolite biogenicity in peritidal silicified carbonates of the Mesoproterozoic Billyakh Group, Siberia. SEPM Special Publication 67. pp. 59–73.
Bartley, J.K., Kah, L.C., McWilliams, J.L., Stagner, A.F., 2007. Carbon isotope chemostratigraphy of the Middle Riphean type section (Avzyan Formation, Southern Urals, Russia): signal recovery in a fold-and-thrust belt. Chem. Geol. 237, 229–250. https://doi.org/10.1016/j.chemgeo.2006.06.018.
Bartley, J.K., Kah, L.C., Frank, T.D., Lyons, T.W., 2014. Deep-water microbialites of the Mesoproterozoic Dismal Lakes Group: microbial growth, lithification, and implications for coniform stromatolites. Geobiology 13, 15–32. https://doi.org/10.1111/gbi.12114.
Bartley, J.K., Kah, L.C., Frank, T.D., Lyons, T.W., 2015. Deep-water microbialites of the Mesoproterozoic Dismal Lakes Group: microbial growth, lithification, and implications for coniform stromatolites. Geobiology 13 (1), 15–32 Chicago.
Bathurst, R.G., 1972. Carbonate Sediments and Their Diagenesis. Elsevier.
Bergmann, K.D., 2013. Constraints on the Carbon Cycle and Climate during the Early Evolution of Animals. California Institute of Technology.
Bergmann, K.D., Grotzinger, J.P., Fischer, W.W., 2013. Biological influences on seafloor carbonate precipitation. Palaios 28, 99–115. https://doi.org/10.2110/palo.2012.p12-088r.
Berner, R.A., 1992. Weathering, plants, and the long-term carbon cycle. Geochimica et Cosmochimica Acta 56, 3225–3231. https://doi.org/10.1016/0016-7037(92)90300-8.
Bertrand-Sarfati, J., Moussine-Pouchkine, A., 1988. Is cratonic sedimentation consistent with available models? An example from the Upper Proterozoic of the West African craton. Sediment. Geol. 58, 255–276. https://doi.org/10.1016/0037-0738(88)90072-3.
Bertrand-Sarfati, J., Trompette, R., 1976. Use of Stromatolites for Intrabasinal Correlation: Example from the Late Proterozoic of the Northwestern Margin of the Taoudenni Basin. In: Stromatolites.
Bertrand-Sarfati, J., Walter, M.R., 1981. Stromatolite biostratigraphy. Precambrian Res. 15, 353–371.
Bindeman, I.N., Zakharov, D.O., Palandri, J., Greber, N.D., Dauphas, N., Retallack, G.J., Hofmann, A., Lackey, J.S., Bekker, A., 2018. Rapid emergence of subaerial landmasses and onset of a modern hydrologic cycle 2.5 billion years ago. Nature 557, 545–548. https://doi.org/10.1038/s41586-018-0131-1.
Bishop, J.W., Sumner, D.Y., 2006. Molar tooth structures of the Neoarchean Monteville formation, Transvaal Supergroup, South Africa. I: Constraints on microcrystalline CaCO3 precipitation. Sedimentology 53, 1049–1068. https://doi.org/10.1111/j.1365-3091.2006.00801.x.
Blake, R.E., Chang, S.J., Lepland, A., 2010. Phosphate oxygen isotopic evidence for a temperate and biologically active Archaean ocean. Nature 464, 1029–1032. https://doi.org/10.1038/nature08952.
Blättler, C.L., et al., 2018. Two-billion-year-old evaporites capture Earth's great oxidation. Science 360, 320–323. https://doi.org/10.1126/science.aar2687.
Bold, U., Smith, E.F., Rooney, A.D., Bowring, S.A., Buchwaldt, R., Dudás, F.O., Ramezani, J., Crowley, J.L., Schrag, D.P., Macdonald, F.A., 2016. Neoproterozoic stratigraphy of the Zavkhan terrane of Mongolia: the backbone for Cryogenian and early Ediacaran chemostratigraphic records. Am. J. Sci. 315, 1–63. https://doi.org/10.2475/01.2016.01.
Brasier, M.D., Hewitt, R.A., Brasier, C.J., 1978. On the Late Precambrian-Early Cambrian Hartshill Formation of Warwickshirt. Geol. Mag. 115, 21–36.
Braterman, P.S., Cairns-smith, A.G., Sloper, R.W., 1983. Photo-oxidation of hydrated banded iron formations Postglacial population expansion of forest trees in Norfolk. UK 05, 6–7.
Brennan, S.T., Lowenstein, T.K., Horita, J., 2004. Seawater chemistry and the advent of biocalcification. Geology 32, 473–476. https://doi.org/10.1130/G20251.1.
Brocks, J.J., Jarrett, A.J.M., Sirantoine, E., Hallmann, C., Hoshino, Y., Liyanage, T., 2017. The rise of algae in Cryogenian oceans and the emergence of animals. Nature 548, 578–581. https://doi.org/10.1038/nature23457.
Buatois, L.A., Mángano, M.G., Brussa, E.D., Benedetto, J.L., Pompei, J.F., 2009. The changing face of the deep: colonization of the Early Ordovician deep-sea floor, Puna, northwest Argentina. Palaeogeogr. Palaeoclimatol. Palaeoecol. 280, 291–299. https://doi.org/10.1016/j.palaeo.2009.06.014.
Buatois, L.A., Mángano, M.G., Olea, R.A., Wilson, M.A., 2016. Decoupled evolution of soft and hard substrate communities during the Cambrian Explosion and Great Ordovician Biodiversification Event. Proc. Natl. Acad. Sci. 113, 6945–6948. https://doi.org/10.1073/pnas.1523087113.
Buick, R., Des Marais, D.J., Knoll, A.H., 1995. Stable isotopic compositions of carbonates from the Mesoproterozoic Bangemall group, northwestern Australia. Chem. Geol. 123, 153–171. https://doi.org/10.1016/0009-2541(95)00049-R.
Burdett, J.W., Grotzinger, J.P., Arthur, M.A., 1990. Did major changes in the stable-isotope composition of Proterozoic seawater occur? Geology 18, 227–230. https://doi.org/10.1130/0091-7613(1990)018<0227:DMCITS>2.3.CO;2.
Burns, S.J., Mckenzie, J.A., Vasconcelos, C., 2000. Dolomite formation and biogeochemical cycles in the Phanerozoic. Sedimentology 47, 49–61. https://doi.org/10.1046/j.1365-3091.2000.00004.x.
Butterfield, N.J., 1995. Secular distribution of Burgess-Shale-type preservation. Lethaia 28, 1–13. https://doi.org/10.1111/j.1502-3931.1995.tb01587.x.
Butterfield, N.J., 2009. Oxygen, animals and oceanic ventilation: an alternative view. Geobiology 7, 1–7. https://doi.org/10.1111/j.1472-4669.2009.00188.x.
Cairns-Smith, A.G., 1978. Precambrian solution photochemistry, inverse segregation, and banded iron formations. Nature 276, 807–808.
Campanha, G.A.C., Basei, M.S., Tassinari, C.C.G., Nutman, A.P., Faleiros, F.M., 2008. Constraining the age of the Iporanga Formation with SHRIMP U-Pb zircon: implications for possible Ediacaran glaciation in the Ribeira Belt, SE Brazil. Gondwana Res. 13, 117–125. https://doi.org/10.1016/j.gr.2007.05.010.
Campbell, I.H., Allen, C.M., 2008. Formation of supercontinents linked to increases in atmospheric oxygen. Nat. Geosci. 1. https://doi.org/10.1038/ngeo259.
Canfield, D.E., 2004. The evolution of the Earth surface sulphur reservoir. Am. J. Sci. 304, 839–861.
Canfield, D.E., Farquhar, J., 2009. Animal evolution, bioturbation, and the sulfate concentration of the oceans. Proc. Natl. Acad. Sci. 106, 8123–8127. https://doi.org/10.1073/pnas.0902037106.
Canfield, D.E., Teske, A., 1996. Late proterozoic rise in atmospheric oxygen concentration inferred from phylogenetic and sulphur-isotope studies. Nature 382, 127–132. https://doi.org/10.1038/382127a0.
Canfield, D.E., Poulton, S.W., Narbonne, G.M., 2007. Late-Neoproterozoic deep-ocean oxygenation and the rise of animal life. Science 315, 92–95. https://doi.org/10.1126/science.1135013.
Cawood, P.A., Hawkesworth, C.J., 2014. Earth's middle age. Geology 42, 503–506. https://doi.org/10.1130/G35402.1.
Cawood, P.A., Hawkesworth, C.J., Dhuime, B., 2013. The continental record and the generation of continental crust. Bull. Geol. Soc. Am. 125, 14–32. https://doi.org/10.1130/B30722.1.
Chakrabarti, G., Shome, D., Kumar, S., Stephens, G.M., Kah, L.C., 2014. Carbonate platform development in a Paleoproterozoic extensional basin, Vempalle formation, Cuddapah Basin, India. J. Asian Earth Sci. 91, 263–279. https://doi.org/10.1016/j.jseaes.2013.09.028.
Chen, C.-T.A., Wang, S.-L., 1999. Carbon, alkalinity and nutrient budgets on the East China Sea continental shelf. J. Geophys. Res. 104, 20675–20686. https://doi.org/10.1029/1999jc900055.
Chough, S.K., Lee, H.S., Woo, J., Chen, J., Choi, D.K., Lee, S., Kang, I., Park, T., Han, Z., 2010. Cambrian stratigraphy of the North China Platform: revisiting principal sections in Shandong Province, China. Geosci. J. 14, 235–268. https://doi.org/10.1007/s12303-010-0029-x.
Cloud, P.E., 1962. Behaviour of calcium carbonate in sea water. Geochimica et Cosmochimica Acta 26, 867–874. https://doi.org/10.1016/0016-7037(62)90117-5.
Cloud, P.E., Semikhatov, M.A., 1969. Proterozoic stromatolite zonation. Am. J. Sci. 267, 1017–1061. https://doi.org/10.2475/ajs.267.9.1017.
Cloud, P.E., Wright, L.A., Williams, E.G., Diehl, P., Walter, M.R., 1969. Giant stromatolites and associated vertical tubes from the upper proterozoic noonday dolomite.

Geol. Soc. Am. Bull. 85, 1869–1882.
Clough, J.G., Goldhammer, R.K., 2000. Evolution of the Neoproterozoic Katakturuk Dolomite Ramp Complex, Northeastern Brooks Range. Alaska 67, 209–241. https://doi.org/10.1093/acprof:oso/9780199540914.003.0017.
Coffey, J.M., Flannery, D.T., Walter, M.R., George, S.C., 2013. Sedimentology, stratigraphy and geochemistry of a stromatolite biofacies in the 2.72Ga Tumbiana Formation, Fortescue Group, Western Australia. Precambrian Res. 236, 282–296. https://doi.org/10.1016/j.precamres.2013.07.021.
Cohen, P.A., Macdonald, F.A., 2015. The Proterozoic record of eukaryotes. Paleobiology 41, 610–632. https://doi.org/10.1017/pab.2015.25.
Corsetti, F.A., Lorentz, N.J., Pruss, S.B., 2004. Formerly-aragonite seafloor fans from Neoproterozoic strata, Death valley and southeastern Idaho, United States: implications for “cap carbonate” formation and Snowball earth. Geophys. Monogr. Series 146, 33–44. https://doi.org/10.1029/146GM04.
Corsetti, F.A., Kidder, D.L., Marenco, P.J., 2006. Trends in oolite dolomitization across the Neoproterozoic-Cambrian boundary: a case study from Death Valley, California. Sediment. Geol. 191, 135–150. https://doi.org/10.1016/j.sedgeo.2006.03.021.
Cowan, C.A., 1992. Facies and stratigraphic analysis of an ancient carbonate platform, Upper Cambrian, western Newfoundland. Queen’s University, Canada.
Craddock, P.R., Dauphas, N., 2011. Iron and carbon isotope evidence for microbial iron respiration throughout the Archean. Earth Planet. Sci. Lett. 303, 121–132. https://doi.org/10.1016/j.epsl.2010.12.045.
Creveling, J.R., Fernández-Remolar, D., Rodriguez-Martinez, M., Menéndez, S., Bergmann, K.D., Gill, B.C., Abelson, J., Zone, M., 2013. Geobiology of a Lower Cambrian Carbonate Platform, Pedroche Formation, Ossa Morena Zone, Spain. Citation Accessed Citable Lin. Palaeogeogr. Palaeoclimatol. Palaeoecol. https://doi.org/10.1016/j.palaeo.2013.06.015.
Creveling, J.R., Johnston, D.T., Poulton, S.W., Kotrc, B., März, C., Schrag, D.P., Knoll, A.H., 2014. Phosphorus sources for phosphatic Cambrian carbonates. GSA Bull. 126 (1–2), 145–163. https://doi.org/10.1130/B30819.1.
Creveling, J.R., Bergmann, K.D., Grotzinger, J.P., 2016. Cap carbonate platform facies model, Noonday Formation, SE California. Bull. Geol. Soc. Am. 128, 1249–1269. https://doi.org/10.1130/B31442.1.
Crowe, S.A., Jones, C., Katsev, S., Neill, A.H.O., Sturm, A., Canfield, D.E., Haffner, G.D., Mucci, A., Sundby, B., Fowle, D.A., 2008. Photoferrotrophs thrive in an Archean Ocean analogue. PNAS 105, 1–6.
Dahl, T.W., Hammarlund, E.U., Anbar, A.D., Bond, D.P.G., Gill, B.C., Gordon, G.W., Knoll, A.H., Nielsen, A.T., Schovsbo, N.H., Canfield, D.E., 2010. Devonian rise in atmospheric oxygen correlated to the radiations of terrestrial plants and large predatory fish. Proc. Natl. Acad. Sci. 107, 17911–17915. https://doi.org/10.1073/pnas.1011287107.
Daly, R.A., 1909. First calcareous fossils and the evolution of limestones. Bull. Geol. Soc. Am. 20, 153–170.
De Deckker, P., Last, W.M., 1988. Modern dolomite deposition in continental, saline lakes, western Victoria, Australia. Geology 16, 29–32.
Dewing, K., Harrison, J., Pratt, B.R., Mayr, U., 2004. A probable late Neoproterozoic age for the Kennedy Channel and Ella Bay formations, northeastern Ellesmere Island and its implications for passive margin history of the Canadian Arctic. Can. J. Earth Sci. 41.
Diaz, M.R., Swart, P.K., Eberli, G.P., Oehlert, A.M., Devlin, Q., Saeid, A., Altabet, M.A., 2015. Geochemical evidence of microbial activity within ooids. Sedimentology 62, 2090–2112. https://doi.org/10.1111/sed.12218.
Dilliard, K.A., 2006. Sequence stratigraphy and chemostratigraphy of the lower Cambrian Sewki Formation. Washington State University, Northwest Territories, Canada.
Dongjie, T., Xiaoying, S., Ganqing, J., Yunpeng, P., Wenhao, Z., Yuan, W., Min, L., 2013. Environment controls on Mesoproterozoic thrombolite morphogenesis: a case study from the North China Platform. J. Palaeogeogr. 2, 275–296. https://doi.org/10.3724/SP.J.1261.2013.00031.
Droser, M.L., Finnegan, S., 2003. The Ordovician radiation: a follow-up to the Cambrian explosion? Integ. Comp. Biol. 43, 178–184.
Dunham, R.J., 1962. Classification of carbonate rocks according to depositional textures. In: Classification of Carbonate Rocks–A Symposium.
Dupraz, C., Pattisina, R., Verrecchia, E.P., 2007. Translation of Energy into Morphology : Simulation of Stromatolite Morphospace Using a Stochastic Model. pp. 185–203.
Embry, A.F., Klovan, J.E., 1971. A late Devonian reef tract on northeastern Banks Island, N.W.T. Bull. Can. Petrol. Geol. 19, 730–781.
Eriksson, P.G., 1999. Sea level changes and the continental freeboard concept: general principles and application to the Precambrian. Precambrian Res. 97, 143–154. https://doi.org/10.1016/S0301-9268(99)00029-7.
Erwin, D.H., 2008. Macroevolution of ecosystem engineering, niche construction and diversity. Trends Ecol. Evol. 23, 304–310. https://doi.org/10.1016/j.tree.2008.01.013.
Erwin, D.H., Laflamme, M., Tweedt, S.M., Sperling, E.A., Pisani, D., Peterson, K.J., 2011. The Cambrian conundrum: Early divergence and later ecological success in the early history of animals. Science 334, 1091–1097. https://doi.org/10.1126/science.1206375.
Fairbridge, R.W., 1957. The Dolomite Question: Regional Aspects of Carbonate Deposition. pp. 125–178. https://doi.org/10.2110/pec.57.01.0125.
Fairchild, I.J., 1980. Stages in a Precambrian dolomitization, Scotland: cementing versus replacement textures. Sedimentology 27, 631–650. https://doi.org/10.1111/j.1365-3091.1980.tb01652.x.
Fairchild, I.J., 1983. Effects of glacial transport and neomorphism on Precambrian dolomite crystal sizes. Nature 304, 28–30.
Fairchild, I.J., 1991. Origins of Carbonate in Neoproterozoic Stromatolites and the Identification of Modern Analogues. 53. pp. 281–299.
Fairchild, I.J., Knoll, A.H., Swett, K., 1991. Coastal lithofacies and biofacies associated with syndepositional dolomitization and silicification (Draken Fm, Upper Riphean, Svalbard). Precambrian Res. 53, 165–197.
Farquhar, J., Bao, H., Thiemens, M., 2000. Atmospheric Influence of Earth’s Earliest Sulfur Cycle. Science 289, 756–758.
Feldmann, M., Mckenzie, J.A., 1998. Stromatolite-Thrombolite Associations in a Modern Environment, Lee Stocking Island. Bahamas: Palaios 13, 201–212.
Fischer, W.W., Hemp, J., Johnson, J.E., 2015. Manganese and the evolution of photosynthesis. Orig. Life Evol. Biosph. 45, 351–357. https://doi.org/10.1007/s11084-015-9442-5.
Fischer, W.W., Hemp, J., Johnson, J.E., 2016. Evolution of oxygenic photosynthesis. Ann. Rev. Earth Planet. Sci. 44, 647–683. https://doi.org/10.1146/annurev-earth-060313-054810.
Furniss, G., Rittel, J.F., Winston, D., 1998. Gas bubble and expansion crack origin of “molar-tooth” calcite structures in the Middle Proterozoic Belt Supergroup, western Montana. J. Sediment. Res. 68, 104–114.
Galer, S.J.G., 1991. Interrelationships between continental freeboard, tectonics and mantle temperature. Earth Planet. Sci. Lett. 105, 214–228. https://doi.org/10.1016/0012-821X(91)90132-2.
Gallagher, K.L., Kading, T.J., Braissant, O., Dupraz, C., Visscher, P.T., 2012. Inside the alkalinity engine: the role of electron donors in the organomineralization potential of sulfate-reducing bacteria. Geobiology 10, 518–530. https://doi.org/10.1111/j.1472-4669.2012.00342.x.
Garrels, R.M., Perry, E.A., Mackenzie, F.T., 1973. Genesis of Precambrian iron-formations and the development of atmospheric oxygen. Geology 68, 1173–1179.
Gaucher, C., 2000. Sedimentology, palaeontology, and stratigraphy of the Arroyo del Soldado group (Vendian to Cambrian, Uruguay): Beringeria.
Gaucher, E.A., Govindarajan, S., Ganesh, O.K., 2008. Palaeotemperature trend for Precambrian life inferred from resurrected proteins. Nature 451, 704–707. https://doi.org/10.1038/nature06510.
Gebelein, C.D., 1969. Distribution, morphology and accretion rate of recent subtidal algal stromatolites, Bermuda. J. Sediment. Petrol. 39, 49–69.
Gill, B.C., Lyons, T.W., Young, S.A., Kump, L.R., Knoll, A.H., Saltzman, M.R., 2011. Geochemical evidence for widespread euxinia in the Later Cambrian ocean. Nature 469, 80–83. https://doi.org/10.1038/nature09700.
Gischler, E., Zingeler, D., 2002. The origin of carbonate mud in isolated carbonate platforms of Belize, Central America. Int. J. Earth Sci. 91, 1054–1070. https://doi.org/10.1007/s00531-002-0288-5.
Gischler, E., Dietrich, S., Harris, D., Webster, J.M., Ginsburg, R.N., 2013. A comparative study of modern carbonate mud in reefs and carbonate platforms: mostly biogenic, some precipitated. Sediment. Geol. 292, 36–55. https://doi.org/10.1016/j.sedgeo.2013.04.003.
Given, R.K., Wilkinson, B.H., 1987. Dolomite abundance and stratigraphic age; constraints on rates and mechanisms of Phanerozoic dolostone formation; discussion and reply. J. Sediment. Petrol. 57, 1068–1078. https://doi.org/10.1306/212f8f3f-2b24-11d7-8648000102c1865d.
Gomez, F.J., Astini, R.A., 2015. Sedimentology and sequence stratigraphy from a mixed (carbonate-siliciclastic) rift to passive margin transition: The early to middle Cambrian of the Argentine Precordillera. Sediment. Geol. https://doi.org/10.1016/j.sedgeo.2014.11.003.
Griffith, D.M., Veech, J.A., Marsh, C.J., 2016. Cooccur: Probabilistic Species Co-Occurrence Analysis in R. J. Stat. Softw. 69, 1–17. https://doi.org/10.18637/jss.v069.c02.
Grotzinger, J.P., 1981. The stratigraphy and sedimentation of the Wallace Formation, Northwestern Montana and Northern. University of Montana, Idaho. https://doi.org/10.1613/jair.301.
Grotzinger, J.P., 1985. Evolution of Early Proterozoic Passive-Margin Carbonate Platform. Rocknest Formation, Wopmay Orogen, N.W.T., Canada.
Grotzinger, J.P., 1989. Facies and evolution of the Precambrian carbonate depositional systems: emergence of the modern platform archetype. In: Controls on carbonate platform and basin development.
Grotzinger, J.P., James, N.P., 2000. Precambrian Carbonates: Evolution of Understanding: Carbonate Sedimentation and Diagenesis in the Evolving Precambrian World. pp. 3–20. https://doi.org/10.2110/pec.00.67.
Grotzinger, J.P., Kasting, J.F., 1993. New constraints on Precambrian Ocean composition. J. Geol. 101, 235–243. https://doi.org/10.1086/648218.
Grotzinger, J.P., Knoll, A.H., 1999. Stromatolites in Precambrian carbonates: evolutionary mileposts or environmental dipsticks? Ann. Rev. Earth Planet. Sci. 27, 313–358. https://doi.org/10.1146/annurev.earth.27.1.313.
Grotzinger, J.P., Read, J.F., 1983. Evidence for primary aragonite precipitation, lower Proterozoic (1.9 Ga) Rocknest dolomite, Wopmay orogen, northwest Canada. Geology 11, 710–713. https://doi.org/10.1130/0091-7613(1983)11<710:EFPAPL>2.0.CO;2.
Grotzinger, J.P., Rothman, D.H., 1996. An abiotic model for stromatolite morphogenesis. Nature 383, 423–425. https://doi.org/10.1038/383423a0.
Grotzinger, J.P., McCormick, D.S., Peletchaty, S.M., 1987. Progress report on the stratigraphy, sedimentology and significance of the Kimerot and Bear Creek groups, Kilohigok Basin, District of Mackenzie. Geol. Surv. Canada Curr. Res. 87, 219–238.
Halevy, I., Bachan, A., 2017. The geologic history of seawater pH. Science 355, 1069–1071.
Halverson, G.P., Kunzmann, M., Strauss, J.V., Maloof, A.C., 2018. The Tonian-Cryogenian transition in Northeastern Svalbard. Precambrian Res. 319, 79–95. https://doi.org/10.1016/j.precamres.2017.12.010.
Hammarlund, E.U., Smith, M.P., Rasmussen, J.A., Nielsen, A.T., Canfield, D.E., Harper, D.A.T., 2019. The Sirius Passet Lagerstätte of North Greenland—A geochemical window on early Cambrian low-oxygen environments and ecosystems. Geobiology 17, 12–26. https://doi.org/10.1111/gbi.12315.

Hannisdal, B., Peters, S.E., 2011. Phanerozoic earth system evolution and marine biodiversity. Science 334, 1121–1124.
Hardie, L.A., 2003. Secular variations in Precambrian seawater chemistry and the timing of Precambrian aragonite seas and calcite seas. Geology 31, 785–788. https://doi.org/10.1130/G19657.1.
Harper, D.A.T., 2006. The Ordovician biodiversification: setting an agenda for marine life: Palaeogeography, Palaeoclimatology. Palaeoecology 232, 148–166. https://doi.org/10.1016/j.palaeo.2005.07.010.
Harwood, C.L., 2013. Microbial And Metazoan Influences on Microbialite Growth Structures : Insights from Recent Lacustrine Microbialites in Pavilion Lake, BC, and Cambrian Thrombolites from the Great Basin, CA and NV. University of California Davis.
Harwood, C.L., Sumner, D.Y., 2011. Microbialites of the Neoproterozoic Beck Spring Dolomite, Southern California. Sedimentology 58, 1648–1673. https://doi.org/10.1111/j.1365-3091.2011.01228.x.
Harwood, C.L., Sumner, D.Y., 2012. Origins of microbial microstructures in the Neoproterozoic Beck Spring Dolomite: variations In microbial community and timing of lithification. J. Sediment. Res. 82, 709–722. https://doi.org/10.2110/jsr.2012.65.
Harwood Theisen, C., Sumner, D.Y., 2016. Thrombolite fabrics and origins: Influences of diverse microbial and metazoan processes on Cambrian thrombolite variability in the Great Basin, California and Nevada. Sedimentology 63, 2217–2252. https://doi.org/10.1111/sed.12304.
Hendry, J.P., 1993. Calcite cementation during bacterial manganese, iron and sulphate reduction in Jurassic shallow marine carbonates. Sedimentology 40, 87–106. https://doi.org/10.1111/j.1365-3091.1993.tb01093.x.
Higgins, J.A., Fischer, W.W., Schrag, D.P., 2009. Oxygenation of the ocean and sediments: consequences for the seafloor carbonate factory. Earth Planet. Sci. Lett. 284, 25–33. https://doi.org/10.1016/j.epsl.2009.03.039.
Hodgskiss, M.S.W., Kunzmann, M., Poirier, A., Halverson, G.P., 2018. The role of microbial iron reduction in the formation of Proterozoic molar tooth structures. Earth Planet. Sci. Lett. 482, 1–11. https://doi.org/10.1016/j.epsl.2017.10.037.
Hoffman, P.F., 1968. Stratigraphy of the lower Proterozoic (Aphebian). Great Slave Supergroup, East Arm of Great Slave Lake, District of Mackenzie, pp. 100.
Hoffman, P., 1969. Proterozoic Paleocurrents and Depositional History of the East Arm Fold Belt. Great Slave Lake, Northwest Territories.
Hoffman, P.F., 2013. The Great Oxidation and a Siderian snowball Earth: MIF-S based correlation of Paleoproterozoic glacial epochs. Chem. Geol. 362, 143–156. https://doi.org/10.1016/j.chemgeo.2013.04.018.
Hoffman, P.F., Schrag, D.P., 2002. The snowball Earth hypothesis: testing the limits of global change. Terra 14, 129–155. https://doi.org/10.1080/713604466.
Hoffman, P.F., Kaufman, A.J., Halverson, G.P., 1999. Comings and Goings of Global Glaciations on a Neoproterozoic Tropical Platform in Namibia. GSA Today 9, 1–7. https://doi.org/10.1130/GSAT01707GW.1.
Hoffman, P.F., Halverson, G.P., Domack, E.W., Husson, J.M., Higgins, J.A., Schrag, D.P., 2007. Are basal Ediacaran (635 Ma) post-glacial "cap dolostones" diachronous? Earth Planet. Sci. Lett. 258, 114–131. https://doi.org/10.1016/j.epsl.2007.03.032.
Hoffman, P.F., et al., 2017. Snowball Earth Climate Dynamics and Cryogenian Geology-Geobiology.
Hofmann, H.J., 1973. Stromatolites: characteristics and Utility. Earth Sci. Rev. 9, 339–373.
Hofmann, H.J., Jackson, G.D., 1987. Proterozoic ministromatolites with radial-fibrous fabric. Sedimentology 34, 963–971. https://doi.org/10.1111/j.1365-3091.1987.tb00586.x.
Hofmann, A., Dirks, P.H.G.M., Jelsma, H.A., 2004. Shallowing-Upward Carbonate Cycles in the Belingwe Greenstone Belt, Zimbabwe: A Record of Archean Sea-Level Oscillations. J. Sediment. Res. 74, 64–81. https://doi.org/10.1306/052903740064.
Hofmann, M., Linnemann, U., Hoffmann, K., Germs, G., 2014. The four Neoproterozoic glaciations of southern Namibia and their detrital zircon record: The fingerprints of four crustal growth events during two supercontinent cycles. Precambrian Res. https://doi.org/10.1016/j.precamres.2014.07.021.
Holland, H.D., 1999. When did the Earth's atmosphere become oxic? A Reply. Geochem. News 100, 20–22.
Holland, H.D., 2006. The origin of the atmosphere and of the oceans. Philos. Trans. R. Soc. B 361, 903–915. https://doi.org/10.1007/3-540-33088-7_2.
Holland, H.D., Zimmermann, H., 2000. The dolomite problem revisited. Int. Geol. Rev. 42, 481–490. https://doi.org/10.1080/00206810009465093.
Horodyski, R.J., 1976. Stromatolites from the Middle Proterozoic Altyn Limestone, Belt Supergroup, Glacier National Park, Montana. Dev. Sedimentol. 20, 585–597.
Horodyski, R.J., 1977. Environmental Influences on Columnar Stromatolite Branching Patterns: Examples from the Middle Proterozoic Belt Supergroup, Glacier National Park, Montana. J. Paleontol. 51.
Hoshino, Y., et al., 2017. Cryogenian evolution of stigmasterol biosysnthesis. Sci. Adv. 3. https://doi.org/10.1126/sciadv.1700887.
Hren, M.T., Tice, M.M., Chamberlain, C.P., 2009. Oxygen and hydrogen isotope evidence for a temperate climate 3.42 billion years ago. Nature 462, 205–208. https://doi.org/10.1038/nature08518.
Hsu, K.J., 1966. Origin of Dolomite in Sedimentary Sequences: A Critical Analysis: Criteria for Dolomite Stability: Mineralium Deposita. 138.
Hsu, K.J., Siegenthaler, C., 1969. Preliminary Experiments on Hydrodynamic Movement induced by evaporation and their bearing on the dolomite problem. Sedimentology 12, 11–25.
Hu, X., Burdige, D.J., 2008. Shallow marine carbonate dissolution and early diagenesis—Implications from an incubation study. J. Mar. Res. 66, 489–527.
Hulth, S., Aller, R.C., Gilbert, F., 1999. Coupled anoxic nitrification/manganese reduction in marine sediments. Geochimica et Cosmochimica Acta 63, 49–66. https://doi.org/10.1016/S0016-7037(98)00285-3.
Hurtgen, M.T., Halverson, G.P., Arthur, M.A., Hoffman, P.F., 2006. Sulfur cycling in the aftermath of a 635-Ma snowball glaciation: Evidence for a syn-glacial sulfidic deep ocean. Earth Planet. Sci. Lett. 245, 551–570.
Husson, J.M., Peters, S.E., 2017. Atmospheric oxygenation driven by unsteady growth of the continental sedimentary reservoir. Earth Planet. Sci. Lett. 460, 68–75. https://doi.org/10.1016/j.epsl.2016.12.012.
Husson, J.M., Peters, S.E., 2018. Nature of the sedimentary rock record and its implications for Earth system evolution: Emerging Topics in Life Sciences. ETLS20170152. https://doi.org/10.1042/ETLS20170152.
James, N.P., Narbonne, G.M., Sherman, A.G., 1998. Molar-tooth carbonates: shallow subtidal facies of the mid- to late Proterozoic - reply. J. Sediment. Res. 68, 716–722. https://doi.org/10.2110/jsr.68.716.
James, N.P., Narbonne, G.M., Kyser, T.K., 2001. Late Neoproterozoic cap carbonates: Mackenzie Mountains, northwestern Canada: precipitation and global glacial meltdown. Can. J. Earth Sci. 38, 1229–1262. https://doi.org/10.1139/e01-046.
James, N.P., Narbonne, G.M., Sherman, A.G., 2012. Molar-tooth carbonates: shallow subtidal facies of the mid- to late Proterozoic. J. Sediment. Res. 68, 716–722. https://doi.org/10.2110/jsr.68.716.
Jiang, G., Christie-Blick, N., Kaufman, A.J., Banerjee, D.M., Rai, V., 2002. Sequence stratigraphy of the Neoproterozoic Infra Krol Formation and Krol Group, Lesser Himalaya, India. J. Sediment. Res. 72, 524–542. https://doi.org/10.1306/120301720524.
Jiang, G., Christie-Blick, N., Kaufman, A.J., Banerjee, D.M., Rai, V., 2003. Carbonate platform growth and cyclicity at a terminal Proterozoic passive margin, Infra Krol Formation and Krol Group, Lesser Himalaya, India. Sedimentology 50, 921–952. https://doi.org/10.1046/j.1365-3091.2003.00589.x.
Jiang, G., Kaufman, A.J., Christie-Blick, N., Zhang, S., Wu, H., 2007. Carbon isotope variability across the Ediacaran Yangtze platform in South China: Implications for a large surface-to-deep ocean ?δ13C gradient. Earth Planet. Sci. Lett. 261, 303–320. https://doi.org/10.1016/j.epsl.2007.07.009.
Johnson, J.E., Webb, S.M., Thomas, K., Ono, S., Kirschvink, J.L., Fischer, W.W., 2013. Manganese-oxidizing photosynthesis before the rise of cyanobacteria. Proc. Natl. Acad. Sci. 110, 11238–11243. https://doi.org/10.1073/pnas.1305530110.
Johnston, D.T., Wing, B.A., Farquhar, J., Kaufman, A.J., Strauss, H., Lyons, T.W., Kah, L.C., Canfield, D.E., 2005. Active microbial sulfur disproportionation in the Mesoproterozoic. Science 310, 1477–1479. https://doi.org/10.1126/science.1117824.
Jones, D.S., Maloof, A.C., Hurtgen, M.T., Rainbird, R.H., Schrag, D.P., 2010. Regional and global chemostratigraphic correlation of the early Neoproterozoic Shaler Supergroup, Victoria Island, Northwestern Canada. Precambrian Res. 181, 43–63. https://doi.org/10.1016/j.precamres.2010.05.012.
Kah, L.C., 1997. Sedimentological, geochemical, and paleobiological interactions on a Mesoproterozoic carbonate platform: Society Cliffs Formation. Northern Baffin Island, Arctic Canada, pp. 298.
Kah, L.C., 2000. Depositional δ 18 O Signatures in Proterozoic Dolostones: Constraints on Seawater Chemistry and Early Diagenesis. SEPM Special Publication 67, 345–360. https://doi.org/10.2110/pec.00.67.0345.
Kah, L.C., Grotzinger, J.P., 1992. Early Proterozoic (1.9 Ga) thrombolites of the Rocknest Fm, NW Territories, Canada: Palaios. Palaios 7, 305–315.
Kah, L.C., Knoll, A.H., 1996. Microbenthic distribution of Proterozoic tidal flats: environmental and taphonomic considerations. Geology 24, 79–82. https://doi.org/10.1130/0091-7613(1996)024<0079:MDOPTF>2.3.CO;2.
Kah, L.C., Sherman, A.G., Narbonne, G.M., Knoll, A.H., Kaufman, A.J., 1999. δ ^{13}C stratigraphy of the Proterozoic Bylot Supergroup, Baffin Island, Canada: implications for regional lithostratigraphic correlations. Can. J. Earth Sci. 36, 313–332. https://doi.org/10.1139/e98-100.
Kah, L.C., Lyons, T.W., Frank, T.D., 2004. Low marine sulphate and protracted oxygenation of the Proterozoic biosphere. Nature 431, 834–838. https://doi.org/10.1038/nature02974.
Kah, L.C., Bartley, J.K., Frank, T., Lyons, T.W., 2006. Reconstructing sea-level change from the internal architecture of stromatolite reefs: an example from the Mesoproterozoic Sulky Formation, Dismal Lakes Group, arctic Canada. Can. J. Earth Sci. 43.
Kah, L.C., Bartley, J.K., Stagner, A.F., 2009. Reinterpreting a Proterozoic enigma: Conophyton – Jacutophyton. Africa 277–296.
Kah, L.C., Bartley, J.K., Teal, D.A., 2012. Chemostratigraphy of the Late Mesoproterozoic Atar Group, Taoudeni Basin, Mauritania: Muted isotopic variability, facies correlation, and global isotopic trends. Precambrian Res. 200–203, 82–103. https://doi.org/10.1016/j.precamres.2012.01.011.
Kappler, A., Pasquero, C., Konhauser, K.O., Newman, D.K., 2005. Deposition of banded iron formations by anoxygenic phototrophic Fe(II)-oxidizing bacteria. Geology 33, 865–868. https://doi.org/10.1130/G21658.1.
Kastner, M., 1983. Origin of Dolomite and Its Spatial and Chronological Distribution–A new insight. AAPG Bull. 67 (11), 2156.
Kaufman, A.J., Knoll, A.H., Semikhatov, M.A., Grotzinger, J.P., Jacobsen, S.B., Adams, W., 1996. Integrated chronostratigraphy of Proterozoic–Cambrian boundary beds in the western Anabar region, northern Siberia. Geol. Mag. 133, 509–533. https://doi.org/10.1017/s0016756800007810.
Kearns, C., 1982. Sedimentology and stratigraphy of the Dismal Lakes Group, Proterozoic. Northwest Territories.
Kearns, C., 1983. Sedimentology and Stratigraphy of the Dismal Lakes Group. Carleton University.
Keller, C.B., Husson, J.M., Mitchell, R.N., Bottke, W.F., Gernon, T.M., Boehnke, P., Bell, E.A., Swanson-Hysell, N.L., Peters, S.E., 2019. Neoproterozoic glacial origin of the Great Unconformity. Proc. Natl. Acad. Sci. 116, 1136–1145. https://doi.org/10.1073/pnas.1804350116.

Kempe, S., Degens, E.T., 1985. An Early Soda Ocean? Chem. Geol. 53, 95–108.
Kennard, J.M., James, N.P., 1986. Thrombolites and stromatolites: two distinct types of microbial structures. PALAIOS 1, 492–503. https://doi.org/10.2307/3514631.
Kirschvink, J.L., Gaidos, E.J., Bertani, L.E., Beukes, N.J., Gutzmer, J., Maepa, L.N., Steinberger, R.E., 2000. Paleoproterozoic snowball Earth: extreme climatic and geochemical global change and its biological consequences. Proc. Natl. Acad. Sci. 97, 1400–1405. https://doi.org/10.1073/pnas.97.4.1400.
Klaebe, R.M., Smith, M.P., Fairchild, I.J., Fleming, E.J., Kennedy, M.J., 2018. Facies-dependent δ13C variation and diagenetic overprinting at the onset of the Sturtian glaciation in North-East Greenland. Precambrian Res. 319, 96–113.
Knauth, L.P., 2005. Temperature and salinity history of the Precambrian ocean: implications for the course of microbial evolution: Palaeogeography. Palaeoclimatol. Palaeoecol. 219, 53–69. https://doi.org/10.1016/j.palaeo.2004.10.014.
Knoll, A.H., 2003. Biomineralization and Evolutionary History. Rev. Mineral. Geochem. 54, 329–356. https://doi.org/10.2113/0540329.
Knoll, A.H., 2011. The multiple origins of complex multicellularity. Ann. Rev. Earth Planet. Sci. 39, 217–239. https://doi.org/10.1146/annurev.earth.031208.100209.
Knoll, A.H., 2015. Paleobiological perspectives on early microbial evolution. Cold Spring Harb. Perspect. Biol. 7, 1–17. https://doi.org/10.1101/cshperspect.a018093.
Knoll, A.H., Beukes, N.J., 2009. Introduction: Initial investigations of a Neoarchean shelf margin-basin transition (Transvaal Supergroup, South Africa). Precambrian Res. 169 (1-4), 1–14.
Knoll, A.H., Semikhatov, M.A., 1998. The genesis and time distribution of two distinctive Proterozoic stromatolite microstructures. Palaios 13, 408–422. https://doi.org/10.1043/0883-1351(1998)013<0408:TGATDO>2.0.CO;2.
Knoll, A.H., Swett, K., 1990. Carbonate deposition during the late Proterozoic era: an example from Spitsbergen. Am. J. Sci. 290, 104–132.
Knoll, A.H., Javaux, E.J., Hewitt, D., Cohen, P., 2006. Eukaryotic organisms in Proterozoic oceans. Philos. Trans. R. Soc. B 361, 1023–1038. https://doi.org/10.1098/rstb.2006.1843.
Knoll, A.H., Worndle, S., Kah, L.C., 2013. Covariance of microfossil assemblages and microbialite textures across a late Mesoproterozoic carbonate platform. Palaios 28, 453–470. https://doi.org/10.2110/palo.2013.p13-005r.
Knoll, A.H., Bergmann, K.D., Strauss, J.V., Knoll, A.H., 2016. Life : The First Two Billion Years.
Konhauser, K.O., Hamade, T., Raiswell, R., Morris, R.C., Southam, G., Canfield, D.E., Konhauser, K.O., Grant Ferris, F., 2002. Could bacteria have formed the Precambrian banded iron formations? Geology 30, 1079. https://doi.org/10.1130/0091-7613(2002)030<1079:cbhftp>2.0.co;2.
Konhauser, K.O., Amskold, L., Lalonde, S.V., Posth, N.R., Kappler, A., Anbar, A., 2007. Decoupling photochemical Fe(II) oxidation from shallow-water BIF deposition. Earth Planet. Sci. Lett. 258, 87–100. https://doi.org/10.1016/j.epsl.2007.03.026.
Korenaga, J., Planavsky, N.J., Evans, D.A.D., 2017. Global water cycle and the coevolution of the Earth's interior and surface environment. Philos. Trans. R. Soc. A 375. https://doi.org/10.1098/rsta.2015.0393.
Krapez, B., Muller, S.G., Bekker, A., 2015. Stratigraphy of the Late Palaeoproterozoic (~2.03Ga) Wooly Dolomite, Ashburton Province, Western Australia: A carbonate platform developed in a failed rift basin. Precambrian Res. 271, 1–19. https://doi.org/10.1016/j.precamres.2015.09.022.
Krause, A.J., Poulton, S.W., Planavsky, N.J., Lenton, T.M., 2018. Stepwise oxygenation of the Paleozoic atmosphere. Nat. Commun. 1–10. https://doi.org/10.1038/s41467-018-06383-y.
Kuivila, K.M., Murray, J.W., 1984. Organic matter diagenesis in freshwater sediments: The alkalinity and total CO2 balance and methane production in the sediments of Lake Washington. Limnol. Oceanogr. 29, 1218–1230. https://doi.org/10.4319/lo.1984.29.6.1218.
Kump, L.R., 2008. The rise of atmospheric oxygen. Nature 451, 277–278. https://doi.org/10.1038/nature06587.
Kump, L.R., Brantley, S.L., Arthur, M.A., 2000. Chemical Weathering, Atmospheric CO2, and Climate. Ann. Rev. Earth Planet. Sci. 28, 611–667.
Kump, L.R., Kasting, J.F., Barley, M.E., 2001. Rise of atmospheric oxygen and the ``up-side-down" Archean mantle. Geochem. Geophys. Geosyst. 2.
Kunzmann, M., Gibson, T.M., Halverson, G.P., Hodgskiss, M.S.W., Bui, T.H., Carozza, D.A., Sperling, E.A., Poirier, A., Cox, G.M., Wing, B.A., 2017. Iron isotope biogeochemistry of Neoproterozoic marine shales. Geochimica et Cosmochimica Acta 209, 85–105.
Kurzweil, F., Wille, M., Gantert, N., Beukes, N.J., Schoenberg, R., 2016. Manganese oxide shuttling in pre-GOE oceans – evidence from molybdenum and iron isotopes. Earth Planet. Sci. Lett. 452, 69–78. https://doi.org/10.1016/j.epsl.2016.07.013.
Lamb, M.P., Fischer, W.W., Raub, T.D., Perron, J.T., Myrow, P.M., 2012. Origin of giant wave ripples in snowball Earth cap carbonate. Geology 40, 827–830.
Le Hir, G., Donnadieu, Y., Goddéris, Y., Pierrehumbert, R.T., Halverson, G.P., Macouin, M., Nédélec, A., Ramstein, G., 2009. The snowball Earth aftermath: exploring the limits of continental weathering processes. Earth Planet. Sci. Lett. 277, 453–463. https://doi.org/10.1016/j.epsl.2008.11.010.
Lee, C.T.A., Yeung, L.Y., McKenzie, N.R., Yokoyama, Y., Ozaki, K., Lenardic, A., 2016. Two-step rise of atmospheric oxygen linked to the growth of continents. Nat. Geosci. 9, 417–424. https://doi.org/10.1038/ngeo2707.
Li, Z.X., et al., 2008. Assembly, configuration, and break-up history of Rodinia: a synthesis. Precambrian Res. 160, 179–210. https://doi.org/10.1016/j.precamres.2007.04.021.
Liu, C., Knoll, A.H., Hazen, R.M., 2017. Geochemical and mineralogical evidence that Rodinian assembly was unique. Nat. Commun. 8, 1–7. https://doi.org/10.1038/s41467-017-02095-x.
Lovley, D.R., 1987. Organic matter mineralization with the reduction of ferric iron: a review. Geomicrobiol. J. 5, 375–399. https://doi.org/10.1080/01490458709385975.
Lowenstam, H.A., Epstein, S., 1957. On the Origin of Sedimentary Aragonite Needles of the Great Bahama Bank. J. Geol. 65, 364–375.
Lyons, T.W., Reinhard, C.T., Planavsky, N.J., 2014. The rise of oxygen in Earth's early ocean and atmosphere. Nature 506, 307–315. https://doi.org/10.1038/nature13068.
MacIntyre, I.G., Reid, R.P., 1992. Comment on the Origin of Aragonite Needle Mud: A Picture is Worth a Thousand Words. SEPM J. Sediment. Res. 62, 1095–1097. https://doi.org/10.1306/d4267a5a-2b26-11d7-8648000102c1865d.
Mackenzie, F.T., Pigott, J.D., 1982. Tectonic controls of Phanerozoic sedimentary rock cycling. J. Geol. Soc. Lond. 138, 183–196. https://doi.org/10.1144/gsjgs.138.2.0183.
Mackey, T.J., Sumner, D.Y., Hawes, I., Jungblut, A.D., Lawrence, J., Leidman, S., Allen, B., 2017. Increased mud deposition reduces stromatolite complexity. Geology 45, 663–666. https://doi.org/10.1130/G38890.1.
Maloof, A.C., Porter, S.M., Moore, J.L., Dudás, F.Ö., Bowring, S.A., Higgins, J.A., Fike, D.A., Eddy, M.P., 2010a. The Earliest Cambrian Record of Animals and Ocean Geochemical Change. pp. 1731–1774. https://doi.org/10.1130/B30346.1.
Maloof, A.C., Ramezani, J., Bowring, S.A., Fike, D.A., Porter, S.M., Mazouad, M., 2010b. Constraints on early Cambrian carbon cycling from the duration of the Nemakit-Daldynian-Tommotian boundary? δ13C shift, Morocco. Geology. https://doi.org/10.1130/G30726.1.
Mángano, M.G., Buatois, L.A., 2016. The Cambrian Explosion. In: The Trace-Fossil Record of Major Evolutionary Events. 39. pp. 73–126. https://doi.org/10.1007/978-94-017-9600-2.
Mángano, M.G., Buatois, L.A., Wilson, M.A., Droser, M.L., 2016. The Great Ordovician Biodiversification event: The Trace-Fossil Record of Major Evolutionary Events. pp. 127–156. https://doi.org/10.1007/978-94-017-9600-2.
Martindale, R.C., et al., 2015. Sedimentology, chemostratigraphy, and stromatolites of lower Paleoproterozoic carbonates, Turee Creek Group, Western Australia. Precambrian Res. 266, 194–211. https://doi.org/10.1016/j.precamres.2015.05.021.
McIntyre, T., Fralick, P., 2017. Sedimentology and Geochemistry of the 2930 Ma Red Lake-Wallace Lake Carbonate Platform, Western Superior Province, Canada. Depos. Rec. 3, 258–287. https://doi.org/10.1002/dep2.36.
Medig, K.P.R., Turner, E.C., Thorkelson, D.J., Rainbird, R.H., 2016. Rifting of Columbia to form a deep-water siliciclastic to carbonate succession: The Mesoproterozoic Pinguicula Group of northern Yukon. Precambrian Research, Canada. https://doi.org/10.1016/j.precamres.2016.03.021.
Melezhik, V.A., Prave, A.R., Hanski, E.J., Fallick, A.E., Lepland, A., Kump, L.R., Strauss, H., 2013. Reading the Archive of Earth's Oxygenation: Volume 2: The Core Archive of the Fennoscandian Arctic Russia - Drilling Early Earth Project.
Merdith, A.S., et al., 2017. A full-plate global reconstruction of the Neoproterozoic. Gondwana Res. 50, 84–134. https://doi.org/10.1016/j.gr.2017.04.001.
Meysman, F.J.R., Middelburg, J.J., Heip, C.H.R., 2006. Bioturbation: a fresh look at Darwin's last idea. Trends Ecol. Evol. 21, 688–695. https://doi.org/10.1016/j.tree.2006.08.002.
Milliman, J.D., 1993. Production and accumulation of calcium carbonate in the ocean: Budget of a nonsteady state. Global Biogeochem. Cycles 7, 927–957. https://doi.org/10.1029/93GB02524.
Milliman, J.D., Freile, D., Steinen, R.P., Wilber, R.J., 1993. Great Bahama Bank aragonitic muds; mostly inorganically precipitated, mostly exported; discussion and reply. J. Sediment. Res. 63, 589–595. https://doi.org/10.2110/jsr.64.921.
Montanez, I.P., Osleger, D.A., 1993. Parasequence Stacking Patterns, Third-Order Accommodation Events, and Sequence Stratigraphy of Middle to Upper Cambrian Platform Carbonates, Bonanza King Formation, Southern Great Basin. In: Carbonate Sequence Stratigraphy: Recent Developments and Applications.
Morse, J.W., Gledhill, D.K., Millero, F.J., 2003. CaCO3 precipitation kinetics in waters from the Great Bahama Bank: implications for the relationship between Bank hydrochemistry and whitings. Geochimica et Cosmochimica Acta 67, 2819–2826. https://doi.org/10.1016/S0016-7037(03)00103-0.
Morse, J.W., Arvidson, R.S., Lüttge, A., 2007. Calcium carbonate formation and dissolution. Chem. Rev. 107, 342–381. https://doi.org/10.1021/cr050358j.
Murphy, M.A., Sumner, D.Y., 2008. Variations in Neoarchean microbialite morphologies: clues to controls on microbialite morphologies through time. Sedimentology 55, 1189–1202. https://doi.org/10.1111/j.1365-3091.2007.00942.x.
Narbonne, G.M., James, N.P., 1996. Mesoproterozoic deep-water reefs from Borden Peninsula, Arctic Canada. Sedimentology 43, 827–848.
Nealson, K.H., Myers, C.R., 1992. Microbial reduction of manganese and iron: New approaches to carbon cycling. Appl. Environ. Microbiol. 58, 439–443.
Neumann, A.C., Land, L.S., 1975. Lime mud deposition and calcareous algae in the Bight of Abaco, Bahamas: A Budget. J. Sediment. Petrol. 45, 763–786.
O'Connell, L.G., James, N.P., 2015. Composition and Genesis of Temperate: Shallow-Marine Carbonate Muds: Spencer Gulf, South Australia. J. Sediment. Res. 85, 1275–1291. https://doi.org/10.2110/jsr.2015.73.
O'Reilly, S.S., Mariotti, G., Winter, A.R., Newman, S.A., Matys, E.D., McDermott, F., Pruss, S.B., Bosak, T., Summons, R.E., Klepac-Ceraj, V., 2017. Molecular biosignatures reveal common benthic microbial sources of organic matter in ooids and grapestones from Pigeon Cay, The Bahamas. Geobiology 15, 112–130. https://doi.org/10.1111/gbi.12196.
Osburn, M., Grotzinger, J., Bergmann, K., 2014. Facies, stratigraphy, and evolution of a middle ediacaran carbonate ramp: Khufai formation, sultanate of Oman. AAPG Bull. 98, 1631–1667.
Osburn, M.R., Owens, J., Bergmann, K.D., Lyons, T.W., 2015. Dynamic changes in sulfate sulfur isotopes preceding the Ediacaran Shuram Excursion. Geochimica et Cosmochimica Acta 170, 204–224.
Pacton, M., Ariztegui, D., Wacey, D., Kilburn, M.R., Rollion-Bard, C., Farah, R., Vasconcelos, C., 2012. Going nano: A new step toward understanding the processes

governing freshwater ooid formation. Geology 40, 547–550. https://doi.org/10.1130/G32846.1.
Parfrey, L.W., Lahr, D.J.G., Knoll, A.H., Katz, L.A., 2011. Estimating the timing of early eukaryotic diversification with multigene molecular clocks. Proc. Natl. Acad. Sci. 108, 13624–13629. https://doi.org/10.1073/pnas.1110633108.
Peryt, T., 1983. Classification of coated grains. In: Coated grains. Springer, Berlin, Heidelberg, pp. 3–6. https://doi.org/10.1007/978-3-642-10415-2.
Peters, S.E., 2006. Macrostratigraphy of North America. J. Geol. 114, 391–412.
Peters, S.E., Gaines, R.R., 2012. Formation of the 'Great Unconformity' as a trigger for the Cambrian explosion. Nature 484, 363–366. https://doi.org/10.1038/nature10969.
Peters, S.E., Husson, J.M., 2017. Sediment cycling on continental and oceanic crust. Geology 45, 323–326. https://doi.org/10.1130/G38861.1.
Peters, S.E., Husson, J.M., Wilcots, J., 2017. The rise and fall of stromatolites in shallow marine environments. Geology 45, 487–490. https://doi.org/10.1130/G38931.1.
Petrov, P.Y., Semikhatov, M.A., 2009. Platforms: Shorikha formation of the Turukhansk uplift, Siberia. Stratigr. Geol. Corr. 17, 461–475. https://doi.org/10.1134/S0869593809050013.
Pfeil, P.W., Read, J.F., 1980. Cambrian carbonate platform margin facies, Shady Dolomite, southwestern Virgina, USA. J. Sediment. Petrol. 50, 91–116.
Pierrehumbert, R.T., 2005. High levels of atmospheric carbon dioxide necesarry for the termination of global glaciation. Nature 429, 646–649. https://doi.org/10.1038/nature02571.1.
Pigott, J.D., 1981. Global Tectonic Control of Secular Variations in Phanerozoic Sedimentary Rock/Ocean/Atmosphere Chemistry. Northwestern University, pp. 196.
Planavsky, N.J., Ginsburg, R.N., 2009. Taphonomy of Modern Marine Bahamian Microbialites. Palaios 24, 5–17. https://doi.org/10.2110/palo.2008.p08-001r.
Pollock, M.D., Kah, L.C., Bartley, J.K., 2006. Morphology of Molar-Tooth Structures in Precambrian Carbonates: influence of Substrate Rheology and Implications for Genesis. J. Sediment. Res. 76, 310–323. https://doi.org/10.2110/jsr.2006.021.
Pope, M.C., Grotzinger, J.P., 2000. Controls on fabric development and morphology of tufas and stromatolites: SEPM (Society for Sedimentary Geology) Special Publication. 67.
Pope, M.C., Grotzinger, J.P., Schreiber, B.C., 2000. Evaporitic Subtidal Stromatolites Produced by in situ Precipitation: Textures, Facies Associations, and Temporal Significance. J. Sediment. Res. 70, 1139–1151. https://doi.org/10.1306/062099701139.
Pope, E.C., Bird, D.K., Rosing, M.T., 2012. Isotope composition and volume of Earth's early oceans. Proc. Natl. Acad. Sci. 109, 4371–4376. https://doi.org/10.1073/pnas.1115705109.
Posth, N.R., Konhauser, K.O., Kappler, A., 2011. Banded Iron Formations: Encyclopedia of Earth Sciences Series.
Preiss, W.V., 1977. The biostratigraphic potential of Precambrian stromatolites. Precambrian Res. 5, 207–219. https://doi.org/10.1016/0301-9268(77)90028-6.
Pruss, S.B., Clemente, H., 2011. Assessing the role of skeletons in early Paleozoic carbonate production: insights from Cambro-Ordovician strata, Western Newfoundland. Quant. Evol. Early Life 36, 321–354. https://doi.org/10.1007/978-94-007-0680-4.
Pruss, S.B., Knoll, A.H., 2017. Environmental covariation of metazoans and microbialites in the Lower Ordovician Boat Harbour Formation, Newfoundland. Palaeogeogr. Palaeoclimatol. Palaeoecol. 485, 917–929. https://doi.org/10.1016/j.palaeo.2017.08.007.
Pruss, S.B., Corsetti, F.A., Fischer, W.W., 2008. Seafloor-precipitated carbonate fans in the Neoproterozoic Rainstorm Member, Johnnie Formation, Death Valley Region, USA. Sediment. Geol. 207, 34–40. https://doi.org/10.1016/j.sedgeo.2008.03.005.
Pruss, S.B., Finnegan, S., Fischer, W.W., Andrew, H., Pruss, S.B., Finnegan, S., Fischer, W.W., Knoll, A.H., 2010a. Carbonates in skeleton-poor seas: new insights from Cambrian and Ordovician strata of Laurentia. 25. pp. 73–84.
Pruss, S.B., Finnegan, S., Fischer, W.W., Knoll, A.H., 2010b. Carbonates in Skeleton-Poor Seas: New Insights From Cambrian and Ordovician Strata of Laurentia. Palaios 25, 73–84. https://doi.org/10.2110/palo.2009.p09-101r.
Pu, J.P., Bowring, S.A., Ramezani, J., Myrow, P., Raub, T.D., Landing, E., Mills, A., Hodgin, E., Macdonald, F.A., 2016. Dodging snowballs: Geochronology of the Gaskiers glaciation and the first appearance of the Ediacaran biota. Geology 44, 955–958. https://doi.org/10.1130/G38284.1.
Rainbird, R.H., 1991. Stratigraphy, sedimentology and tectonic setting of the Upper Shaler Group. Victoria Island, Northwest Territories.
Reinhard, C.T., Planavsky, N.J., Robbins, L.J., Partin, C.A., Gill, B.C., Lalonde, S.V., Bekker, A., Konhauser, K.O., Lyons, T.W., 2013. Proterozoic ocean redox and biogeochemical stasis. Proc. Natl. Acad. Sci. 110, 5357–5362. https://doi.org/10.1073/pnas.1208622110.
Riding, R., 2011. The nature of stromatolites: 3,500 million years of history and a century of research. In: Advances in Stromatolite Geobiology. 131https://doi.org/10.1007/978-3-642-10415-2.
Robbins, L.L., Blackwelder, P.L., 1992. Biochemical and ultrastructural evidence for the origin of whitings: a biologically induced calcium carbonate precipitation mechanism. Geology 20, 464–468. https://doi.org/10.1130/0091-7613(1992)020<0464:BAUEFT>2.3.CO;2.
Roberts, J.A., Kenward, P.A., Fowle, D.A., Goldstein, R.H., González, L.A., Moore, D.S., 2013. Surface chemistry allows for abiotic precipitation of dolomite at low temperature. Proc. Natl. Acad. Sci. 110, 14540–14545. https://doi.org/10.1073/pnas.1305403110.
Ronov, A.B., 1968. Probable changes in the composition of sea water during the course of geological time. Sedimentology 10 (1), 25–43 Chicago.
Ronov, A.B., 1982. The Earth's sedimentary shell (quantitative patterns of its structure, compositions, and evolution): the 20th V.I. Vernadskiy Lecture, March 12, 1978. Int. Geol. Rev. 24, 1365–1388. https://doi.org/10.1080/10643389.2012.728825.
Ronov, A.B., 1984. Common tendencies in the chemical evolution of the Earth's crust, ocean and atmosphere. Geochem. Int. https://doi.org/10.1080/10643389.2012.728825.
Ronov, A.B., 1985. The Distribution of Basalts, Andesites, and Rhyolites on the Continents and Continental Margins and in the Oceans. Int. Geol. Rev. 27, 1276–1284. https://doi.org/10.1080/10643389.2012.728825.
Ronov, A.B., Khain, V.E., Balukhovsky, A.N., Seslavinsky, K.B., 1980. Quantitative analysis of Phanerozoic sedimentation. Sediment. Geol. 25, 311–325. https://doi.org/10.1016/0037-0738(80)90067-6.
Ronov, A.B., Khain, V.E., Seslavinsky, K.B., 1981. Vendian lithologic complexes of the world. Soviet Geol. 5, 37–59. https://doi.org/10.1080/10643389.2012.728825.
Ronov, A.B., Khain, V.E., Seslavinsky, K.B., 1982. Lower and middle Riphean lithologic complexes of the world. Int. Geol. Rev. 5, 509–525. https://doi.org/10.1080/10643389.2012.728825.
Rooney, A.D., Strauss, J.V., Brandon, A.D., Macdonald, F.A., 2015. A Cryogenian chronology: Two long-lasting synchronous neoproterozoic glaciations. Geology 43, 459–462. https://doi.org/10.1130/G36511.1.
Rose, C.V., 2012. Comings and goings of the end-Cryogenian ice sheet: a stratigraphic study of the pre-, syn-, and post-glacial deposits. Princeton University, South Australia.
Saltzman, M.R., Edwards, C.T., Adrain, J.M., Westrop, S.R., 2015. Persistent oceanic anoxia and elevated extinction rates separate the Cambrian and Ordovician radiations. Geology 43, 807–811. https://doi.org/10.1130/G36814.1.
Sánchez-Baracaldo, P., Raven, J.A., Pisani, D., Knoll, A.H., 2017. Early photosynthetic eukaryotes inhabited low-salinity habitats. Proc. Natl. Acad. Sci. https://doi.org/10.1073/pnas.1620089114. 201620089.
Saylor, B.Z., 1996. Sequence stratigraphic and chemostratigraphic constraints on the evolution of the terminal Proterozoic to Cambrian Nama Basin. Massachusetts Institute of Technology, Namibia.
Schirrmeister, B.E., Sanchez-Baracaldo, P., Wacey, D., 2016. Cyanobacterial evolution during the Precambrian. Int. J. Astrobiol. 15, 187–204. https://doi.org/10.1017/S1473550415000579.
Schmidt, P.W., Williams, G.E., 2008. Palaeomagnetism of red beds from the Kimberley Group, Western Australia: Implications for the palaeogeography of the 1.8 Ga King Leopold glaciation. Precambrian Re. 167, 267–280. https://doi.org/10.1016/j.precamres.2008.09.002.
Schopf, J.W., Klein, C., 1992. The Proterozoic Biosphere: A Multidisciplinary Study. Cambridge University Press, Cambridge, pp. 1348.
Semikhatov, M.A., Raaben, M.E., 1996. Dynamics of the global diversity of Proterozoic stromatolites. Stratigr. Geol. Corr. 4, 492–513.
Semikhatov, M.A., Polevaya, N.I., Volobuev, M.A., Kazakov, G.A., 1973. Late Precambrian of the Siberian Platform and its Folded Framing. Geochronol. USSR. 1, 268–280.
Semikhatov, M.A., Gebelein, C.D., Cloud, P.E., Awramik, S.M., Benmore, W.C., 1979. Stromatolite morphogenesis–progress and problems. Can. J. Earth Sci. 16, 992–1015.
Semikhatov, M.A., Kuznetsov, A.B., Maslov, A.V., Gorokhov, I.M., Ovchinnikova, G.V., 2009. Stratotype of the Lower Riphean, the Burzyan Group of the Southern Urals: Lithostratigraphy, paleontology, geochronology, Sr- and C-isotopic characteristics of its carbonate rocks. Stratigr. Geol. Corr. 17, 574–601. https://doi.org/10.1134/S0869593809060021.
Serebryakov, S.N., Semikhatov, M.A., 1974. Riphean and Recent stromatolites: a comparison. Am. J. Sci. 274, 556–574. https://doi.org/10.2475/ajs.274.6.556.
Sergeev, V.N., Knoll, A.H., Kolosova, S., Kolosov, P., 1994. Silicified microfossils from the Mesoproterozoic Debengda Formation, northern Siberia. Stratigr. Geol. Corr. 2, 19–33.
Sergeev, V.N., Knoll, A.H., Grotzinger, J.P., 1995. Paleobiology of the Mesoproterozoic Billyakh Group, Anabar Uplift, Northern Siberia. J. Paleontol. 39, 1–37.
Sergeev, V.N., Knoll, A.H., Petrov, P.Y., 1997. Paleobiology of the Mesoproterozoic-Neoproterozoic transition: the Sukhaya Tunguska Formation, Turukhansk Uplift, Siberia. Precambrian Res. 85, 201–239. https://doi.org/10.1016/S0301-9268(97)00035-1.
Shields, G., 2002. A chemical explanation for the mid-Neoproterozoic disappearance of molar-tooth structure ~750 Ma. Terra Nova 14, 108–113.
Shinn, E.A., Lloyd, R.M., Ginsburg, R.N., 1969. Anatomy of a modern carbonate tidal-flat, Andros Island, Bahamas. J. Sediment. Petrol. 39, 1202–1228.
Shinn, E.A., Steinen, R.P., Lidz, B.H., Swart, P.K., 1989. Whitings, a Sedimentologic Dilemma. J. Sediment. Petrol. 59, 147–161. https://doi.org/10.1306/212F8F3A-2B24-11D7-8648000102C1865D.
Siahi, M., Hofmann, A., Master, S., Mueller, C.W., Gerdes, A., 2017. Carbonate ooids of the Mesoarchaean Pongola Supergroup, South Africa. Geobiology 15, 750–766. https://doi.org/10.1111/gbi.12249.
Sibley, D.F., 1991. Secular changes in the amount and texture of dolomite. Geology 19, 151–154. https://doi.org/10.1130/0091-7613(1991)019<0151:SCITAA>2.3.CO.
Siever, R., 1992. The silica cycle in the Precambrian. Geochimica et Cosmochimica Acta 56, 3265–3272. https://doi.org/10.1016/0016-7037(92)90303-Z.
Sigg, L., Johnson, C.A., Kuhn, A., 1991. Redox conditions and alkalinity generation in a seasonally anoxic lake (Lake Greifen). Marine Chem. 36, 9–26. https://doi.org/10.1016/S0304-4203(09)90051-2.
Smith, E.F., 2015. Constraints on global carbon cycling, basin formation and early animal evolution during the Neoproterozoic and Early Cambrian. pp. 357. https://doi.org/10.1017/CBO9781107415324.004.
Soetaert, K., Soetaert, K., Hofmann, A.F., Hofmann, A.F., Middelburg, J.J., Middelburg, J.J., Meysman, F.J.R., Meysman, F.J.R., Greenwood, J., Greenwood, J., 2007. The effect of biogeochemical processes on pH. Marine Chem. 105, 30–51. https://doi.org/10.1016/j.marchem.2006.12.012.
Sperling, E.A., Frieder, C.A., Raman, A.V., Girguis, P.R., Levin, L.A., Knoll, A.H., 2013. Oxygen, ecology, and the Cambrian radiation of animals. Proc. Natl. Acad. Sci. 110,

13446–13451. https://doi.org/10.1073/pnas.1312778110.
Sperling, E.A., Wolock, C.J., Morgan, A.S., Gill, B.C., Kunzmann, M., Halverson, G.P., Macdonald, F.A., Knoll, A.H., Johnston, D.T., 2015. Statistical analysis of iron geochemical data suggests limited late Proterozoic oxygenation. Nature 523, 451–454. https://doi.org/10.1038/nature14589.
Sprinkle, J., Guensburg, T.E., 1995. Origin of Echinoderms in the Paleozoic Evolutionary Fauna: The Role of Substrates. Palaios 10, 437. https://doi.org/10.2307/3515046.
Srinivasan, K., Walker, K.R., 1993. Sequence stratigraphy of an intrashelf basin carbonate ramp to rimmed platform transition: Maryville Limestone (Middle Cambrian), southern Appalachians. Geol. Soc. Am. Bull. 105.
Stewart, J.H., 1970. Upper Precambrian and Lower Cambrian Strata. Southern Great Basin California and Nevada.
Stewart, J.J.H., Amaya-Martinez, R., Palmer, A.R., Amaya-Martínez, R., 2002. Neoproterozoic and Cambrian strata of Sonora, Mexico: Rodinian supercontinent to Laurentian Cordilleran margin. Geol. Soc. Am. Spec. Papers 365, 5–20. https://doi.org/10.1130/0-8137-2365-5.5.
Stolper, D.A., Keller, C.B., 2018. A record of deep-ocean dissolved O2 from the oxidation state of iron in submarine basalts. Nature 553, 323–327.
Strauss, J.V., 2015. The Neoproterozoic and Early Paleozoic Tectonic and Environmental Evolution of Alaska and Northwest Canada. pp. 348.
Summa, C.L., 1993. Sedimentologic, stratigraphic, and tectonic controls of a mixed carbonate-siliciclastic succession: Neoproterozoic Johnnie Formation, southeast California. Massachusetts Institute of Technology, pp. 616.
Sumner, D.Y., 1997. Late Archean calcite-microbe interactions; two morphologically distinct microbial communities that affected calcite nucleation differently. Palaios1 12 (4), 302–318.
Sumner, D., 2000. Microbial vs Environmental Influences on the Morphology of Late Archean Fenestrate Microbialites. In: Microbial Sediments, pp. 307–314.
Sumner, D.Y., Grotzinger, J.P., 1986. Herringbone calcite; petrography and environmental significance. J. Sediment. Res. 66, 419–429.
Sumner, D.Y., Grotzinger, J.P., 1993. Numerical modeling of ooid size and the problem of Neoproterozoic giant ooids. J. Sediment. Petrol. 63, 974–982. https://doi.org/10.1306/D4267C5D-2B26-11D7-8648000102C1865D.
Sumner, D.Y., Grotzinger, J.P., 1996. Were kinetics of Archean calcium carbonate precipitation related to oxygen concentration? Geology 24, 119–122. https://doi.org/10.1130/0091-7613(1996)024<0119:WKOACC>2.3.CO;2.
Sumner, D.Y., Grotzinger, J.P., 2000. Late Archean Aragonite Precipitation: Petrography, Facies Associations, and Environmental Significance: SEPM Special Publication 67. Carbonate Sedimentation and Diagenesis in the Evolving Precambrian World 67, 123–144. https://doi.org/10.2110/pec.00.67.0123.
Sumrall, C.D., Sprinkle, J., Guensburg, T.E., 1997. Paleontological Society Systematics and Paleoecology of Late Cambrian Echinoderms from the Western United States. J. Paleontol. 71, 1091–1109.
Sun, S.Q., 2003. A reappraisal of dolomite abundance and occurrence in the Phanerozoic; discussion and reply. J. Sediment. Res. 65, 244–246. https://doi.org/10.1306/d4268086-2b26-11d7-8648000102c1865d.
Swett, K., Knoll, A.H., 1985. Stromatolitic bioherms and microphytolites from the late proterozoic draken conglomerate formation, spitsbergen. Precambrian Res. 28, 327–347. https://doi.org/10.1016/0301-9268(85)90037-3.
Tang, D., Shi, X., Jiang, G., 2013. Mesoproterozoic biogenic thrombolites from the North China platform. Int. J. Earth Sci. 102, 401–413. https://doi.org/10.1007/s00531-012-0817-9.
Tang, D., Shi, X., Jiang, G., 2014. Sunspot cycles recorded in Mesoproterozoic carbonate biolaminites. Precambrian Res. 248, 1–16. https://doi.org/10.1016/j.precamres.2014.04.009.
Tang, D., Shi, X., Shi, Q., Wu, J., Song, G., Jiang, G., 2015. Organomineralization in Mesoproterozoic giant ooids. J. Asian Earth Sci. 107, 195–211.
Tarhan, L.G., 2018a. Phanerozoic shallow marine sole marks and substrate evolution. Geology 46, 755–758.
Tarhan, L.G., 2018b. The early Paleozoic development of bioturbation—Evolutionary and geobiological consequences. Earth Science Rev. 178, 177–207.
Tarhan, L.G., Droser, M.L., Planavsky, N.J., Johnston, D.T., 2015. Protracted development of bioturbation through the early Paleozoic Era. Nat. Geosci. 8, 865–869.
Thomas, R.D.K., Reif, W.-E., 1993. The skeleton space: a finite set of organic designs. Evolution 47, 341–360.
Thompson, C.K., Kah, L.C., 2012. Sulfur isotope evidence for widespread euxinia and a fluctuating oxycline in Early to Middle Ordovician greenhouse oceans. Palaeogeogr. Palaeoclimatol. Palaeoecol. 313–314, 189–214. https://doi.org/10.1016/j.palaeo.2011.10.020.
Tice, M., 2005. Life and evolution in the early Archean: New data from the 3416 Ma Buck Reef Chert. Stanford University, Barberton Greenstone Belt, South Africa, pp. 121.
Tosca, N.J., Guggenheim, S., Pufahl, P.K., 2016. An authigenic origin for Precambrian greenalite: Implications for iron formation and the chemistry of ancient seawater. Bull. Geol. Soc. Am. 128, 511–530. https://doi.org/10.1130/B31339.1.
Tostevin, R., Clarkson, M.O., Gangl, S., Shields, G.A., Wood, R.A., Bowyer, F., Penny, A.M., Stirling, C.H., 2019. Uranium isotope evidence for an expansion of anoxia in terminal Ediacaran oceans. Earth Planet. Sci. Lett. 506, 104–112. https://doi.org/10.1016/j.epsl.2018.10.045.
Trower, E.J., Grotzinger, J.P., 2010. Sedimentology, diagenesis, and stratigraphic occurrence of giant ooids in the Ediacaran Rainstorm Member, Johnnie Formation, Death Valley region, California. Precambrian Res. 180, 113–124. https://doi.org/10.1016/j.precamres.2010.03.007.
Trower, E.J., et al., 2018. Active ooid growth driven by sediment transport in a high energy shoal, Little Ambergris Cay, Turks and Caicos, British Overseas Territories. J. Sediment. Res. 88 (9), 1132–1151.
Trower, E.J., Lamb, M.P., Fischer, W.W., 2019. The origin of carbonate mud. Geophys. Res. Lett. 2. https://doi.org/10.1029/2018GL081620.
Tucker, M.E., 1977. Stromatolite biostromes and associated facies in the late precambrian porsanger dolomite formation of Finnmark, Arctic Norway. Palaeogeogr. Palaeoclimatol. Palaeoecol. 21, 55–83. https://doi.org/10.1016/0031-0182(77)90004-9.
Tucker, M.E., 1982. Precambrian dolomites: petrographic and isotopic evidence that they differ from Phanerozoic dolomites. Geology 10, 7–12. https://doi.org/10.1130/0091-7613(1982)10<7:PDPAIE>2.0.CO;2.
Tucker, M.E., 1983. Diagenesis, geochemistry and origin of a Precambrian dolomite: The Beck Spring Dolomite of Eastern California. J. Sev. 53.
Tucker, M.E., 1984. Calcitic, aragonitic and mixed calcitic-aragonitic ooids from the mid-Proterozoic Belt Supergroup, Montana. Sedimentology 31, 627–644. https://doi.org/10.1111/j.1365-3091.1984.tb01227.x.
Turner, E.C., 1999. Growth dynamics, framework composition, and microstructure of giant early Neoproterozoic calcimicrobial reefs, Little Dal Group, Mackenzie Mountains, NWT. Queen's Universityhttps://doi.org/10.16953/deusbed.74839.
Turner, E.C., 2009. Mesoproterozoic carbonate systems in the Borden Basin. Nunavut. https://doi.org/10.1139/E09-062.
Turner, E.C., James, N.P., Narbonne, G.M., 2000. Taphonomic control on microstructure in early Neoproterozoic reefal stromatolites and thrombolites. Palaios 15, 87–111. https://doi.org/10.1669/0883-1351(2000)015<0087:TCOMIE>2.0.CO;2.
Tyler, S.A., Barghoorn, E.S., 1954. Occurrence of Structurally Preserved Plants in Pre-Cambrian Rocks of the Canadian Shield. Science 119, 606–608.
Van Ee, N.J., Wanless, H.R., 2008. Ooids and grapestones: a significant source of mud on Caicos Platform. In: Developing Models and Analogs for Isolated Carbonate Platforms: Holocene and Pleistocene Carbonates of Caicos Platform, British West Indies: SEPM, Core Workshop, pp. 121–125.
van Smeerdijk Hood, A., Wallace, M.W., 2015. Extreme ocean anoxia during the Late Cryogenian recorded in reefal carbonates of Southern Australia. Precambrian Res. 261, 96–111. https://doi.org/10.1016/j.precamres.2015.02.008.
van Smeerdijk Hood, A., Wallace, M.W., 2018. Neoproterozoic marine carbonates and their paleoceanographic significance. Global Planet. Change 160, 28–45. https://doi.org/10.1016/j.gloplacha.2017.11.006.
van Smeerdijk Hood, A., Wallace, M.W., Drysdale, R.N., 2011. Neoproterozoic aragonite-dolomite seas? Widespread marine dolomite precipitation in Cryogenian reef complexes. Geology 39, 871–874. https://doi.org/10.1130/G32119.1.
Van Tuyl, F.M., 1915. The origin of dolomite(Vol. 25). State Printer, R. Henderson.
Vasconcelos, C., Mckenzie, J.A., 1997. Microbial mediation of modern dolomite precipitation and diagenesis under anoxic conditions (Lagoa Vermelha, Rio de Janeiro, Brazil). J. Sediment. Res. 67, 378–390.
Vernhet, E., Youbi, N., Chellai, E.H., Villeneuve, M., El Archi, A., 2011. The Bou-Azzer glaciation: Evidence for an Ediacaran glaciation on the West African Craton (Anti-Atlas, Morocco). Precambrian Res. 196–197, 106–112. https://doi.org/10.1016/j.precamres.2011.11.009.
Vorob'eva, N.G., Petrov, P.Y., 2014. The genus Vendomyces Burzin and facies-ecological specificity of the Staraya Rechka microbiota of the Late Vendian of the Anabar Uplift of Siberia and its stratigraphic analogues. Paleontol. J. 48, 655–666. https://doi.org/10.1134/S003103011406015X.
Vorob'eva, N.G., Sergeev, V.N., Semikhatov, M., 2006. Unique lower Vendian Kel'tma microbiota, Timan ridge: New evidence for the paleontological essence and global significance of the Vendian system: Doklady. Earth Sci. 410, 1038–1043. https://doi.org/10.1134/S1028334X06070087.
Wacey, D., Saunders, M., Kong, C., Brasier, A., Brasier, M., 2016. 3.46 Ga Apex chert 'microfossils' reinterpreted as mineral artefacts produced during phyllosilicate exfoliation:, v. 36, p. 296–313. Gondwana Res. 36, 296–313. https://doi.org/10.1016/j.gr.2015.07.010.
Walker, J.C.G., Hays, P.B., Kasting, J.F., 1981. A negative feedback mechanism for the long-term stabilization of the earth's surface temperature. J. Geophys. Res. 86, 9776. https://doi.org/10.1029/JC086iC10p09776.
Wallace, M.W., 1990. Origin of dolomitization on the Barbwire Terrace, Canning Basin, Western Australia. Sedimentology 37, 105–122. https://doi.org/10.1111/j.1365-3091.1990.tb01985.x.
Wallace, M.W., Hood, A.V.S., Woon, E.M., Hoffmann, K.H., Reed, C.P., 2014. Enigmatic chambered structures in Cryogenian reefs: The oldest sponge-grade organisms? Precambrian Res. 255, 109–123.
Walter, M., 1976. Stromatolites: New York. pp. 790.
Walter, L.M., Burton, E.A., 1990. Dissolution of recent platform carbonate sediments in marine pore fluids. Am. J. Sci. 601–643.
Walter, M.R., Heys, G.R., 1985. Links between the rise of the Metazoa and the decline of stromatolites. Precambrian Res. 29, 149–174.
Wang, D., Wallace, A.F., De Yoreo, J.J., Dove, P.M., 2009. Carboxylated molecules regulate magnesium content of amorphous calcium carbonates during calcification. Proc. Natl. Acad. Sci. 106, 21511–21516. https://doi.org/10.1073/pnas.0906741106.
Warren, J., 2000. Dolomite: occurrence, evolution, and economically important associations. Earth Science Rev. 52, 1–82.
Warthmann, R., van Lith, Y., Vasconcelos, C., Mckenzie, J.A., Karpoff, A.M., 2000. Bacterially induced dolomite precipitaion in anoxic culture experiments. Geology 28, 1091–1094. https://doi.org/10.1130/0091-7613(2000)028<1091:BIDPIA>2.3.CO;2.
Wei, G., Planavsky, N.J., Tarhan, L.G., Chen, X., Wei, W., Li, D., Ling, H., 2018. Marine redox fluctuation as a potential trigger for the Cambrian explosion. 46. pp. 1–5. https://doi.org/10.1130/G40150.1.
Widdel, F., Schnell, S., Heising, S., Ehrenreich, A., Assmus, B., Schink, B., 1993. Ferrous iron oxidation by anoxygenic phototrophic bacteria. Nature 362, 834–836. https://doi.org/10.1038/362834a0.

Williams, G.E., 2005. Subglacial meltwater channels and glaciofluvial deposits in the Kimberley Basin, Western Australia: 1.8 Ga low-latitude glaciation coeval with continental assembly. J. Geol. Soc. 162, 111–124. https://doi.org/10.1144/0016-764903-157.

Wilson, J.P., et al., 2010. Geobiology of the late Paleoproterozoic Duck Creek Formation. Precambrian Research, Western Australia. https://doi.org/10.1016/j.precamres.2010.02.019.

Windley, B.F., 1977. Timing of continental growth and emergence. Nature 270 (5636), 426.

Wise, D.U., 1974. Continental Margins, Freeboard and the Volumes of Continents and Oceans Through Time: The Geology of Continental Margins. pp. 45–58. https://doi.org/10.1007/978-3-662-01141-6_4.

Wood, R., 2018. Exploring the Drivers of Early Biomineralization. pp. 201–212.

Wood, R.A., Zhuravlev, A.Y., Sukhov, S.S., Zhu, M., Zhao, F., 2017. Demise of Ediacaran dolomitic seas marks widespread biomineralization on the Siberian Platform. Geology 45, 27–30. https://doi.org/10.1130/G38367.1.

Wood, R., Bowyer, F., Penny, A., Poulton, S.W., 2018. Did anoxia terminate Ediacaran benthic communities? Evidence from early diagenesis. Precambrian Res. 313, 134–147. https://doi.org/10.1016/j.precamres.2018.05.011.

Wright, D.T., 2000. Benthic Microbial Communities and Dolomite Formation in Marine and Lacustrine Environments–a new dolomite model. In: Marine Authigenesis: From Global to Microbial, pp. 7–20.

Wright, V.P., Cherns, L., 2016. How far did feedback between biodiversity and early diagenesis affect the nature of early Palaeozoic sea floors? Palaeontology 59, 753–765.

Xiao, S., Bao, H., Wang, H., Kaufman, A.J., Zhou, C., Li, G., Yuan, X., Ling, H., 2004. The Neoproterozoic Quruqtagh Group in eastern Chinese Tianshan: Evidence for a post-Marinoan glaciation. Precambrian Res. 130, 1–26. https://doi.org/10.1016/j.precamres.2003.10.013.

Yates, K.K., Robbins, L.L., 1998. Production of carbonate sediments by a unicellular green alga. Am. Mineral. 83, 1503–1509. https://doi.org/10.2138/am-1998-11-1238.

Young, G.M., 1982. The late Proterozoic Tindir Group, east-central Alaska: evolution of a continental margin. Geol. Soc. Am. Bull. 93, 759–783. https://doi.org/10.1130/0016-7606(1982)93<759:TLPTGE>2.0.CO;2.

Young, G.M., 2013. Precambrian supercontinents, glaciations, atmospheric oxygenation, metazoan evolution and an impact that may have changed the second half of Earth history. Geosci. Front. 4, 247–261. https://doi.org/10.1016/j.gsf.2012.07.003.

Young, G.M., von Brunn, V., Gold, D.J.C., Minter, W.E.L., 2009. Earth's Oldest Reported Glaciation: Physical and Chemical Evidence From the Archean Mozaan Group (~2.9 Ga) of South Africa. J. Geol. 106, 523–538. https://doi.org/10.1086/516039.

Zempolich, W.G., Baker, P.A., 1993. Experimental and Natural Mimetic Dolomitization of Aragonite Ooids. SEPM J. Sediment. Res. 63. https://doi.org/10.1306/D4267B86-2B26-11D7-8648000102C1865D.

Zempolich, W.G., Wilkinson, B.H., Lohmann, K.C., Spring, S., 1988. Diagenesis of late Proterozoic carbonates: The Beck Spring Dolomite of Eastern California. J. Sediment. Petrol. 58, 656–672.

Zentmyer, R.A., Pufahl, P.K., James, N.P., Hiatt, E.E., 2011. Dolomitization on an evaporitic Paleoproterozoic ramp: Widespread synsedimentary dolomite in the Denault Formation, Labrador Trough, Canada. Sediment. Geol. 238, 116–131. https://doi.org/10.1016/j.sedgeo.2011.04.007.